ALERT Geomaterials

Alliance of laboratories in Europe for Research and Technology
Aussois, September 30 – October 02, 2024

35th ALERT Workshop / POSTER SESSION

Booklet of abstracts

Editors: Nadia BENAHMED
Antoine WAUTIER

(INRAE, France)

ALERT Geomaterials

The Alliance of Laboratories in Europe for Education, Research and Technology

35th ALERT Workshop

Poster Session

Aussois 2024

Editors:

Nadia BENAHMED
Antoine WAUTIER

(INRAE, Aix-en-Provence – France)

ISBN: 978-2-9584769-4-6

Dear colleagues,

We are pleased to welcome you to Aussois and to our 35th ALERT Workshop and School.

As always, it is an exciting time for us to continue to meet and bring together inspired people for fruitful days with interesting, stimulating discussions, exchange of knowledge and experience on Geomechanics. Presentations of recent advances offer the chance to get up-to-date and to remain at the cutting edge.

We would like to express our thanks to all of you who contributed to the success of this poster session. The number of received posters this year is historical compared to previous editions, with more than 50 contributions (!) gathering contributors from 17 countries (Czech Republic, Germany, France, Canada, The Netherlands, UK, , Belgium, Australia, Italy, Austria, USA, Swiss, Spain, Japan, Sweden, Colombia, China) and belonging from 41 different research institutions. They are summarized in the histogram below together with the corresponding number of posters (>1).

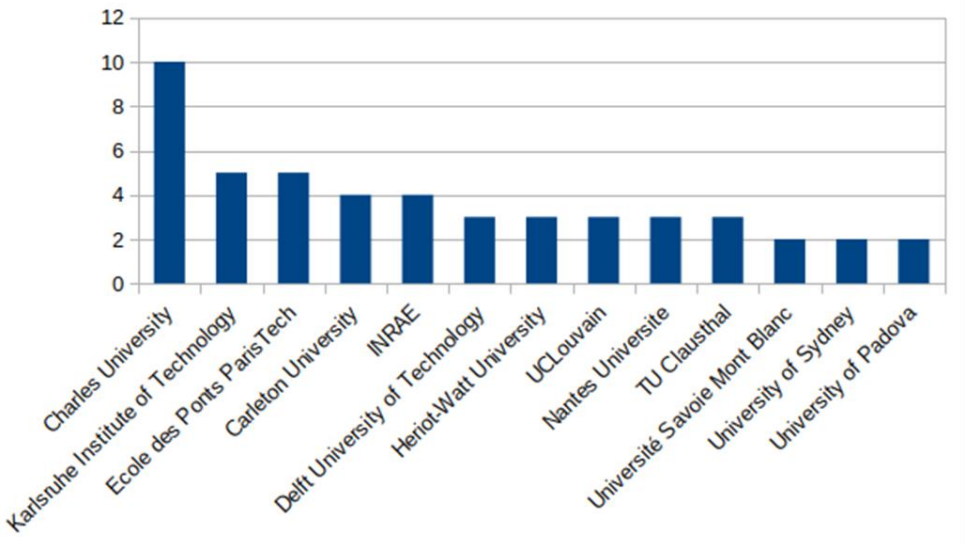

The posters cover numerical, experimental and analytical approaches with the following repartition.

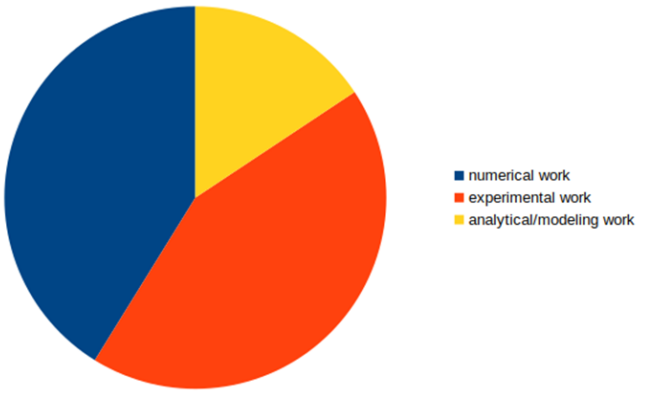

From the reading of the abstracts, we can propose the following analysis, counting the number of abstracts dealing with different types of materials, numerical tools, specific loadings, experimental techniques, types of loading and fields of application. This gives an idea of the current hot topics in geomechanics.

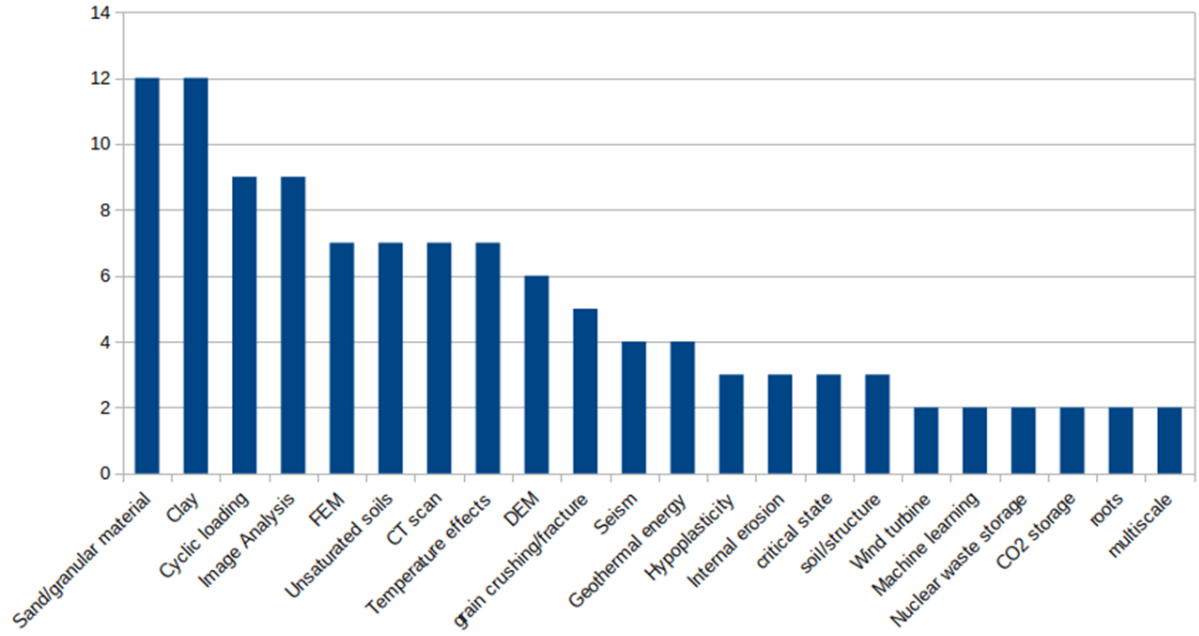

Twenty posters were eligible for the poster competition 2024. The Poster Prize was granted to:

Zhaochen XU (ENPC)

*for his poster entitled "**Behaviour of reservoir rocks under hydrostatic cyclic loading for hydrogen storage application**". Congratulations!*

Congratulations also to the two other nominees, Faranak SAHRAGARD (Carleton University) and Antoine GUGGISBERG (EPFL) for their posters of excellent quality.

Looking forward to see you next year in Aussois!

Kind regards,

Nadia Benahmed and Antoine Wautier.

Table of contents

Delaying Grain Breakage Phenomenon in a Lightweight Granular Material 8
Hamza Loubane, Ali Daouadji

On the Friction Dependency of the Stress Lode Angle 10
Gertraud Medicus, Mehdi Pouragha, Alexander Ostermann, Wolfgang Fellin

The Generalized Intergranular Strain Concept and its Confrontation with Experimental Data 12
Luis Mugele, Hanz Hennig Stutz, David Mašín

Why Are Boreholes in Sand Stable? 14
Tessel Grubben, Alexis Koulidis, Martin van der Schans, Niels Hartog, Martin Bloemendal Philip Vardon

Fabric-Strain Relationship in REVs Inside a Shear Band for a Sand Specimen in Triaxial Compression 16
Selma Schmidt, Ivo Herle

Tensile Strength of Compacted Boom Clay 18
Ties de Jong, Bhini Chandan Malagar, Philip J. Vardon, Anne-Catherine Dieudonné

Mechanical Responses of Willow Roots Under Different Loading Modes 20
Shanshan Li, Hans Henning Stutz

Rate Effects on Evolution of Pore Water Pressure at Fine-Grained Soil - Structure Interfaces 22
Bereket Mamo Gebremeskel, Hans Henning Stutz

Compound Centipede-Root-Vortex Inspired Penetration 24
Meron Belachew, Chloé Arson, J. David Frost 24

Investigating the Effect of Na^{+}, Ca^{2+}, and Cu^{2+} Adsorption on Bentonite Using Multi-Scale Simulation 26
Yalda Pedram, Yaoting Zhang, Scott Briggs, Chang Seok Kim, Laurent Brochard, Laurent Béland 26

Effective Management of Induced Seismicity for the Net Zero Energy Transition 28
Birhanmeskel Woldemichael, Alexis Cartwright–Taylor, Elli-Maria Charalampidou, Nathaniel Forbes Inskip, Ian G. Main, Ian B. Butler, Maria-Daphne Mangriotis 28

The Effective Fracture Energy of Shear Frictionless Cracks 30
Serafim Egorov, Jean Sulem, Mathias Lebihain

Numerical Investigations of Chemical Damage-Healing in Geomaterials at the Microstructural Level 32
Alexandre Sac-Morane, Hadrien Rattez, Manolis Veveakis

Stiffness of Weathered Limestone: From Laboratory Data to In-Situ Measurements Beneath Wind Turbine Foundations 34
Carlos Peña, Sabine Gehring, Hans Henning Stutz

Sustainable Repurposing of Reiche Zeche Mine for Geothermal Energy and Water Storage: A Geomechanical and Hydrological Approach 36
Ali Ahmadi, Tomiwa Aderemi, Eleni Gerolymatou, Elli-Maria Charalampidou

Reinforcement Learning-Based Adaptive Time-Integration for Nonsmooth Dynamics . 38
David Riley, Alexandros Stathos, Diego Gutierrez-Oribio, Ioannis Stefanou

On The Automated Calibration of Elastoplasticity Constitutive Model: The Hardening Soil ... 40
Phuong C. Do, Tomáš Kadlíček, David Mašín, Jan Najser

Compressibility Characteristics of Malaysian Kaolin Considering Different Thermo-Hydro-Mechanical Conditions 42
Rodrigo Polo-Mendoza, David Mašín, Jan Najser, Jakub Roháč, Jose Duque

Experimental Investigation of the Influence of Soil Plasticity on Compression and Creep Behaviour of Clayey Soils 44
Manh Nguyen Duy, Jan Jerman, Jan Najser

Influence of Anisotropic Structure on the Interface Shear Strength of Fine-Grained Soil 46
Sabine Gehring, Hans Henning Stutz, Andrzej Niemunis

Rock Boring Process Simulation: A Coupled Approach with OpenFOAM and YADE 48
Manikandan Valliappan, Eleni Gerolymatou

A Discrete Elements Study of Flash Heating in Fault Gouges 50
Hossein Shahabi, Hadrien Rattez

Considering the Ductile Behavior of Altered Volcanic Rocks in the Flank Stability of Volcanoes and Their Response to Earthquakes 52
Jens Niclaes, Pierre Delmelle, Hadrien Rattez

Accelerated Implicit Cyclic Loading 53
Kadlíček Tomáš, Mašín David

A Rheological Model for Ice 56
Faranak Sahragard, Mehdi Pouragha, Mohammad Rayhani

Experimental Approaches to Evaluate Temperature and Time-Dependent Effects in Sheared Soil 58
Tomáš Mladý, Om Prasad Dhaka, Bhargavi Chowdepalli

Geotechnical Clay Core Characterisation for Deep Geological Disposal of Radioactive Waste in the Netherlands 60
Vidushi Toshniwal, Ties de Jong, Hemmo Abels, Wout Broere, Ana Maria Fernández, Michael A. Hicks, Dirk Munsterman, Erika Neeft, Philip J. Vardon, Anne-Catherine Dieudonné

Evolution of Clay Microstructure Under 1-D Consolidation 62
Rishabh Tiwari, Béatrice Baudet, Matthew Richard Coop, Jean-Michel Pereira, Pierre Delage

Hydromechanical Coupling in the Rupture of Saturated Geomaterials 64
Antoine Guggisberg, Mehana Allache, Philipp Braun, Marie Violay, Mathias Lebihain

Influence of the Sample Preparation Method on the Monotonic and Cyclic Response of Malaysian Kaolin 66
Elvis Covilla, David Mašín, Jose Duque, Jakub Roháč, Jan Najser

A Constitutive Model for Predicting Soil Strength and Compressibility Under Grain Crushing 68
David León-Vanegas, Lluís Monforte, Marcos Arroyo, Antonio Gens

Coupled Thermo-Hydro-Mechanical Behavior of Clays: From Constitutive Modelling with Hypoplasticity to Finite Element Simulations 70
Pico Maria, Mašín, David

Influence of Suction and Saturation on Accumulated Axial Strain and Post-Cyclic Strength of Unsaturated Soils 72
Bhargavi Chowdepalli, Kenji Watanabe

Widgets for Teaching in Geomechanics 75
Eleni Gerolymatou, Erik Bruer, Maryam Zali, Yousef Al-Hadhrami, Franck Andy Dzoupet Yimtchi, Farzaneh Rajabi Monfared

Microstructural Insights Into the Failure Mechanism of Lightweight Cemented Soils Coupling In-Situ X-Ray Microtomography and Digital Image Correlation 76
Laura Perrotta, Enza Vitale, Emmanuel Roubin, Alessandro Tengattini, Giacomo Russo, Gioacchino Viggiani

Multiscale Modeling of Granular Materials: A Statistical Homogenization Strategy Relying on Mesoscale DEM Simulations 78
Aoxin Li, Antoine Wautier, François Nicot, Mehdi Pouragha, Claudio Carvajal

Behaviour of Reservoir Rocks Under Hydrostatic Cyclic Loading for Hydrogen Storage Application 80
Zhaochen Xu, Philipp Braun, Jean Sulem

Microscale Precursors of Failure in Fine Grained Porous Sandstone under Cyclic Thermo-Mechanical Coupling: A Grain Based Model (GBM) Study 82
Jinci Chen, Elli-Maria Charalampidou, Ali Ozel, Audrey Ougier-Simonin

Thermal Effect on the Residual Shear Strength and its Correlation to the Available Clay Fraction **84**
Om Prasad Dhakal, Bhargavi Chowdepalli, Tomas Mlady, Marco Loche, Gianvito Scaringi

Strategies for Extending Saturated Constitutive Soil Models to Unsaturated Tailings ... **86**
Mina Mofrad, Mehdi Pouragha, Paul H. Simms

Terracotta: A Simple Hydrodynamic Model for Clays **88**
Max Wiebicke, Itai Einav

Multiphysics Modelling of Slope Instability of a Large-Scale Physical Model **90**
Maria Lazari, Matteo Camporese, Lorenzo Sanavia

Multiphysics Modelling of Desaturation Cracks in Non-Isothermal Multiphase Porous Media **92**
Zechao Chen, Laura De Lorenzis, Lorenzo Sanavia

Three-Dimensional Numerical Study on the Internal Erosion Mechanism of the Agly Dike **94**
Zezhi Deng, Nadia Benahmed, Laurence Girolami, Pierre Philippe, Stephane Bonelli, Gang Wang

A Novel Testing System for Particle-Scale Investigation of Clay in Nano-X-Ray Imaging Instruments **96**
Angela Casarella, Anders Karlsson, Gustave Pinzón, Olga Stamati, Julie Villanova, Jelke Dijkstra

DEM-Based Model of PVC Geomembranes to Understand the Mechanical Behavior **98**
Nesrin Akel, Antoine Wautier, François Nicot, Guillaume Stoltz, Nathalie Touze-Foltz

The Sand Atlas **100**
Ilija Vego, Benjy Marks

Altering the Macroscopic Behavior of Granular Materials by Adding Fines **102**
Abhijit Hegde, Nadia Benahmed, Antoine Wautier, Pierre Philippe

Advances in Earthquake Prevention: Controlling Slip-Rate in Seismic Faults and Seismicity Rate in Underground Reservoirs **104**
Diego Gutiérrez-Oribio, Alexandros Stathas, Ioannis Stefanou

On the Emergence of Micromorphic Continua through the Upscaling of a Cauchy Medium **106**
Alexandros Stathas, Ioannis Stefanou

Delaying Grain Breakage Phenomenon in a Lightweight Granular Material

Hamza Loubane, Ali Daouadji

INSA LYON, Laboratoire GEOMAS

17 rue des Arts, 69621 Villeurbanne, France

Hamza.loubane@insa-lyon.fr

Keywords: grain breakage, particle size effect, particle crushing, granular material, lightweight expanded clay aggregate

Abstract

This study investigates the effect of particle grading on grain breakage in granular materials subjected to one-dimensional compression tests. The hypothesis is that altering the grading of the granular material by introducing a fraction of smaller particles to fill void spaces can reduce grain breakage. Initial tests were conducted on a monodisperse lightweight clay aggregates material with grain sizes ranging from 12.5 to 16 mm (Dmax/Dmin = 1.28), subjected to various levels of compression.

To enhance the material's density and potentially delay grain breakage, smaller particles (8-10 mm in diameter) were introduced into the monodisperse material, this led to a Dmax/Dmin = 2, with a bidisperse material distribution. The effectiveness of this densification was quantified using a classical breakage index, which considers both the potential breakage (up to a fractal distribution) and the actual breakage (area behind the PSD curve).

Key findings indicate that the addition of smaller particles slightly reduced grain breakage under lower compression levels (Figure 1). This effect was more noticeable at lower stress levels but diminished as the applied stress increased to higher levels (such as 5000 kPa). The modified material exhibited less breakage compared to the monodisperse material, demonstrating that a smaller fraction addition can influence the material's response to compression. Additionally, the individual strength of the grains was tested and can be approximated using the Weibull distribution (Figure 2).

The conclusions drawn from these experiments suggest that the densification of granular materials through the addition of smaller particles can be an effective strategy for reducing grain breakage, particularly under lower stress conditions.

Figures

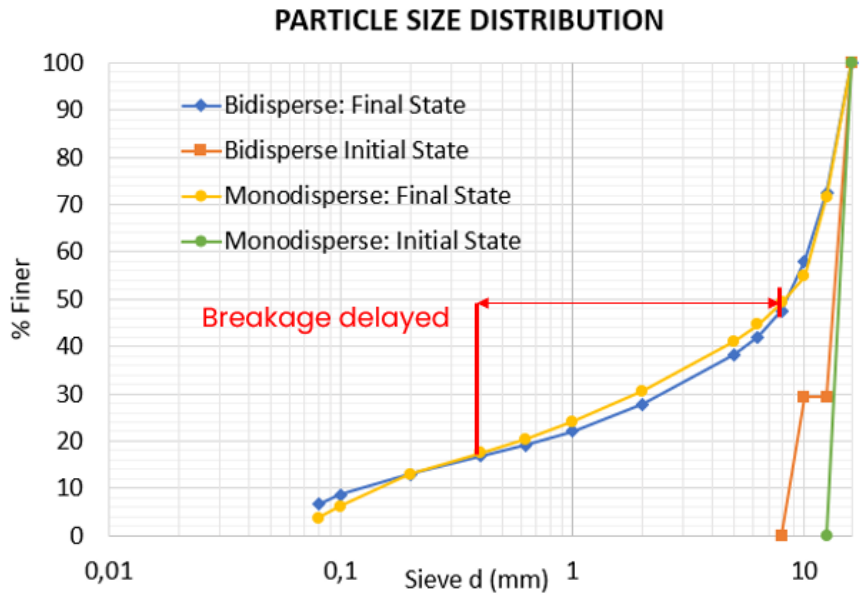

***Figure 1**: Percentage of passing particles as a function of their diameter for monodisperse and bidispers samples before and after being subjected to a stress of 2500 kPa.*

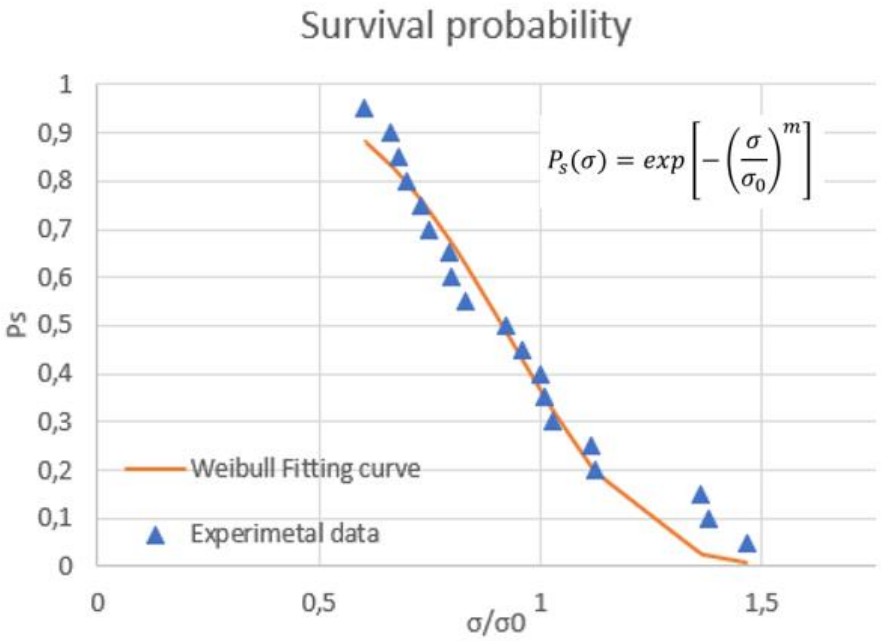

***Figure 2**: Survival probability distribution for lightweight clay appregates (12.5<d<16mm) as a function of normalized failure stress.*

On the Friction Dependency of the Stress Lode Angle

Gertraud Medicus[1], Mehdi Pouragha[2], Alexander Ostermann[1], Wolfgang Fellin[1]

[1]University of Innsbruck, Austria

[2]Carleton University, Canada

gertraud.medicus@uibk.ac.at, mehdi.pouragha@carleton.ca, alexander.ostermann@uibk.ac.at, wolfgang.fellin@uibk.ac.at

Keywords: critical state, hypoplasticity; barodesy, DEM, Lode angle, alignment

Abstract

The shape of the failure locus of a material is significant for its strength predictions. Even when constitutive models include the same critical stress surface, different critical stress ratios can be predicted for an identical applied isochoric strain path. In this study, we investigate critical stress predictions of different constitutive models, which include the surface according to Matsuoka–Nakai. We perform analytical investigations, true triaxial test simulations with hypoplasticity (von Wolffersdorff, 1996; Mašín, 2013) and barodesy (Kolymbas, 2015; Medicus & Fellin, 2017), and discrete element modelling (DEM) simulations to investigate the friction dependency of the stress Lode angle α_σ. Our results demonstrate that in hypoplasticity, the direction of the deviatoric stress state at critical state depends solely on the direction of the applied deviatoric strain path, characterized through the Lode angle of the strain rate $\alpha_{\dot{\varepsilon}}$, see Figure 1. In contrast, in barodesy, the predictions are also dependent on the friction angle of the material. To validate this friction dependency on the stress Lode angle, we conducted DEM simulations. The DEM results qualitatively support the predictions of barodesy and suggest that a higher friction results in a higher Lode angle at critical stress state, see Figure 2. The complete study can be found in MehdiCus et al. (2024).

Acknowledgement

G.M. is funded by the Austrian Science Fund (FWF) V 918. For the purpose of open access, the authors have applied a CC BY public copyright licence to any Author Accepted Manuscript version arising from this submission. In addition, G.M. is supported by Le Pôle interdisciplinaire d'études françaises de l'Université d'Innsbruck (Frankreich-Schwerpunkt der Universität Innsbruck).

References

P.-A. von Wolffersdorff. A hypoplastic relation for granular materials with a predefined limit state surface. Mechanics of Cohesive-Frictional Materials, 1996.

D. Mašín. Clay hypoplasticity with explicitly defined asymptotic states. Acta Geotechnica, 2013.

D. Kolymbas. Introduction to barodesy. Géotechnique, 2015.

G. Medicus and W. Fellin. An improved version of barodesy for clay. Acta Geotechnica, 2017.

G. Medicus, M. Pouragha, A. Ostermann & W. Fellin. On the friction dependency of the stress lode angle. Int. J. Numer. Anal. Methods Geomech., 2024.

Figures

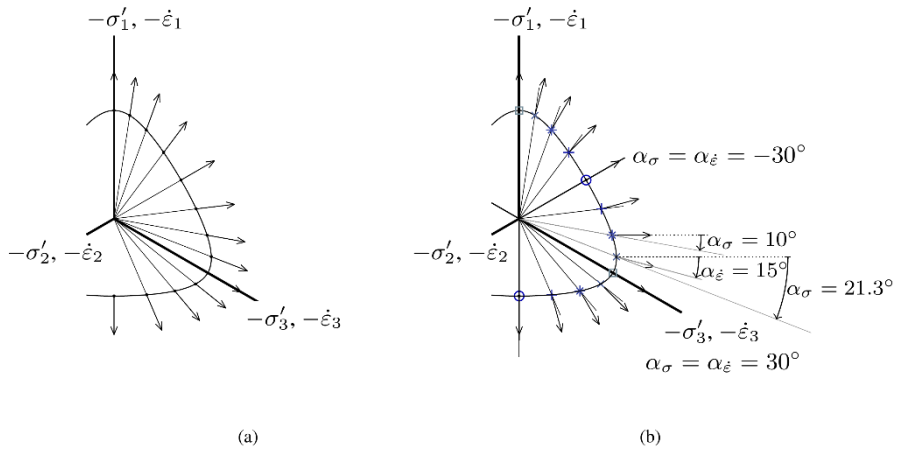

***Figure 1**: Critical stress states in the deviatoric plane. The full line is the cross section of the critical stress surface according to Matsuoka–Nakai with a deviatoric plane, the arrows denote the deviatoric directions of proportional strain paths and are characterised through $\alpha\dot{\varepsilon}$. For isochoric plane-strain compression, it follows $\alpha\dot{\varepsilon}$=0°. In hypoplasticity (Figure a) $\alpha\sigma = \alpha\dot{\varepsilon}$ for isochoric conditions. In barodesy (Figures b), $\alpha\sigma$ differs from $\alpha\dot{\varepsilon}$.*

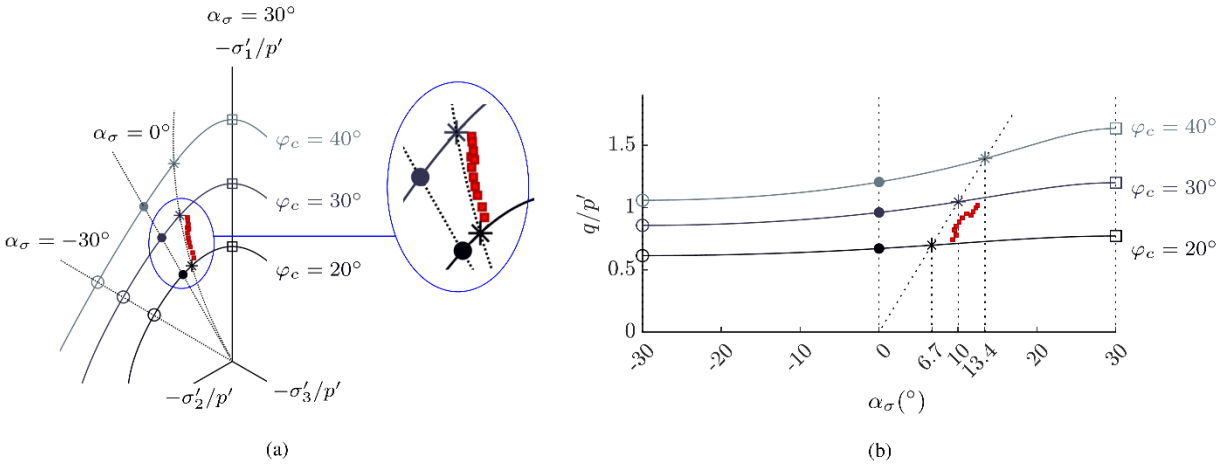

***Figure 2**: Critical stress states of isochoric plane-strain paths ($\alpha\dot{\varepsilon} = 0$) with hypoplasticity, barodesy and DEM are displayed in the deviatoric plane (a), and q/p' vs. $\alpha\sigma$ plane: The DEM results (filled, red squares) show that Lode angle at the critical stress state increases with friction which is consistent with the predictions of barodesy (marked with ∗). Conversely, hypoplasticity (marked with •) shows no dependence of the Lode angle on φc , as $\alpha\dot{\varepsilon} = 0$ implies that $\alpha\sigma = 0$, as shown in Figure 1 a.*

The Generalized Intergranular Strain Concept and its Confrontation with Experimental Data

Luis Mugele[1], Hanz Hennig Stutz[1], David Mašín[2]

[1]Institute of Soil Mechanics and Rock Mechanics, Karlsruhe Institute of Technology, Germany

[2]Faculty of Science, Charles University, Prague, Czech Republic

luis.mugele@kit.edu

Keywords: hypoplasticity, asymptotic states, generalized intergranular strain, cyclic deformation

Abstract

In The holistic constitutive modeling of soil remains a significant challenge in geotechnical research. While advanced constitutive models, such as modern hypoplastic formulations, can effectively reproduce the behavior of soil under monotonic loading, they exhibit considerable deficits when it comes to cyclic deformations. The well-known intergranular strain (IS) concept [1] is often used to account for the small-strain effects in such simulations. However, the original IS concept suffers from two major issues [2]: (1) overshooting and (2) linear accumulation. To address these issues, the generalized intergranular strain (GIS) concept [3] has been introduced. The GIS approach is designed to be adaptable to various constitutive models, including hypoplastic and elasto-plastic formulations. However, the GIS concept has only been discussed in theory. This study therefore aims to compare experimental data with the coupled hypoplastic model HP+GIS to evaluate its practical effectiveness.

First, it is important to give some general remarks on the model formulation. An asymptotic state refers to a state reached after sufficient long monotonic deformation. In the n-dimensional vector space $\mathbb{R}^n$ of state variables, all asymptotic states lie on the so-called asymptotic state boundary surface (ASBS). This surface is utilized in constitutive formulations and is considered in the proposed extended generalized hypoplasticity [3]

$$\dot{\boldsymbol{\sigma}} = \mathrm{E} : (\dot{\boldsymbol{\varepsilon}} - C\, \boldsymbol{m}\, S \parallel \dot{\boldsymbol{\varepsilon}} \parallel + f(\boldsymbol{\alpha}, \dot{\boldsymbol{\varepsilon}}))$$

where E_{ijkl} represents the linear stiffness, m_{ij} the hypoplastic flow rule, $S = f_d \,/\, f_d^A$ (distance from the current state to the ASBS), and further generalized via the tensorial function $f(\boldsymbol{\alpha}, \dot{\boldsymbol{\varepsilon}})$ and scalar value C. The hypoplasticity after von Wolffersdorff [4] (HP) is the most widely used hypoplastic model for sand, depicting asymptotic states implicitly without an explicit definition. In this model, as described in [5], the ASBS can only be determined iteratively. As shown in [3], the HP can be reformulated into the extended generalized hypoplasticity.

The novel GIS formulation addresses the above-mentioned major issues of the original IS concept by incorporating the state variable intergranular strain h_{ij} and a scalar factor k defined as:

$$k = [\rho^{\chi_R} m_T + (1 - \rho^{\chi_R}) m_R] + \begin{cases} \rho^{\chi_R}\,(1 - m_T)\,\vec{\boldsymbol{h}} : \vec{\dot{\boldsymbol{\varepsilon}}} & \text{if} \quad \vec{\boldsymbol{h}} : \dot{\boldsymbol{\varepsilon}} > 0 \\ -\rho^{\chi_R}\,(m_R - m_T)\,\vec{\boldsymbol{h}} : \vec{\dot{\boldsymbol{\varepsilon}}} & \text{if} \quad \vec{\boldsymbol{h}} : \dot{\boldsymbol{\varepsilon}} \leq 0 \end{cases}$$

The factor k is used as a modification of the extended generalized hypoplasticity

$$\dot{\boldsymbol{\sigma}} = k\,\mathrm{E} : (\dot{\boldsymbol{\varepsilon}} - C\,\boldsymbol{m}\; S^{k\gamma}\; \| \dot{\boldsymbol{\varepsilon}} \| + f(\boldsymbol{\alpha}, \dot{\boldsymbol{\varepsilon}}))$$

with $\gamma = f(\Omega \triangleq \text{cyclic preloading})$. After a change in loading direction, this model achieves (1) a reduction of irreversible deformations and (2) an increase in linear stiffness. The original IS issues are thus addressed, resulting in (1) reduced overshooting of the ASBS due to the unaffected value of $S = 1$ and (2) nonlinear accumulation effects due to the state variable Ω [6].

The resulting HP+GIS requires 18 parameters: 8 conventional HP parameters, 5 conventional IS parameters, and 5 additional GIS parameters. The novel constitutive model is calibrated and validated against experimental data from Karlsruhe fine sand (KFS) [7], as shown in Figure 1. The HP and IS parameters have been directly adopted from the HP+IS model [7]. The presented comparison between experimental data and simulations demonstrates the accuracy of the HP+GIS model in simulating soil behavior under cyclic loading and its advantages over the conventional HP+IS formulation.

References

[1] Niemunis, A., & Herle, I. (1997). Hypoplastic model for cohesionless soils with elastic strain range. Mechanics of Cohesive-frictional Materials: An International Journal on Experiments, Modelling and Computation of Materials and Structures, 2(4), 279-299.

[2] Duque, J., Yang, M., Fuentes, W., Mašín, D., & Taiebat, M. (2022). Characteristic limitations of advanced plasticity and hypoplasticity models for cyclic loading of sands. Acta Geotechnica, 1-23.

[3] Mugele, L., Stutz, H. H., & Mašín, D. (2024). Generalized intergranular strain concept and its application to hypoplastic models. Computers and Geotechnics, 173, 106480.

[4] Von Wolffersdorff, P. A. (1996). A hypoplastic relation for granular materials with a predefined limit state surface. Mechanics of Cohesive-frictional Materials: An International Journal on Experiments, Modelling and Computation of Materials and Structures, 1(3), 251-271.

[5] Mašín, D., & Herle, I. (2006). State boundary surface in hypoplasticity. In Modern Trends in Geomechanics (pp. 117-128). Berlin, Heidelberg: Springer Berlin Heidelberg.

[6] Duque, J., Mašín, D., & Fuentes, W. (2020). Improvement to the intergranular strain model for larger numbers of repetitive cycles. Acta Geotechnica, 15, 3593-3604.

[7] Wichtmann, T., & Triantafyllidis, T. (2016). An experimental database for the development, calibration and verification of constitutive models for sand with focus to cyclic loading: part I—tests with monotonic loading and stress cycles. Acta Geotechnica, 11, 739-761.

Figures

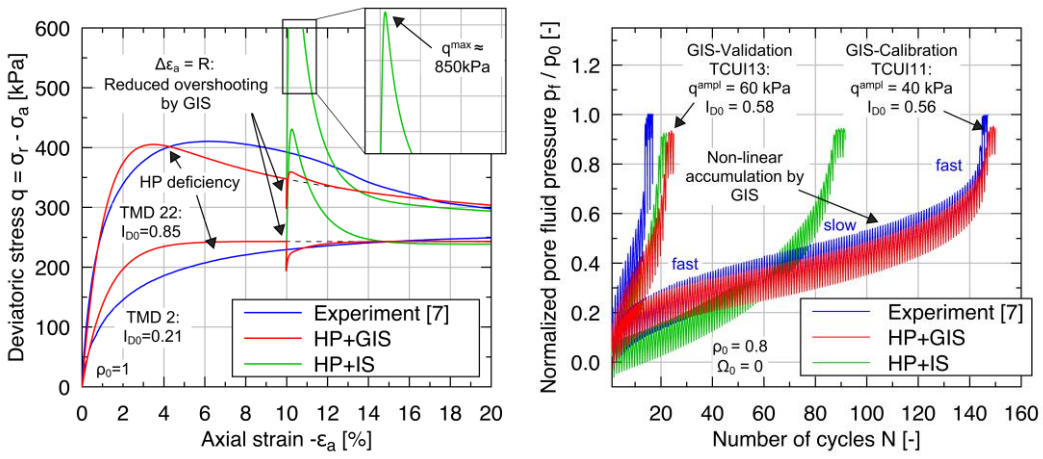

Figure 1: *Experimental data from [7] vs. simulations using the HP+GIS model for drained monotonic triaxial tests (left) and cyclic undrained triaxial tests (right) on Karlsruhe fine sand (KFS).*

Why Are Boreholes in Sand Stable?

Tessel Grubben, Alexis Koulidis, Martin van der Schans, Niels Hartog, Martin Bloemendal Philip Vardon

Delft University of Technology, KWR Water Research Institute, University of Utrecht & Netherlands Organisation for Applied Scientific Research (TNO)

t.m.grubben@tudelft.nl

Keywords: borehole stability, sand, shear strength, dilatancy, soil fabric

Abstract

As space in our shallow subsurface is scarce and groundwater tables are declining, we are forced to target deeper, more challenging aquifers for utilising ground(water) resources [1,2]. Expanding the radius of a borehole at depth has the potential to increase the hydraulic performance, reduce drilling costs and clogging potential, and could thereby enhance the feasibility of these deeper-lying aquifers [3]. However, field experience has indicated that enlarging boreholes may lead to instability problems [4]. This has prompted an in depth analysis of borehole stability in sand, raising the question of why conventional boreholes in cohesionless soils are stable in the first place? According to the Mohr-Coulomb failure criterion [5], any cohesionless soil is at failure if one of the principal stresses is equal to zero. In a borehole supported by an overpressure, the effective radial stress at the borehole wall is by definition zero. Hence, this implies that boreholes in sands are inherently unstable; a conclusion which is heavily contradicted by the successful drilling of millions of boreholes in unconsolidated formations worldwide, e.g. [6] for the application of heat storage systems.

The most straightforward explanation for this contradiction is that the assumption of zero cohesion must be incorrect. There are three possible sources that potentially contribute to the overall cohesion of the sand: Firstly, the presence of clay particles increases the cohesion of the mixture [7]. However, this would not explain stable boreholes in pure sand. A second explanation, which also accounts for the stability of sand castles, are the liquid induced forces caused by an interstitial fluid, i.e. suction forces causing an apparent cohesion [8]. Nonetheless, this suction force diminishes with increasing moisture content and thus is not applicable to fully saturated soils [9]. Finally, a third and seemingly most conceivable explanation is the apparent cohesion caused by the dilation of sand upon yielding [10]. In this work this hypothesis is tested through a series of laboratory experiments investigating the dilative behaviour and critical state of the sand. These first considerations hint at the relevance of the soil fabric and discrete failure mechanisms of the sand. Which implies that a purely continuum description of the borehole stability problem in cohesionless soils is inadequate.

References

[1] Jasechko, S., & Perrone, D. (2021). Global groundwater wells at risk of running dry. Science, 372(6540), 418-421.

[2] Bloemendal, M., Olsthoorn, T., & van de Ven, F. (2015). Combining climatic and geo-hydrological preconditions as a method to determine world potential for aquifer thermal energy storage. Science of the Total Environment, 538, 621-633.

[3] Houben, G. J. (2015). Hydraulics of water wells--flow laws and influence of geometry. Hydrogeology Journal, 23(8), 1633.

[4] van der Schans, M. L., Bloemendal, M., Robat, N., Oosterhof, A., Stuyfzand, P. J., & Hartog, N. (2022). Field Testing of a Novel Drilling Technique to Expand Well Diameters at Depth in Unconsolidated Formations. Groundwater, 60(6), 808-819.

[5] Jaeger, J. C., Cook, N. G., & Zimmerman, R. (2009). Fundamentals of rock mechanics. John Wiley & Sons.

[6] Fleuchaus, P., Godschalk, B., Stober, I., & Blum, P. (2018). Worldwide application of aquifer thermal energy storage–A review. Renewable and Sustainable Energy Reviews, 94, 861-876.

[7] Dafalla, M. A. (2013). Effects of clay and moisture content on direct shear tests for clay-sand mixtures. Advances in Materials Science and Engineering, 2013.

[8] Hornbaker, D. J., Albert, R., Albert, I., Barabási, A. L., & Schiffer, P. (1997). What keeps sandcastles standing?. Nature, 387(6635), 765-765.

[9] Fredlund, D. G. (2006). Unsaturated soil mechanics in engineering practice. Journal of geotechnical and geoenvironmental engineering, 132(3), 286-321.

[10] Rowe, P. W. (1962). The stress-dilatancy relation for static equilibrium of an assembly of particles in contact. Proceedings of the Royal Society of London. Series A. Mathematical and Physical Sciences, 269(1339), 500-527.

Figures

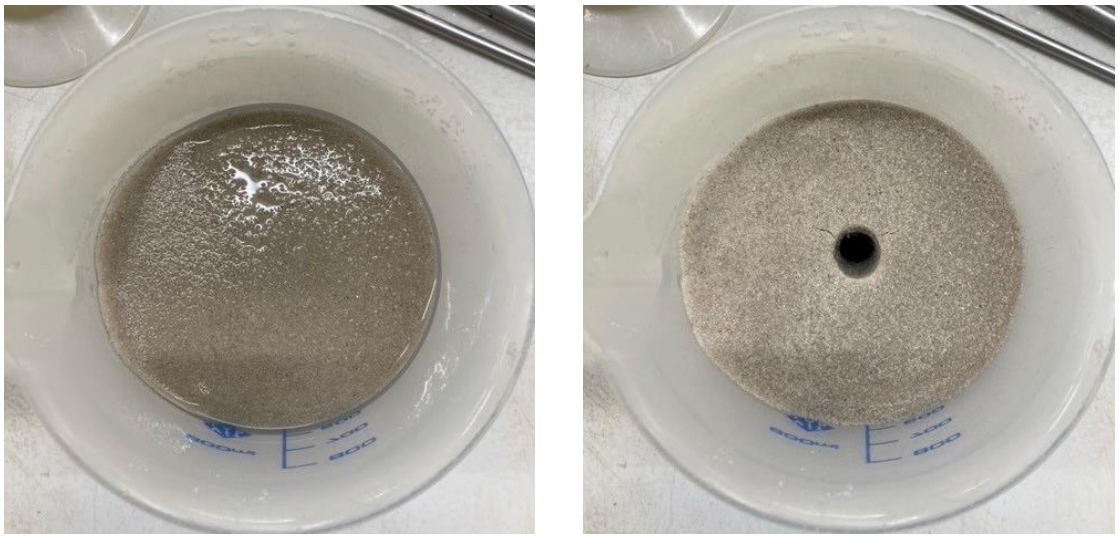

Figure 1: *Mini experiment showing a stable 'borehole' in pure, saturated sand.*

Fabric-Strain Relationship in REVs Inside a Shear Band for a Sand Specimen in Triaxial Compression

Selma Schmidt, Ivo Herle

Institut für Geotechnik, TU Dresden, Germany

selma.schmidt@tu-dresden.de

Keywords: REV scale, fabric, μCT, shear band

Abstract

1. Motivation

When interpreting triaxial tests, the specimen is commonly assumed to be homogeneous. In contrast, it has been shown that the specimen consists of multiple zones behaving very differently [1] and that a true critical state is only reached inside the shear band [2].

Within the shear band, a number of representative elementary volumes (REVs) can be distinguished. The constitutive behaviour on the level of the REVs is fundamental for the material description.

2. Approach

In [3], the soil behaviour inside a shear band is extracted from μCT images. For this purpose, sets of grains, which correspond to a REV, are defined at the initial state of a Hostun sand specimen and then tracked throughout a triaxial test.

5 different variables are considered in [3]:

- The volumetric and deviatoric strain

- The void ratio and

- Two contact fabric variables: the coordination number and the anisotropy.

The strains are calculated for tetrahedra consisting of 4 grains and then averaged over all tetrahedra of an element. For the void ratio and the contact fabric variables, a grain-based approach is adopted. The grains are tracked throughout the test by considering their displacements between two μCT images determined from DDIC.

3. Results

The soil behaviour in REVs placed inside the evolving shear band is observed to be simpler than for the complete specimen [3]. The void ratio shows a linear evolution with increasing deviatoric strain while the relationship between the contact fabric and the strain resembles a “bilinear” relationship.

It has to be noted that it is not possible to directly determine the stresses on the REV scale, but, the evolution of the anisotropy has been shown to resemble the stress evolution in a triaxial test [4].

The results suggest that simple constitutive models might be used to simulate triaxial tests when considering the heterogeneity of the soil specimen. This could be achieved by using a realistic heterogeneous initial state derived from a μCT image as in [5].

References

[1] Schmidt, S., Wiebicke, M., Herle, I. (2022). On the determination and evolution of fabric in representative elementary volumes for a sand specimen in triaxial compression. Granular Matter, 24(4), 97.

[2] Desrues, J., Chambon, R., Mokni, M., Mazerolle, F. (1996). Void ratio evolution inside shear bands in triaxial sand specimens studied by computed tomography. Géotechnique, 46(3), 529–546.

[3] Schmidt, S., Herle, I. (2024). Heterogeneous and scale-dependent behaviour of an initially dense sand specimen in triaxial compression. Preprint.

[4] Wiebicke, M., Andò, E., Viggiani, G., Herle, I. (2020). Measuring the evolution of contact fabric in shear bands with X-ray tomography. Acta Geotechnica, 15(1), 79–93.

[5] Schmidt, S., Wiebicke, M., Herle, I. (2024). Characterisation of the heterogeneity of a sand specimen in triaxial compression using x-ray CT and representative elementary volumes. E3S Web of Conferences, 544, 04003.

Figures

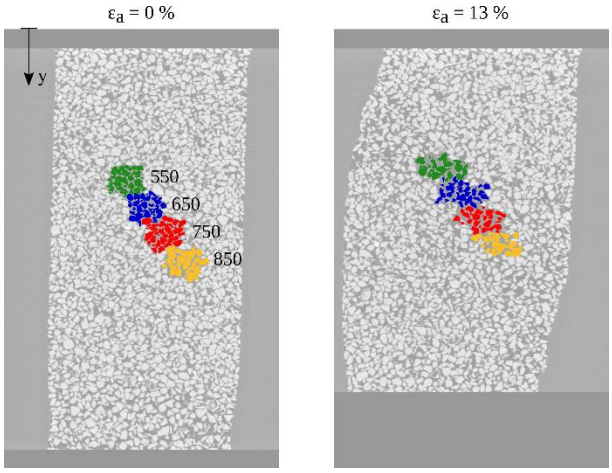

Figure 1: *REV positions at the initial state as labeled in Fig. 3 and deformed REVs at the final state from [3].*

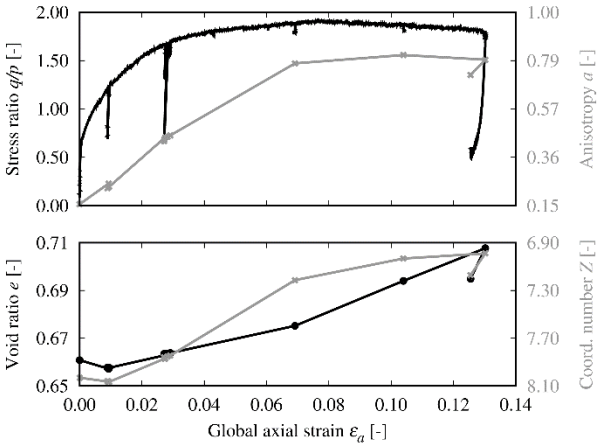

Figure 2: *Macroscopic response of the Hostun sand specimen from [1].*

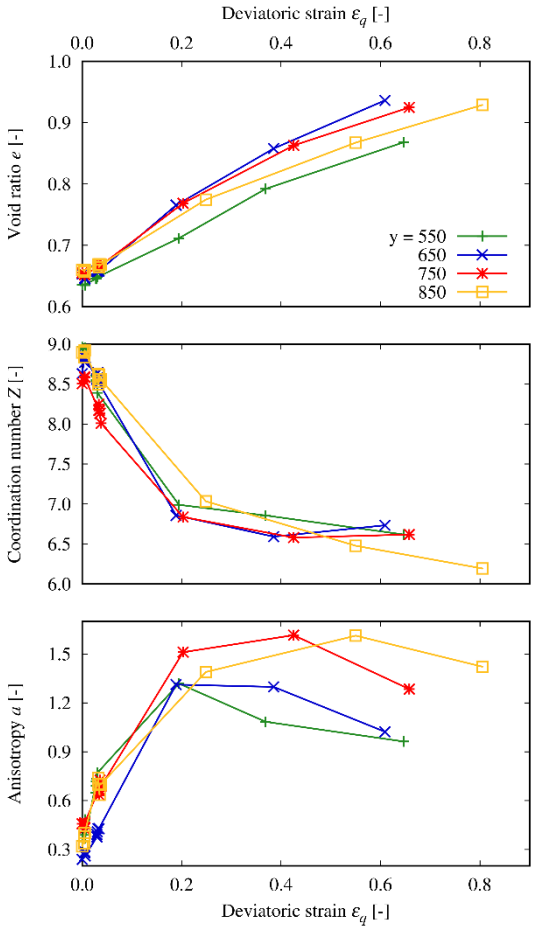

Figure 3: *Evolution of the void ratio and the contact fabric inside 4 deforming REVs with the deviatoric strain of the REVs from [3]. The REVs were placed in the region of the evolving shear band and tracked throughout the triaxial test.*

Tensile Strength of Compacted Boom Clay

Ties de Jong*, Bhini Chandan Malagar, Philip J. Vardon, Anne-Catherine Dieudonné

Delft University of Technology, Delft, The Netherlands

*t.dejong@tudelft.nl

Keywords: tensile strength, Brazilian test, Boom Clay, salinity.

Abstract

The currently, geological disposal is seen as the only safe and feasible option for the long-term management of radioactive waste. Geological disposal facilities (GDFs) are widely designed as networks of galleries and disposal tunnels or drifts. During the construction of a GDF, an excavation damage zone (EDZ) forms, consisting of shear planes and tension fractures (Mertens et al., 2004). The extent of the tension fractures largely depends on the pre-excavation stress field, the excavation method and size, and the tensile strength of the host formation material. While the tensile strength is therefore an important design parameter, it is often not well characterised and inferred from other geotechnical properties (Dehandschutter et al., 2005)

The salinity of the clay's pore water affects the clay microstructure, as the distance between clay particles reduces as the ionic strength of the pore water increases (Dor et al., 2016). This change in microstructure results in changes in geotechnical properties. While the effect of water content and dry density on the tensile strength has been extensively studied (Tang et al., 2015), the effect of pore water salinity on the tensile strength of clays has not yet been investigated. The goal of this study is therefore to estimate the tensile strength of remoulded Boom Clay and develop a fundamental understanding of the interplay between pore water salinity, microstructure and tensile strength of clays.

The tensile strength of remoulded and compacted Boom Clay disks is determined using the indirect Brazilian tensile strength test, a test commonly used in rock mechanics, which is also suitable for compacted clays (Akin & Likos, 2017). Clay disks are prepared by uniaxial load-controlled compaction to different values of dry density (1.5 – 1.8 g/cm^3), water content (0.08 – 0.23) and pore water salinity (0 – 1 mol/L NaCl solution). The disks are then loaded radially until tensile failure occurs, recognised by the formation of a tensile crack, as is shown in figure 1. The forces and displacements during the compaction as well as during the Brazilian test are measured, as is shown in figure 2.

Similar to what has been observed before with direct tensile strength methods (Tang et al., 2015), we observe an increase in tensile strength with increasing dry densities, and an initial increase in tensile strength for decreasing water content. The effects of water salinity on tensile strength, caused by the combined effect of increased (osmotic) suction and the reorganisation of clay aggregates, is further evaluated.

References

Akin, I. D., & Likos, W. J. (2017). Brazilian tensile strength testing of compacted clay. Geotechnical Testing Journal, 40(4), 608-617.

Behrends, T., van der Veen, I., Hoving, A., & Griffioen, J. (2016). First assessment of the pore water composition of Rupel Clay in the Netherlands and the characterisation of its reactive solids. Netherlands Journal of Geosciences, 95(3), 315-335.

Dehandschutter, B., Vandycke, S., Sintubin, M., Vandenberghe, N., & Wouters, L. (2005). Brittle fractures and ductile shear bands in argillaceous sediments: inferences from Oligocene Boom Clay (Belgium). Journal of Structural Geology, 27(6), 1095-1112.

Dor, M., Levi-Kalisman, Y., Day-Stirrat, R. J., Mishael, Y., & Emmanuel, S. (2020). Assembly of clay mineral platelets, tactoids, and aggregates: Effect of mineral structure and solution salinity. Journal of colloid and interface science, 566, 163-170.

Mertens, J., Bastiaens, W., & Dehandschutter, B. (2004). Characterisation of induced discontinuities in the Boom Clay around the underground excavations (URF, Mol, Belgium). Applied clay science, 26(1-4), 413-428.

Tang, C. S., Pei, X. J., Wang, D. Y., Shi, B., & Li, J. (2015). Tensile strength of compacted clayey soil. Journal of Geotechnical and Geoenvironmental Engineering, 141(4), 04014122.

Figures

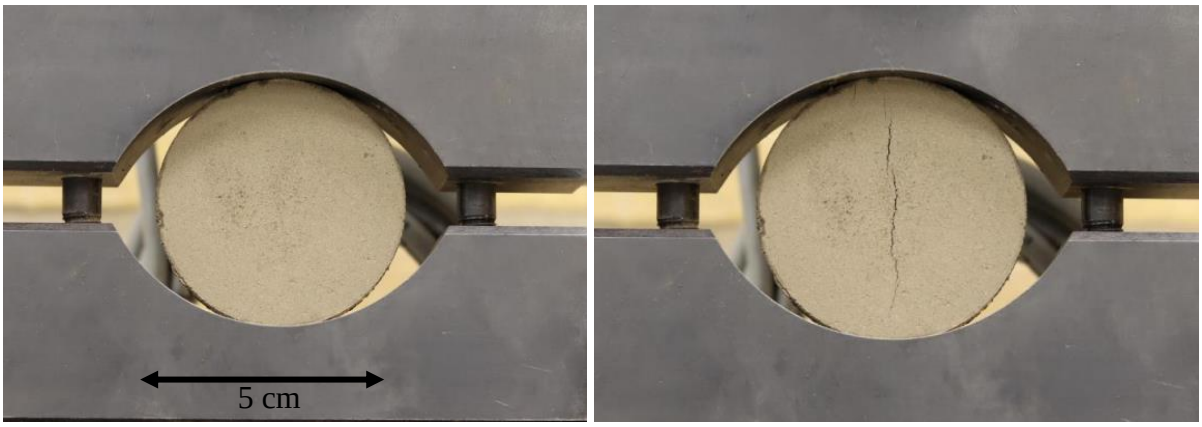

Figure 1: *Tensile failure of compacted Boom Clay under loading.*

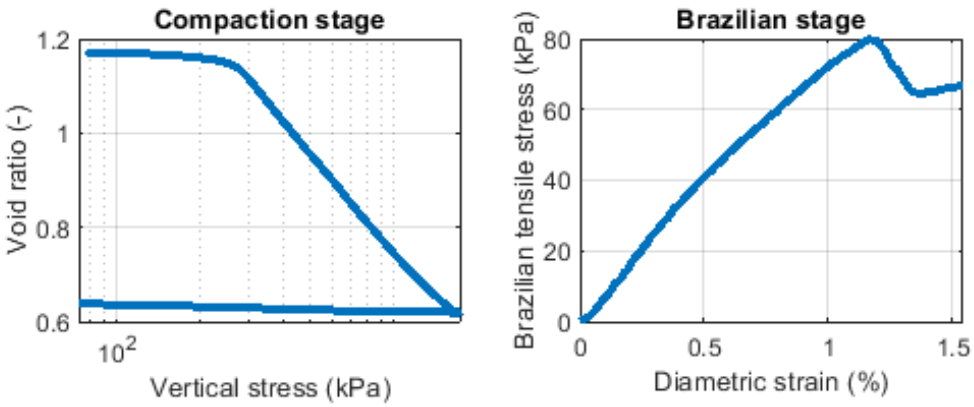

Figure 2: *Example of measurements during the compaction and Brazilian stage.*

Mechanical Responses of Willow Roots Under Different Loading Modes

Shanshan Li, Hans Henning Stutz

Karlsruhe Institute of Technology, Institute of Soil Mechanics and Rock Mechanics, Germany

shan-shan.li@kit.edu , hans.stutz@kit.edu

Keywords: willow roots, uniaxial tension test, off-axis loading test, root mechanical properties

Abstract

Characterizing root mechanical properties is essential for comprehending root-soil interactions [1, 2]. Roots exhibit specific mechanical behaviors, including tensile, compressive, buckling, twisting, and bending responses, under various soil environment such as herbivory, soil compaction, movement and settling [3]. Similar to wood, roots can exhibit directional dependency due to their anisotropic nature [4].

Although previous research has extensively focused on root tensile strength under uniaxial tension, studies on root mechanical response to different loading conditions are limited. To address this gap, a dual-purpose tension tester was modified based on a conventional direct shear apparatus. This work first examined the mechanical response of roots under uniaxial tension, using three species—*Salix viminalis*, *Salix purpurea*, and *Salix alba*. Specially designed clamps were utilized for these tests (Figure 1a). The results from uniaxial tension served as a baseline for further investigation into more complex loading, i.e., off-axis loading. The results of uniaxial tension indicated that, regardless of species, three distinct typical stress-strain curves could be identified under uniaxial tension loading. Roots, considered as composite materials consisting of cortex and stele, exhibited first fracture strains consistently less than 25%, with lower strains in roots showing only elastic behavior or prone to cortex-stele debonding.

Another set of clamps were developed for off-axis loading test (Figure 1b). Preliminary findings from off-axis loading tests showed root failure occurred at a similar off-axis angle regardless of root diameter within a given shear zone. Compared to uniaxial tension, off-axis loading mobilized the lower root ductility, indicating a reduced ability of roots to undergo plastic deformation without breaking (Figure 2).

However, the initial approach of off-axis loading test has limitations in replicating the load on roots in natural soil. The current clamps are too rigid to accommodate root deformation during loading. This high rigidity forces the root to remain fixed in a particular position, causing stress concentration at root-clamp interface, which often leads to root failure near the clamps. In contrast, soil in engineering acts as a flexible medium that deforms under load, resulting in more complex root-soil interaction. As root deforms, soil adjusts its support, in turn affecting the root mechanical response.

Therefore, future research will focus on improving the clamps to better replicating the mechanical behavior of roots in natural environments. This will enhance the understanding of root-soil interaction and improve the applicability of experimental results in engineering contexts. Furthermore, this study will introduce a theoretical framework based on the Johansen model [5] of timber connections, to predict the load-bearing capacity of individual roots during

soil shearing, specifically considering root-soil interactions where thick roots may induce local soil failure, and thin roots are more susceptible to bending or breakage.

References

[1] Martinez, A., Dejong, J., Akin, I., and et al. (2022). Bio-inspired geotechnical engineering: Principles, current work, opportunities and challenges. Géotechnique, 72(8):687–705.

[2] Li, S., Wang, Z., and Stutz, H. H. (2023). State-of-the-art review on plant-based solutions for soil improvement. Biogeotechnics, 1(3):100035.

[3] Mao, Z., Wang, Y., McCormack, M. L., Rowe, N., Deng, X., Yang, X., Xia, S., Nespoulous, J., Sidle, R. C., Guo, D., and Stokes, A. (2018). Mechanical traits of fine roots as a function of topology and anatomy. Annals of Botany, 122(7):1103−1116.

[4] Persson, K. (2000). Micromechanical modelling of wood and fibre properties. Lund University, Department of Mechanics and Materials Lund, Sweden.

[5] Johansen, K. (1949). Theory of Timber Connections. International Assoc. of Bridge and Structural Engineering Publication, 9:249−262.

Figures

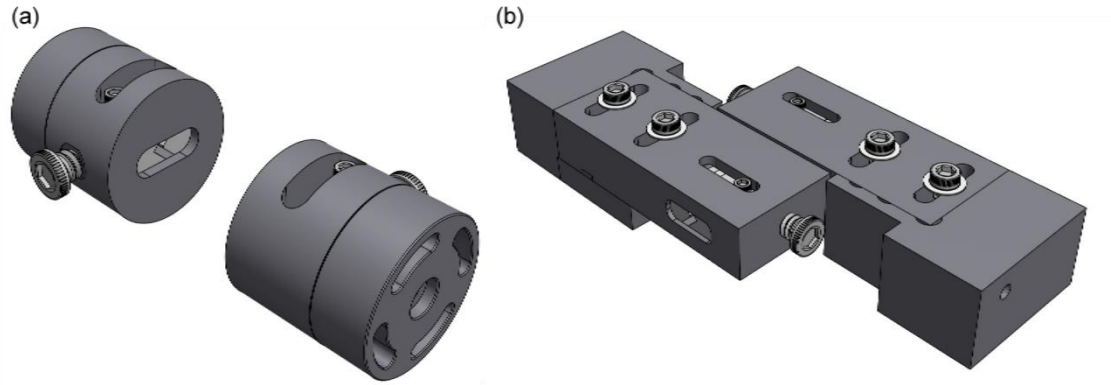

Figure 1: *Clamps designed for (a) uniaxial tension tests and (b) off-axis loading tests.*

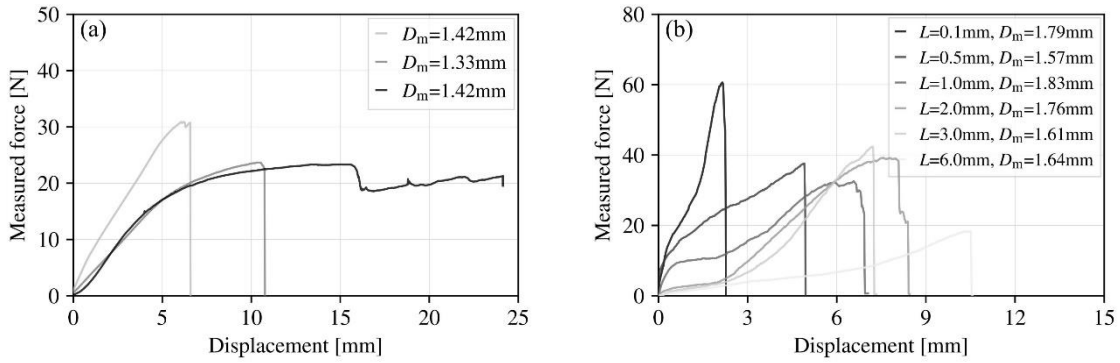

Figure 2: *Stress-strain curves of Salix purpurea roots subjected to (a) uniaxial tension and (b) off-axis loading.*

Rate Effects on Evolution of Pore Water Pressure at Fine-Grained Soil - Structure Interfaces

Bereket Mamo Gebremeskel, Hans Henning Stutz

Karlsruhe Institute of Technology, Institute of Soil Mechanics and Rock Mechanics
Engler- Bunte - Ring 14, 76131, Karlsruhe, Germany

bereket.gebremeskel@kit.edu, hans.stutz@kit.edu

Keywords: rate dependence, velocity of shearing, pile-soil interface

Abstract

Determining the magnitude of excess pore water pressure at fine-grained soil-structure interfaces is an important aspect during pile driving and loading activities [1]. However, due to a lack of instrumentation for measuring the actual excess pore water pressure during pile load testing, the evolution of pore water pressure at the pile-soil interface is not recorded for the majority of tests. As a result, the axial capacity of monopiles and suction buckets is either expressed in terms of total stress parameters or by empirical relationships developed for site-specific situations. On the other hand, the rate of loading affects the drainage conditions in fine-grained materials, which in turn determines the evolution of excess pore water pressure and the resulting interface strength. This research focuses on the effect of the rate of loading on the evolution of pore water pressure and the resulting effect on the interface strength of fine-grained soil-structure interfaces.

In this study, specimens prepared from pure kaolin and kaolin-sand mixtures were tested. The interface shear device is equipped with three pore water pressure transducers [2]. Velocities from different categories, namely fast, medium, and slow, were used in order to subject the test specimens to undrained, partially drained, and drained conditions. All specimens were tested under constant normal load (CNL) conditions.

The excess pore water pressure at the interface increases with shear displacement for relatively faster rates of shearing. However, for intermediate and slower rates of shearing, the excess pore water pressure initially increases until a certain displacement and then starts to decline. The reason for the time-dependent dissipation of excess pore water pressure could be the development of established drainage lines in the specimen over time [3]. For tests performed under the same initial normal stress and shearing rate, the magnitude of excess pore water pressure measured in the Kaolin-sand mixture specimen was significantly greater than that in pure kaolin. The observed differences may be due to variations in the mean particle diameter and permeability of the specimens. The ratio of pore water pressure to total normal stress was found to be larger for faster rates. Effective normal stress values were calculated from the initial normal total stress and the measured pore water pressure values. The calculated effective stress values were observed to vary as a function of shear displacement and pore water pressure. In conclusion, the results of the current study showed that the evolution of excess pore water pressure at the fine-grained soil interface strongly depends on the rate of loading. The mobilized interface strength is found to be affected by the magnitude of the excess pore water pressure.

References

[1] Younghong Wabg, Jiamin Jin, Bo Han, Yishun Jiang, Dongsheng Jeng, Huining Liu, Zuoding Liang and Lin Cui (2023). Distribution and dissipation laws of excess pore water pressure based on soil pile interface during pile-sinking in saturated clay. Soil Dynamics and Earthquake Engineering, 167 :107807.

[2] Martinez and H.H Stutz (2024). Evolution of excess pore water pressure in undrained clay structure interface shear tests. E3S Web of Conf., 544 :01025.

[3] Shi ao Liu, Chencong Liao, Jinjian Chen, Guanlin Ye, and Xiaohe Xia (2024). Shear rate effect on clay-structure interface strength properties in various interface boundary conditions. Soil Dynamics and Earthquake Engineering, 177 :108389.

Figures

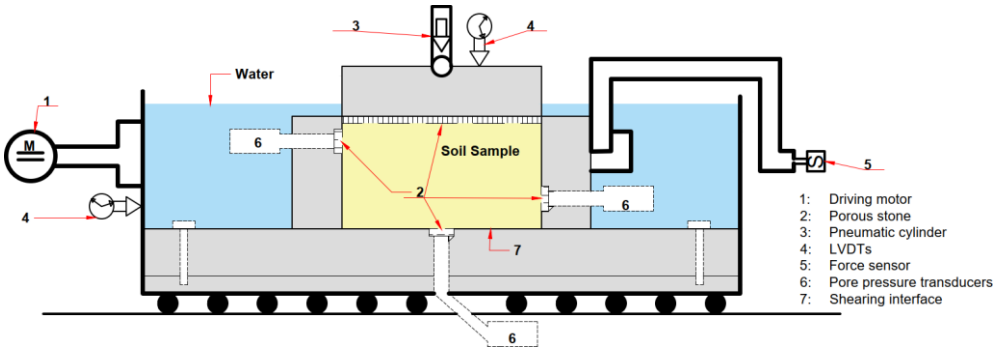

Figure 1: *Interface shear set-up.*

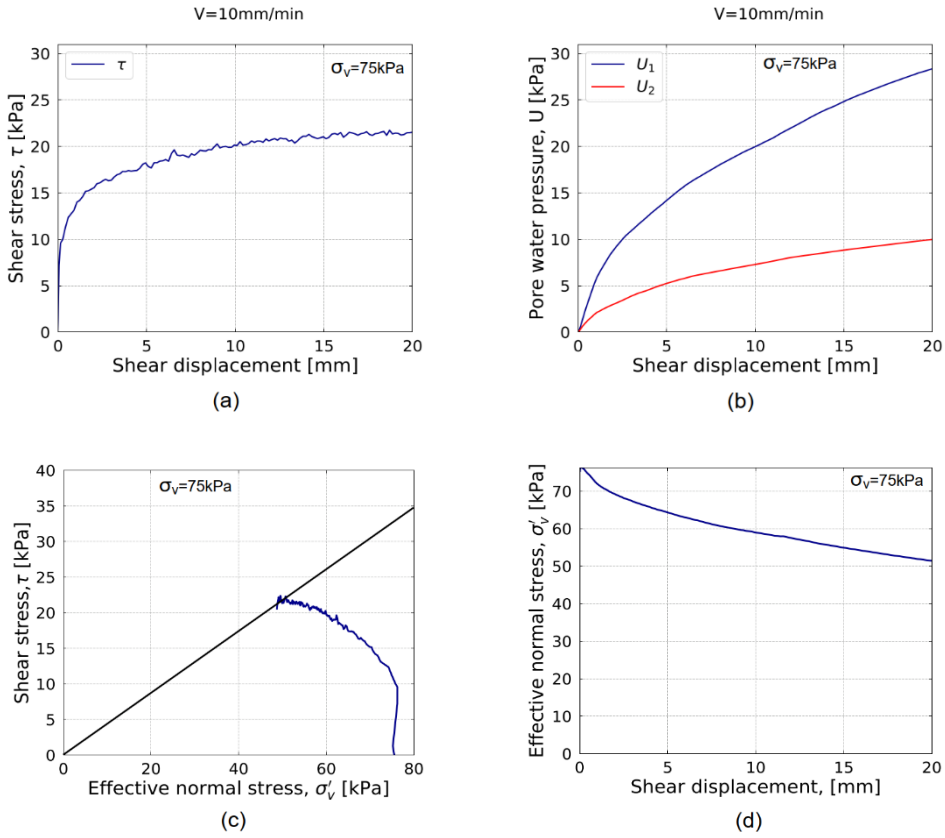

Figure 2: *Results from interface shear tests on kaolin-sand mixtures (a) Relationship between shear stress and shear displacement (b) Variation of pore water pressure with shear displacement (c) Effective stress path during shearing (d) Changes in effective normal stress with shear displacement.*

Compound Centipede-Root-Vortex Inspired Penetration

Meron Belachew[1], Chloé Arson[2], J. David Frost[1]

[1]Georgia Institute of Technology, School of Civil and Environmental Engineering, Atlanta, USA

[2]Cornell University, School of Civil and Environmental Engineering, Ithaca, USA

mbelachew3@gatech.edu

Keywords: bio-inspired design, soil penetration, root tip extension, centipede mobility, vortical motion

Abstract

Bio-inspired design seeks to find sustainable solutions to human challenges by understanding and extracting nature's strategies and applying them to engineering problems. Penetration into the subsurface is a difficult problem in geotechnical engineering as it requires a large reaction force to overcome friction and tip resistance [1]. Interestingly, plant roots are exceptionally efficient at penetrating through different soil types and to great depths. One reason for this is the tip extension mechanism that enables to maintain the sides of the root intact with the surrounding soil [2] as tapered root advances into the soil whilst also radially expanding to create fractures ahead of the penetration front [3]. Furthermore, centipedes use their legs to anchor to the soil on their sides and actively push back to generate sufficient reaction force as they advance forward and penetrate the soil [4]. The mechanism employed by these organisms enables them to generate a reaction force from the soil itself by reversing the direction of the frictional force that is developed on the sides of a penetrating body. In this study, we take inspiration from plant roots and centipedes and introduce an additional rotational motion as used by erodium seeds [5] to incorporate a vortical tip to aid penetration. The vortex shape has been used in the design of water pumps and wind turbines to move fluid efficiently for various applications [6, 7]. Our design merges these different mechanisms to develop a compound efficient soil penetration device that can minimize the reaction force that is needed to advance the penetration.

Our design has evolved through several embodiments as shown in Figure 1, starting with a pseudo-2D version featuring conveyor belts in one direction. This device was able to generate a reaction force that helped it advance into the soil as shown in Figure 2. With these promising results, we plan to expand into 3D versions that combine different shapes and motions in the future as shown in Figure 1.

The results from these studies can be useful in designing penetration probes that introduce new types of motions that are helpful in minimizing the reaction force needed for penetration. These mechanisms can be applied to a wide range of applications such as in-situ testing, sensor installation, foundation installation and micro-tunneling to state a few.

References

[1] A. Eslami, S. Moshfeghi, H. MolaAbasi, and M. M. Eslami, "CPT equipment, performance, and records," *Piezocone Cone Penetration Test (CPTu CPT) Appl. Found. Eng.*, pp. 55–80, 2020, doi: 10.1016/b978-0-08-102766-0.00003-1.

[2] A. Sadeghi, A. Tonazzini, L. Popova, and B. Mazzolai, "A Novel Growing Device Inspired by Plant Root Soil Penetration Behaviors," *PLoS One*, 2014.

[3] A. K. Mishra, F. Tramacere, and B. Mazzolai, "From plant root's sloughing and radial expansion mechanisms to a soft probe for soil exploration," *2018 IEEE Int. Conf. Soft Robot. RoboSoft 2018*, pp. 71–76, 2018, doi: 10.1109/ROBOSOFT.2018.8404899.

[4] J. P. Rieu, H. Delanoë-Ayari, C. Barentin, T. Nakagaki, and S. Kuroda, "Dynamics of centipede locomotion revealed by large-scale traction force microscopy," *J. R. Soc. Interface*, vol. 21, no. 214, 2024, doi: 10.1098/rsif.2023.0439.

[5] N. E. Stamp, "Self-Burial Behaviour of Erodium Cicutarium Seeds," *J. Ecol.*, vol. 72, no. 2, pp. 611–620, 1984, [Online]. Available: http://www.jstor.org/stable/2260070.

[6] I. Abdelghafar, A. G. Refaie, E. Kerikous, D. Thévenin, and S. Hoerner, "Optimum geometry of seashell-shaped wind turbine rotor: Maximizing output power and minimizing thrust," *Energy Convers. Manag.*, vol. 292, no. February, p. 117331, 2023, doi: 10.1016/j.enconman.2023.117331.

[7] L. Jay, "Nature-Inspired Innovation: PAX Water Technologies."

Figures

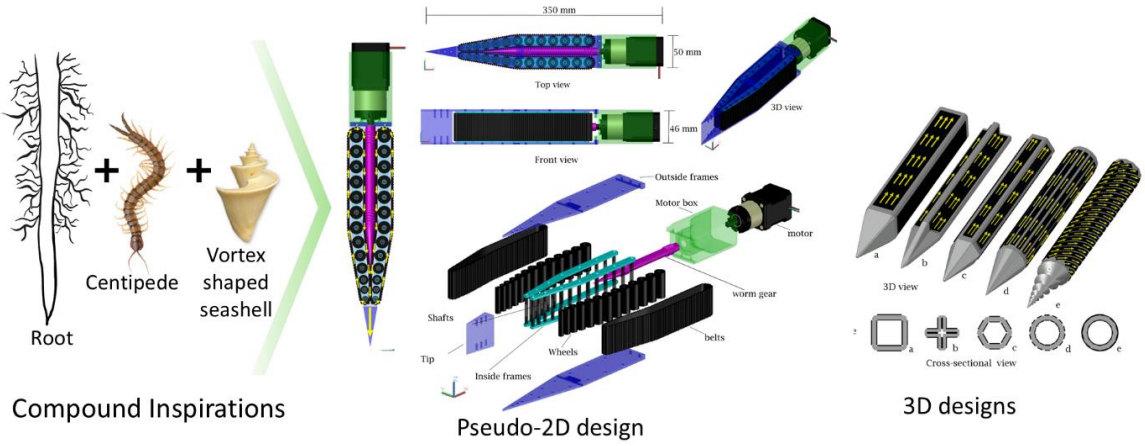

Figure 1: *Compound inspirations, pseudo-2D design and 3D designs.*

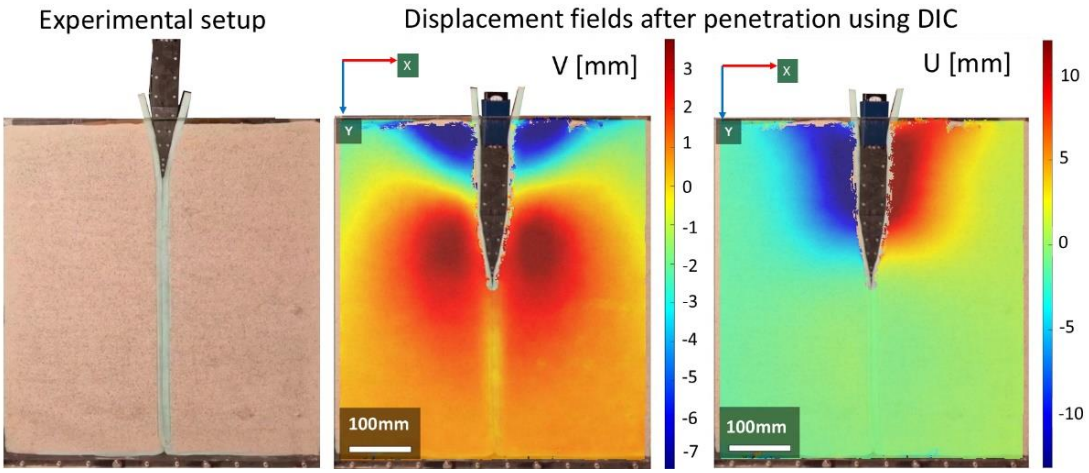

Figure 2: *Experimental setup and displacement field of penetration for the pseudo-2D design.*

Investigating the Effect of Na^+, Ca^{2+}, and Cu^{2+} Adsorption on Bentonite Using Multi-Scale Simulation

Yalda Pedram [1], Yaoting Zhang [1], Scott Briggs [2], Chang Seok Kim [2], Laurent Brochard [3], Laurent Béland [1]

[1]Department of Mechanical and Materials Engineering, Queen's University, Kingston, ON K7L 3N6, Canada

[2]Nuclear Waste Management Organization, Toronto M4T 2S3, Ontario, Canada

[3]Laboratoire Navier, Ecole des Ponts ParisTech, Université Gustave Eiffel, CNRS, Marne-la-Vallée, France

yalda.pedram@queensu.ca, yaoting.zhang@queensu.ca, sbriggs@nwmo.ca, cskim@nwmo.ca, laurent.brochard@enpc.fr, laurent.beland@queensu.ca

Keywords: montmorillonite, density functional theory, molecular dynamics simulations, multi-scale simulation, Cu^{2+} ions, ClayFF model

Abstract

Bentonite, primarily composed of sodium or calcium montmorillonite (Na- or Ca-MMT), is extensively used in geotechnical applications due to its high swelling capacity, ion exchange ability, and low permeability [1-3]. Understanding how various ions, such as Na^+, Ca^{2+}, and Cu^{2+}, interact with MMT is crucial for predicting the material's mechanical behavior under different environmental conditions, particularly in the context of deep geological repositories (DGR) for nuclear waste disposal. [4,5]

This research employs a comprehensive multi-scale simulation approach to investigate the effects of ion adsorption on the mechanical properties of bentonite, focusing on swelling pressure and future calculations of elastic properties. The study begins with Density Functional Theory (DFT) calculations to parametrize and validate an interatomic interaction force-field for Cu^{2+} in clay systems, extending the existing ClayFF model [6,7]. Following this, Molecular Dynamics (MD) simulations are performed to calculate interaction energies between MMT platelets containing different counter-ions (Na^+, Ca^{2+} and Cu^{2+}). These atomistic-level simulations provide detailed interaction profiles in the form of Potentials-of-Mean-Force (PMF) (Figure 1) and swelling pressure results (Figure 2).

To bridge the gap between atomistic and macroscopic scales, the PMF data derived from the MD simulations are integrated into a mesoscale model through Gaussian Process Regression (GPR). This integration enables the prediction of mechanical properties under various ionic conditions, offering insights into the influence of ion adsorption on the structural integrity and performance of bentonite.

The outcomes of this research contribute to a better understanding of the nano to macro link in geomaterials, emphasizing the importance of multi-scale approaches in predicting emergent properties of geomaterials. This study not only enhances predictive accuracy but also provides a framework for understanding the impact of ion adsorption and exchange on material behavior, which is crucial for the safe and efficient design of containment strategies in geotechnical engineering and nuclear waste disposal.

References

[1] Clem, A. G.; Doehler, R. W. Industrial applications of bentonite. Clays and Clay minerals 1961, 10, 272–283.

[2] Abootalebi, P.; Siemens, G. Thermal properties of engineered barriers for a Canadian deep geological repository. Canadian Geotechnical Journal 2018, 55, 759–776.

[3] Uddin, F. Clays, nanoclays, and montmorillonite minerals. Metallurgical and Materials Transactions A 2008, 39, 2804–2814.

[4] Sellin, P.; Leupin, O. X. The use of clay as an engineered barrier in radioactive-waste management–a review. Clays and Clay Minerals 2013, 61, 477–498.

[5] Grambow, B. Geological disposal of radioactive waste in clay. Elements 2016, 12, 239–245.

[6] Cygan, R. T.; Greathouse, J. A.; Kalinichev, A. G. Advances in clayff molecular simulation of layered and nanoporous materials and their aqueous interfaces. The

Journal of Physical Chemistry C 2021, 125, 17573–17589.

[7] Cygan, R. T.; Liang, J.-J.; Kalinichev, A. G. Molecular models of hydroxide, oxyhy-droxide, and clay phases and the development of a general force field. The Journal of Physical Chemistry B 2004, 108, 1255–1266.

Figures

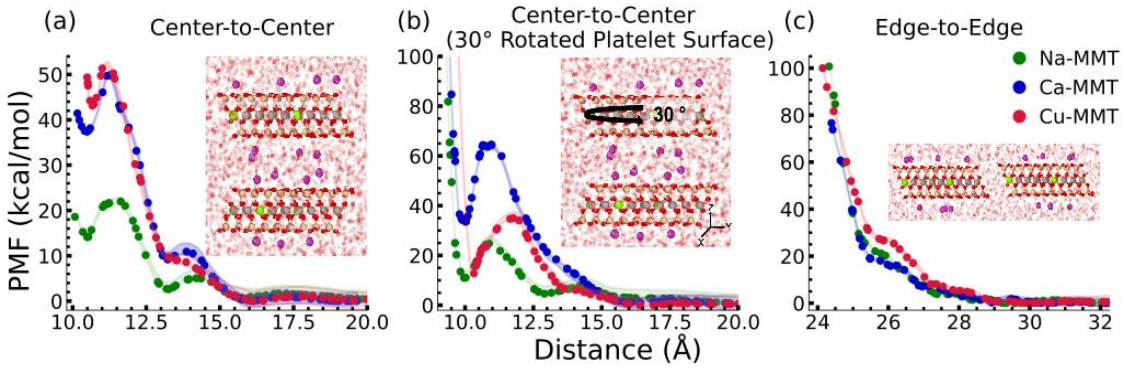

Figure 1: *Potentials of mean force (PMF) for (a) center-to-center, (b) rotated center-to-center, and (c) edge-to-edge interactions of Na-, Ca-, and Cu-MMT platelets.*

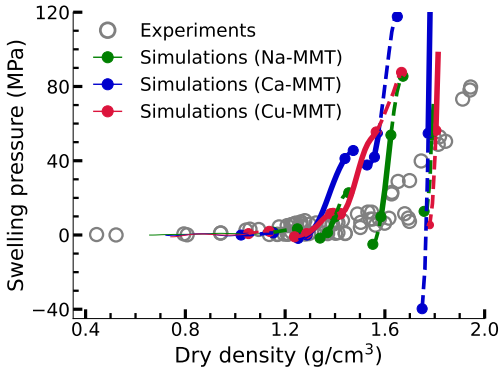

Figure 2: *Simulated versus experimental swelling pressures for Na-, Ca-, and Cu-MMT as a function of dry density, with stability regions indicated by line styles.*

Effective Management of Induced Seismicity for the Net Zero Energy Transition

Birhanmeskel Woldemichael[1*], Alexis Cartwright–Taylor[1,3], Elli-Maria Charalampidou[2], Nathaniel Forbes Inskip[1], Ian G. Main[3], Ian B. Butler[3], Maria-Daphne Mangriotis[4]

[1]Heriot-Watt University, School of Energy, Geoscience, Infrastructure and Society, Edinburgh, Scotland, UK

[2]Heriot-Watt University, Institute of Geoenergy Engineering, Edinburgh, Scotland, UK

[3]University of Edinburgh, School of Geosciences, Edinburgh, UK

[4]National Oceanography Center, Southampton, UK

[*]bhw3000@hw.ac.uk

Keywords: induced seismicity, faulting, rock deformation, subsurface activities, micromechanics

Abstract

Progress towards a net zero carbon economy involves subsurface activities such as geothermal energy production and geological storage of carbon dioxide (long-term) and hydrogen (short-term). These activities involve injection and extraction of fluids, which actively disturb tectonic stresses in the earth's crust. Subsurface ruptures, and associated seismicity, induced by such stress perturbations carry a risk of damage from ground motion, fluid leakage to the surface due to increased flow pathways, and potential loss of public confidence. Safe operation of these requires effective management to minimise induced seismicity.

Induced seismicity has risen significantly over the past decade due to the widespread hydraulic fracturing activities around the globe [1]. This increase has intensified the negative public perception of subsurface engineering activities. It has also led to increased research into optimal approaches for managing induced seismicity. Currently, induced seismicity is regulated using a 'traffic light' system based on the maximum magnitude of recorded seismic events. However, management of induced seismicity requires more advanced systems, such as that varying the injection protocol continuously instead of waiting for the thresholds when it may be too late [2,3].

To reduce the uncertainties involved in managing the risk of induced seismicity, understanding small scale processes such as the evolution of local strains and damage mechanisms in the approach to and during failure or fault reactivation is important to provide fundamental observations for informing process-based models that describe and forecast catastrophic phenomenon. In this project, rock deformation and fluid injection experiments are being conducted to understand how micro-seismicity and rock microstructure evolve during conventional rock deformation and during fault reactivation under fluid injection.

We present here preliminary results from analysis of x-ray volumes tracking the micro-mechanisms involved in conventional rock deformation. These samples were triaxially compressed using an x-ray transparent rock deformation apparatus with integrated mechanical and acoustic monitoring (Fig.1a) [4] that allowed us to capture time-resolved x-ray microtomographic volumes of shear failure by adjusting the loading rate using feedback from detected acoustic emissions (AE) to maintain a constant AE event rate. We used the open-source software spam to calculate the 3D strain fields [5]. We show the evolution of local 3D strain fields in Berea sandstone samples deformed under a constant

micro-cracking rate (Fig.1b and c). In the first case, the maximum principal stress is varied while in the latter case the minimum principal stress is varied.

The results in Figure 1b and c; provide the evolution of differential stress and AE event rate during deformation of the sample. Using AE event rate feedback prolonged the failure time, providing a comprehensive view of how damage and related micro-seismic events develop. These tests and preliminary results will further inform the acquisition and analysis of planned experimental campaigns involving x-ray and seismicity acquisitions, exploring several deformation and injection scenarios.

References

1. Moein et al., (2023). The physical mechanisms of induced earthquakes, Nature Reviews Earth & Environment, 4, 847–863.
2. Kwiatek et al., (2019). Controlling fluid-induced seismicity during a 6.1-km-deep geothermal stimulation in Finland, Science Advances, 5: eaav7224.
3. Mangriotis et al. (in review). Loading of a porous rock with constant micro-seismic event rate suppresses seismicity and promotes subcritical failure, https://doi.org/10.21203/rs.3.rs-3054375/v1
4. Cartwright-Taylor et al., (2022). Seismic events miss important kinematically governed grain scale mechanisms during shear failure of porous, Nature Communications, 13:6169.
5. Stamati et al., (2020). spam : Software for Practical Analysis of Materials. Journal of Open Source Software, 5(51), 2286.

Figures

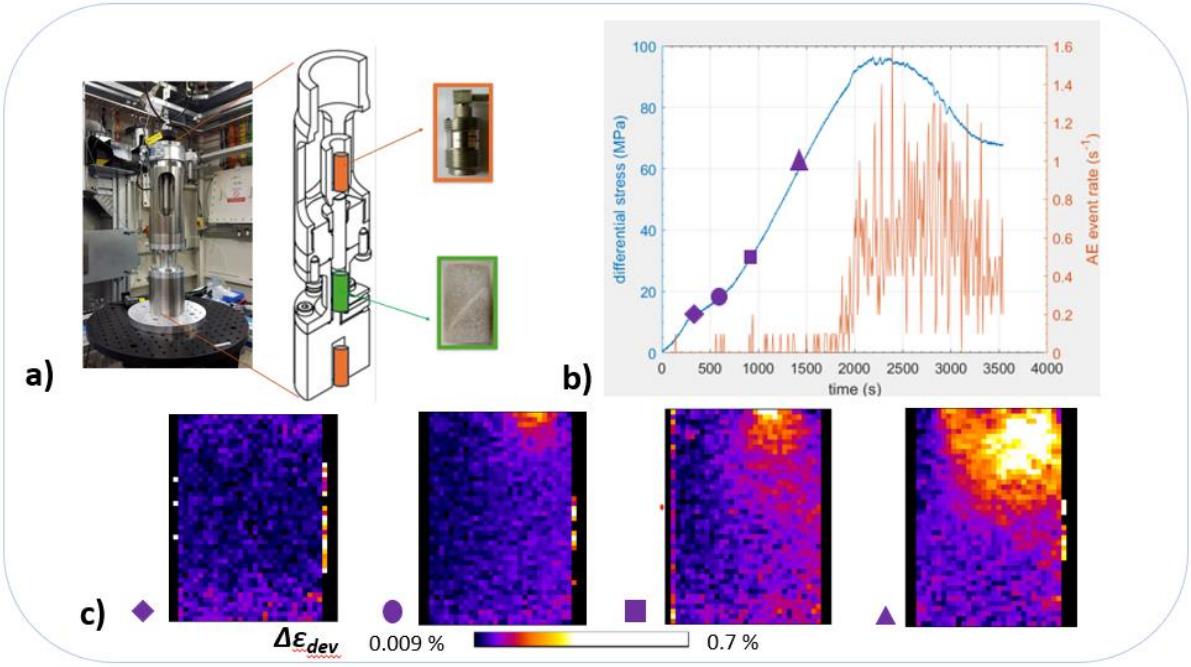

Figure 1: *a) X-ray transparent rock deformation cell, Stór Mjölnir, with AE monitoring [4] b) Stress and acoustic emission event rate evolution over time c) Example showing slices of incremental deviatoric strain in the sample highlighting localisation of strain in the top part of the sample, early loading at four-specific times – see purple in (b).*

The Effective Fracture Energy of Shear Frictionless Cracks

Serafim Egorov, Jean Sulem, Mathias Lebihain

Laboratoire Navier, France

Serafim.Egorov@enpc.fr

Keywords: three-dimensional fracture, perturbation approaches, shear frictionless cracks, effective fracture energy

Abstract

The effective fracture energy of perfectly brittle materials has been extensively studied using the perturbation approach of linear elastic fracture mechanics initiated by Rice [1]. Most of these studies have been conducted for semi-infinite cracks propagating in tensile mode I [2,3]. Yet, cracks are often of finite size, and they can be loaded in mixed (tensile and shear) modes. A profound understanding of the impact of mode mixity and size effects on material toughening by heterogeneities of fracture energy remains up to now elusive.

In this work, we propose a numerical implementation of the energetic variational framework of Francfort and Marigo [4], building on the perturbation theory of Rice. Unlike previous approaches based on a viscous regularization of Griffith's criterion, our method is based on asymptotic estimates of the potential energy of the system. It allows to swiftly compute the successive equilibrium positions of the crack front, by minimizing the sum of the perturbed potential energy, and a dissipated energy, set by the heterogeneous fracture energy field.

Using this novel method, we show how the coupling between shear modes II+III due to non-zero Poisson's ratio impacts the front deformations and ultimately the effective fracture energy. Building on the results of 36,000 Monte Carlo simulations of shear crack propagation in disordered brittle media, we establish a connection between material toughening and disorder intensity. We also emphasize the size effects that emerge from the finite crack size relative to the scale of the heterogeneities.

References

[1] Rice, J., 1985. Journal of Applied Mechanics 52, 571–579. doi:10.1115/1.3169103

[2] Patinet, S., Vandembroucq, D., Roux, S., 2013. Physical Review Letters 110, 165507. doi:10.1103/PhysRevLett.110.165507

[3] Démery, V., Rosso, A., Ponson, L., 2014. Europhysics Letters 105, 34003. doi:10.1209/0295-5075/105/34003

[4] Francfort, G.A., Marigo, J.J., 1998. Journal of the Mechanics and Physics of Solids 46, 1319–1342. doi:10.1016/S0022-5096(98)00034-9

Figures

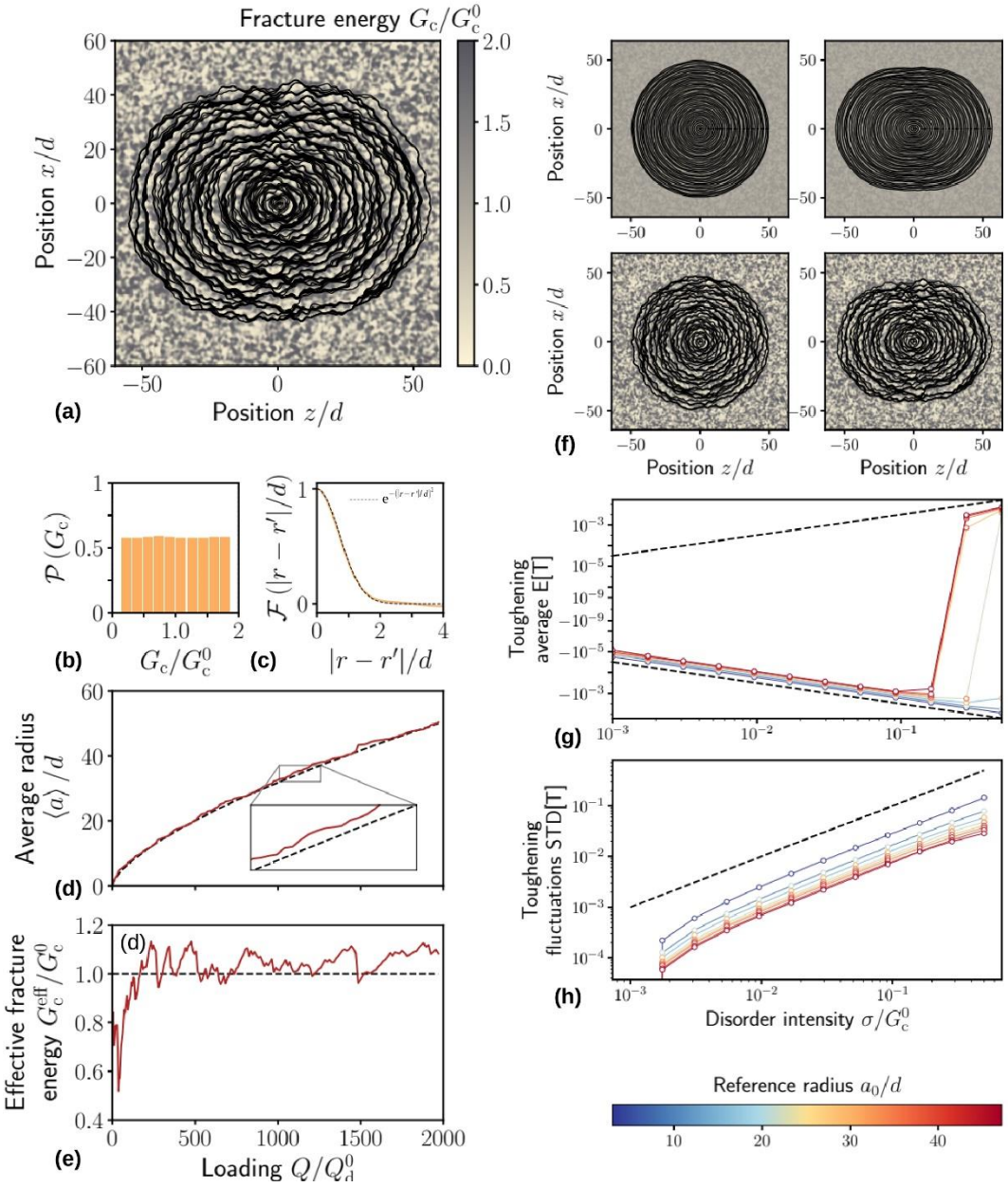

Figure 1: *a) The reference penny-shaped crack in a disordered toughness field, with a circular front of unit radius, propagates within its plane under the action of a pair of normalized shear forces applied with a constant load increment at the crack center. b) The probability density function for the fracture energy is considered within its minimum and maximum values. c) The spatial correlation of the fracture energy field at a characteristic heterogeneity scale. d) The normalized average radius fluctuates around its reference value, corresponding to a uniform toughness field. e) The effective fracture energy required to propagate the crack is estimated for a given loading condition. f) On the left side, Poisson's coefficient is set to zero; on the right side, it is set to 0.2. The top corresponds to a disorder intensity of 0.1, while the bottom corresponds to intensity of 0.5. g) The average toughening depends on both the disorder intensity and the average radius of the crack front position. h) The standard deviation of the toughening depends on the disorder intensity and the average radius of the crack front position.*

Numerical Investigations of Chemical Damage-Healing in Geomaterials at the Microstructural Level

Alexandre Sac-Morane[1,2], Hadrien Rattez[1], Manolis Veveakis[2]

[1]UCLouvain, Louvain-la-Neuve, Belgium

[2]Duke University, Durham, NC, USA

alexandre.sacmorane@duke.edu

Keywords: chemo-mechanical couplings, phase-field, Discrete Element Method debonding, pressure-solution

Abstract

The intricate interplay between chemical and mechanical processes in soil and rocks has emerged as a key factor to consider for numerous engineering applications including underground storage and geothermal energy, as well as for understanding geological processes such as diagenesis or earthquake nucleation. These reactions result in mineral dissolution (chemical damage) or to precipitation (chemical healing), which can modify the different properties of the material. The coupling between mechanics and chemistry has been investigated at the microstructural level considering two different mechanisms: the debonding and the pressure-solution.

The mechanical behavior and rupture of geomaterials are significantly influenced by dissolution (chemical damage) phenomena. In the case of cemented rocks, debonding can occur during weathering and strongly weakens the material. Furthermore, this strength degradation has been observed in oedometric tests conducted on granular materials presenting no cohesion. A new campaign of Discrete Element Modelization (DEM) simulations has been performed to investigate the effect of the debonding on the mechanical properties of the rock in different contexts. The simulations consider a cohesive granular sample under oedometric conditions, while the bonds are dissolved by an acid injection. The DEM allows for straightforward control of numerous parameters, including the initial value of the lateral earth pressure coefficient k_0 $\left(= \frac{lateral\ stress}{vertical\ stress}\right)$ or the weakening law of the cementation. For example, the influence of the degree of cementation, the initial state of stresses, the confining pressure or the history of the loading has been highlighted. It appears that the sample aims to reach an attractor configuration with the chemical damage. This evolution of the mechanical properties can result in a modification of the stress state during the injection of a reactive fluid, which may in turn lead to induced seismicity.

Pressure-solution plays a pivotal role in a number of geological processes, including the nucleation and recurrence of earthquakes, as well as diagenetic processes. It involves three chemo-mechanical processes at the micro-scale: dissolution due to stress concentration at grain contacts, diffusive transport of dissolved mass from the contact to the pore space, and precipitation of the solute on the less stressed surface of the grains. These processes result in a time-dependent compaction of the rock by changing its microstructure, pore structure and composition. Furthermore, it induces a modification of the strength of a wide range of geological materials. A new coupling between a Phase-Field (PF) method and a Discrete Element Modelization (PFDEM) has recently been developed to investigate this phenomenon. The grains are modeled in DEM as polygonal (2D)/polyhedral (3D) particles, in order to

accurately capture their complex shapes, which significantly influence the macroscopic mechanical behavior of the material. Considering the granular material as a phase, PF is a good candidate to model with physics-based laws an addition or reduction of the quantity of material locally. The dissolution/precipitation is controlled by the introduction of mechanical and chemical energy into the Allen-Cahn formulation on the phase variables. Meanwhile, the diffusion and mass conservation are verified by a coupled diffusion formulation on the solute concentration. This method has been applied to reproduce results from previous works on the pressure-solution phenomenon at several grains level. This new framework enables us to model chemo-mechanical couplings, taking into account the true shape of the grain. It is used to investigate the influence of the different physical phenomena (dissolution, precipitation or diffusion) controlling the rate of material compaction and of the macro properties evolutions, as the porosity, permeability or strength.

References

Sac-Morane, A., Veveakis, M., and Rattez, H. (2024) A Phase-Feld Discrete Element Method to study chemo-mechanical coupling in granular materials, Comput. Methods in Appl. Mech. and Eng., 424, 116900

Sac-Morane, A., Rattez, H., and Veveakis, M. Stress state evolution of a cemented granular material subjected to bond dissolution by Discrete Element Modeling, under review in Geomech. for Energy and the Env.

Figures

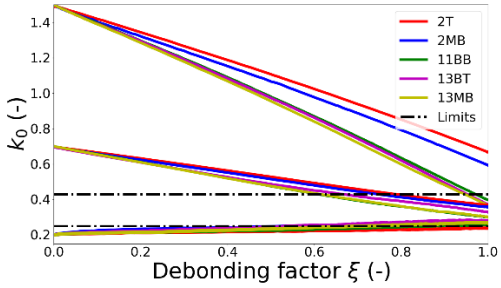

Figure 1: *Evolution of k_0 with the debonding factor (=0 when the bonds are intact and = 1 when all the bond are broken) for different cementation levels and initial state of stress at $P_{confinement}$ = 1 MPa.*

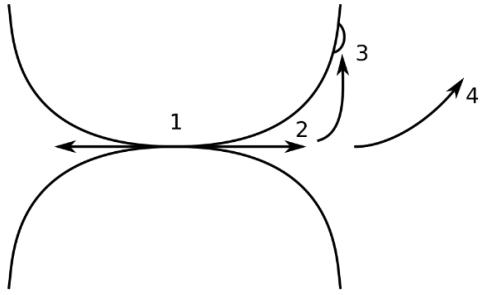

1 Dissolution on the contact
2 Diffusion out of the contact
3 Precipitation on the pore surface
4 Diffusion to other pores

Figure 2: *Pressure-solution is a complex phenomenon divided in three processes: dissolution due to stress concentration (chemical damage), diffusive transport of dissolved mass, and precipitation on the less stressed surface (chemical healing).*

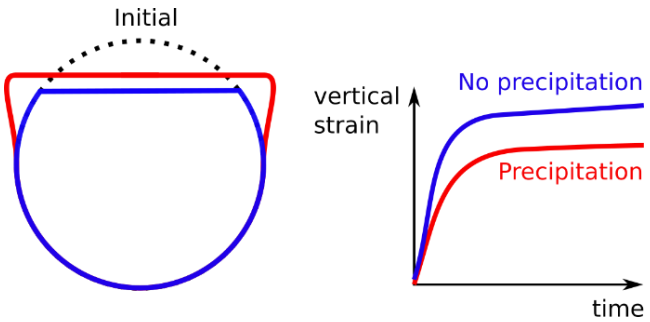

Figure 3: *Influence of the precipitation in pressure-solution at the level of an individual grain. It induces an increase of the contact surface (left), decreasing the pressure transmitted at the contact (motor of the phenomenon). A slowdown of the creep behavior occurs*

Stiffness of Weathered Limestone: From Laboratory Data to In-Situ Measurements Beneath Wind Turbine Foundations

Carlos Peña, Sabine Gehring, Hans Henning Stutz

Karlsruhe Institute of Technology, Institute for soil and rock mechanics

carlos.pinto@kit.edu, sabine.gehring@kit.edu, hans.stutz@kit.edu

Keywords: dynamic and static stiffness, wind turbine foundation, limestone deformation, in-situ instrumentation, finite elements simulation

Abstract

Understanding the mechanical behavior of the foundation zone is pivotal for the design and stability of shallow foundations, particularly in the context of dynamic loaded structures like wind turbines. This study aims to provide an approach into the stress-strain characteristics of weathered limestone through a multi-method that combines laboratory experiments such as axial compression and ultrasonic tests with in-situ measurements and numerical simulation.

The research test field WINSENT was implemented close to Stötten, in the southern part of Germany, within the Albtrauf region. This project offers the unique opportunity to monitor the mechanical behavior of the foundations of two in service onshore wind turbines located in complex terrain conditions by means of extensometers and pressure cells. These instruments were configured in such a way that the elastic and possibly inelastic behavior of the material can be captured. On the other hand, during the investigation phase, core samples from the weathered limestone were collected and consequently uniaxial compression and ultrasonic tests were carried out. They revealed the static stiffness for deformation order of 10^{-3} and the so-called dynamic stiffness within strains below 10^{-5}, respectively.

In order to assess the accuracy of the deformation parameters coming from the laboratory tests, a finite element simulation representing the 3D topography will be carried out and the respective results will be compared with the values of stress and displacement coming from the in-situ instrumentation measurements. For this approach the rock mass quality is also considered to integrate the effects of discontinuities in field. It should be validated if the range of deformations remains in the elastic zone and if the deformation parameters are between the two hypothetic extremes, namely between the dynamic stiffness and the elastic modulus from the uniaxial test reduced by the action of discontinuities. The constitutive model for the simulation will begin as a linear elastic one and, according to the results of the comparison, it can be refined to represent the actual conditions beneath the wind turbines foundations, for example including the effects of a strain accumulation due to the cyclic loading.

The integrated approach of combining laboratory tests with field measurements and numerical modelling can offer a comprehensive understanding of the mechanical response of weathered limestone and a validation of the way the corresponding parameters are acquired and implemented, aimed to improve the reliability of foundation designs in similar geotechnical settings.

References

Davarpanah, S.M., Ván, P. & Vásárhelyi, B. (2020). Investigation of the relationship between dynamic and static deformation moduli of rocks. Geomechanics and Geophysics for Geo-energy and Geo-resources.

Quast A. (2010). Zur Baugrundsteifigkeit bei der gesamtdynamischen Berechnung von Windenergieanlagen. Heft 69. Institut für Grundbau, Bodenmechanik und Energiewasserbau (IGBE) Leibniz Universität Hannover.

Zhang L. (2016). Determination and applications of rock quality designation (RQD). Journal of Rock Mechanics and Geotechnical Engineering.Casini, F., Vaunat, J., Romero, E., & Desideri, A. (2012). Consequences on water retention properties of double-porosity features in a compacted silt. Acta Geotechnica, 7, 139-150.

Figures

Figure 1: *General location of the WINSENT test field.*

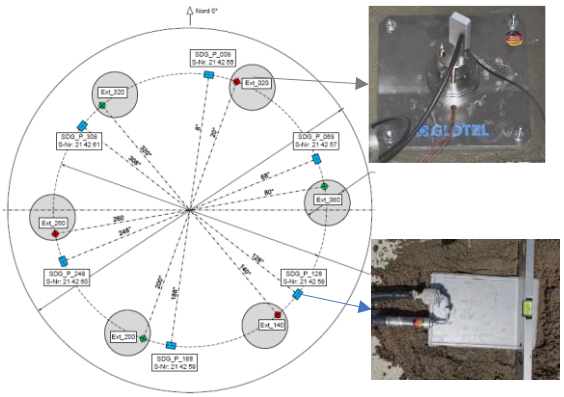

Figure 2: *Top view of a fundament with the layout and example of extensometers and cell pressures.*

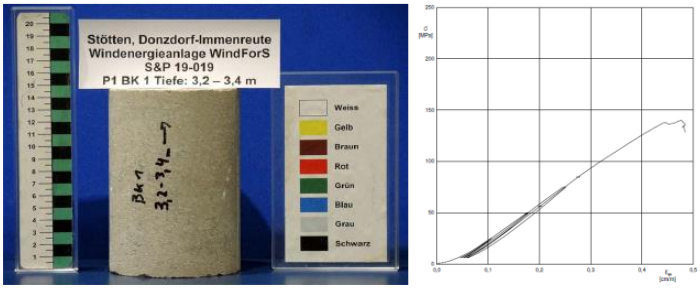

Figure 3: *Uniaxial test performed in the laboratory.*

Sustainable Repurposing of Reiche Zeche Mine for Geothermal Energy and Water Storage: A Geomechanical and Hydrological Approach

Ali Ahmadi, Tomiwa Aderemi, Eleni Gerolymatou, Elli-Maria Charalampidou

Clausthal University of Technology, Heriot-Watt University

Ali.Ahmadi@tu-clausthal.de, aa2142@hw.ac.uk, Eleni.Gerolymatou@tu-clausthal.de, E.Charalampidou@hw.ac.uk

Keywords: Geothermal Energy, Water Reservoirs, Geomechanical Simulations, Sustainable Mining, Renewable Energy, Resource Management, Structural Integrity, Hydrological Analysis, Mine Repurposing, Flac3D, Python

Abstract

The historic Reiche Zeche mine, transformed into a sophisticated research and teaching facility, offers a novel arena for addressing the dual challenges of sustainable energy production and efficient water management. This project investigates the feasibility of repurposing the mine for geothermal energy extraction and as a subterranean water reservoir. Utilizing state-of-the-art geomechanical simulations through Flac3D and detailed data analyses via Python, our research aims to thoroughly assess the structural integrity and adaptability of the mine to these new roles. The collaborative effort, involving experts from Clausthal University of Technology and Heriot-Watt University, integrates extensive point cloud data and historical mining records to construct accurate geomechanical models of the mine.

These models simulate various operational scenarios to predict the mine's behavior under different geothermal and hydrological loads, providing essential insights into its capacity for energy and water storage. Key objectives include evaluating the mine's structural robustness to withstand the operational demands of geothermal heating and water storage, analyzing its hydraulic and thermal properties to ascertain the feasibility of these applications, and developing predictive models that can optimize operational strategies to maximize efficiency and minimize environmental impact.

The outcomes of this project are expected to contribute significantly to the fields of renewable energy and resource management, offering a template for the sustainable conversion of similar infrastructures globally. This research not only seeks to demonstrate the practical capabilities of the Reiche Zeche mine in supporting sustainable energy and water storage solutions but also aims to set a precedent for the repurposing of decommissioned mines worldwide.

Acknowledgment

This research has been supported by the Lower Saxony – Scotland Tandem Fellowship Programme through the European Centre for Advanced Studies (ECAS). We express our sincere gratitude for their financial support and commitment to enhancing collaborative research efforts.

References

Fraser-Harris, A., McDermott, C. I., Receveur, M., Mouli-Castillo, J., Todd, F., Cartwright-Taylor, A., . . . Parsons, M. (2022). The Geobattery Concept: A Geothermal Circular Heat Network for the Sustainable Development of Near Surface Low Enthalpy Geothermal Energy to Decarbonise Heating. Earth Science, Systems and Society, 2. doi:10.3389/esss.2022.10047.

Mischo, H., Barakos, G., Szkliniarz, K., & Kisiel, J. (2021, December 15). Site Description and Data of the Reiche Zeche. Retrieved from https://www.bsuin.eu/wp-content/uploads/2022/02/A3.3_report_Site-Description-Reiche-Zeche_final.pdf.

Monaghan, A. A., Starcher, V., Barron, H. F., Shorter, K., Walker-Verkuil, K., Elsome, J., Callaghan, E. (2022, February). Drilling into mines for heat: geological synthesis of the UK Geoenergy Observatory in Glasgow and implications for mine water heat resources. Quarterly Journal of Engineering Geology and Hydrogeology, 55(1). doi:10.1144/qjegh2021-033.

Figures

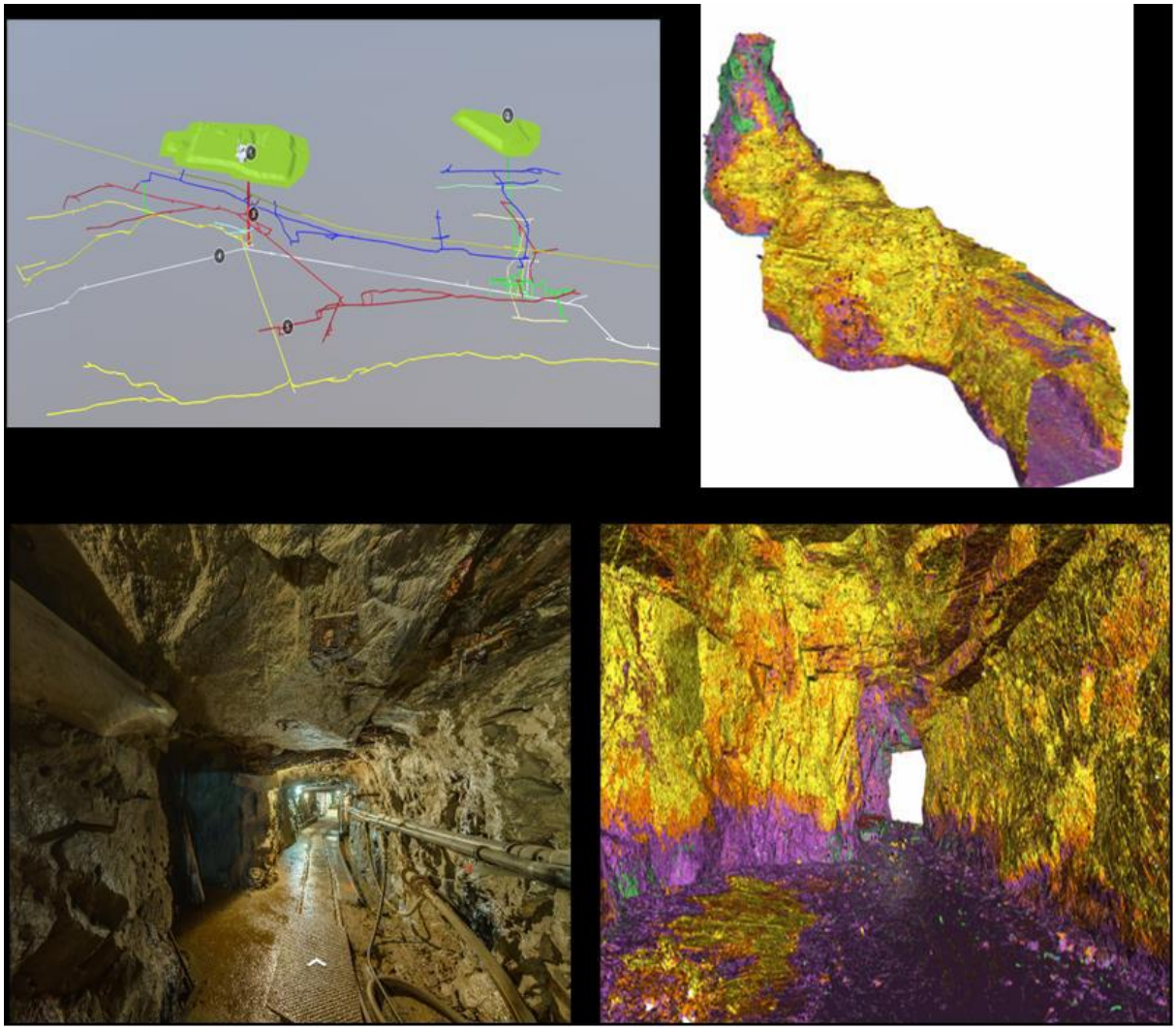

Figure 1: *Top left: 3D Sketchfab model of the Reiche Zeche underground mine network. Top right: An internal view through the front of the point cloud 3D image. Bottom right: a view inside the "Querschlag Ost" tunnelling site. bottom left: Image extracted from the 360 0 virtual reality tour.*

Reinforcement Learning-Based Adaptive Time-Integration for Nonsmooth Dynamics

David Riley, Alexandros Stathos, Diego Gutierrez-Oribio, Ioannis Stefanou

Nantes Universite, Ecole Centrale Nantes, CNRS,GeM, UMR 6183, F-44000, Nantes, France

david.riley@ec-nantes.fr

Keywords: reinforcement learning, time-integration, frictions

Abstract

The numerical time integration of models is fundamental to the simulation of constitutive models and boundary value problems. Traditionally, time integration schemes require adaptive time-stepping to ensure sufficient accuracy. Although these methods are based on mathematical derivations related to the order of accuracy for the chosen integrator, they also rely on heuristic development to determine optimal time steps [1].

In this work we use an alternative approach based on Reinforcement Learning (RL) to select the optimal time step for any time integrator method, balancing computational speed and accuracy. To explore the potential of our RL-based adaptive time-stepping approach, we choose a challenging model problem involving frictional instabilities at various spatiotemporal scales. This problem demonstrates the robustness of our approach in handling nonsmooth problems, which represent a potential worst-case scenario for numerical integration. Specifically, we apply RL to the simulation of a strike-slip fault where friction is governed by Coulomb friction. Our findings indicate that RL can learn an optimal strategy for the time integration of nonsmooth problems as displayed in Figure 1. Our RL-based adaptive integrator offers a new approach for time integration in various other nonsmooth problems in geomechanics.

References

[1] Söderlind, G., & Wang, L. (2006). Adaptive time-stepping and computational stability. *Journal of Computational and Applied Mathematics*, *185*(2), 225-243.

Figures

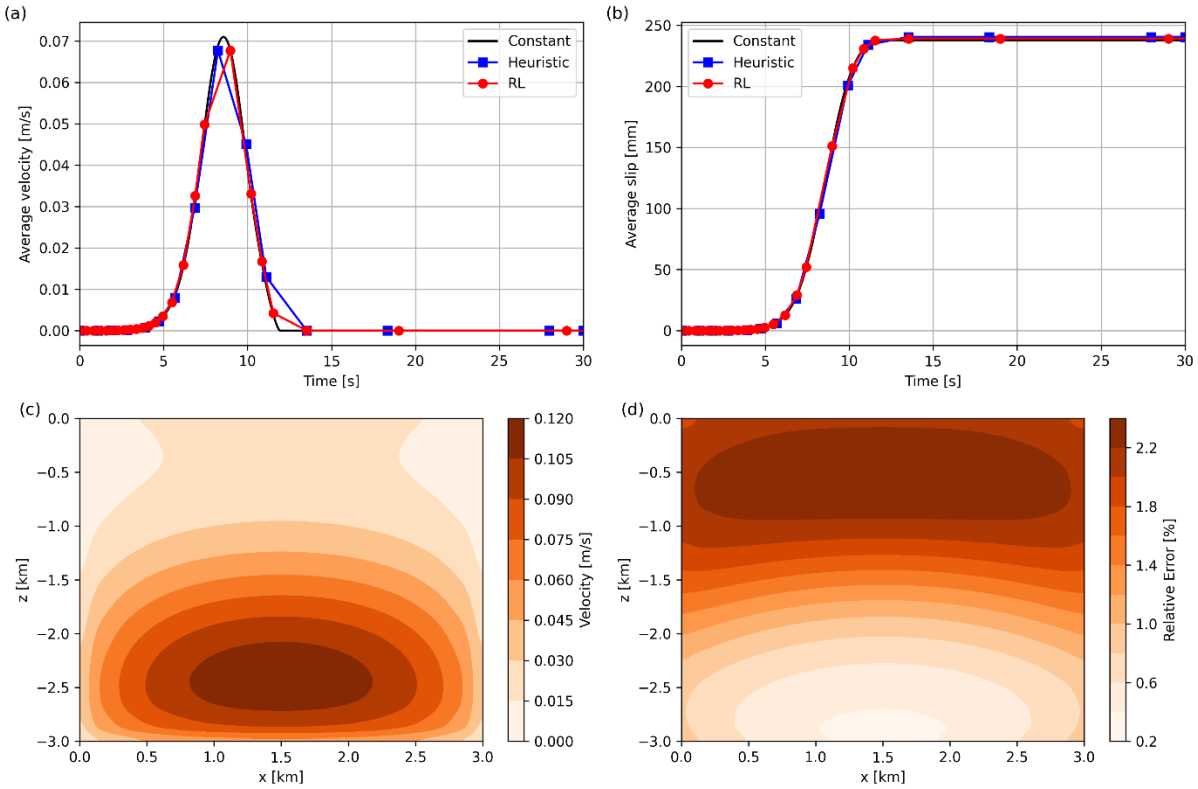

Figure 1: *Results demonstrating the accuracy of the RL-based adaptive time-stepping approach for an evaluation simulation of a frictional instability that was not included in the RL training set. (a) Average velocity over time for three integration methods: a constant time step integrator with h = .001 s, heuristic adaptive time integrator, and RL-based adaptive time integrator. (b) Average slip in time for the three integrators. (c) Velocity distribution along the strike-slip fault at time 8.6 s using the RL-based integrator. (d) Relative error distribution along the strike-slip fault at time 8.6 s between the RL-based integration and constant time step integration.*

On The Automated Calibration of Elastoplasticity Constitutive Model: The Hardening Soil

Phuong C. Do, Tomáš Kadlíček, David Mašín, Jan Najser

Institute of Hydrogeology, Engineering Geology and Applied Geophysics,
Charles University, Czech Republic

dophu@natur.cuni.cz

Keywords: hardening soil model, calibration, ExCalibre

Abstract

Over the decades, researchers have been dedicated to predict soil behaviour under various boundary conditions and developing new advanced constitutive theories. The common goal of these theories is to produce a mathematical relationship between stress and strain components to reliably reproduce experimental data and thus well estimate response and stiffness of soil. Consequently, less conservative and more efficient designs were produced. These theories range widely from the elasticity to the elastoplasticity, which were initially derived from the yielding of metals, to the comprehensive constitutive models based of the critical state soil mechanics such as the hypoplasticity. Among these models, the Hardening Soil Model (HSM) (by Schanz et al. 2000) is one of the most popular constitutive models used by practical engineers. The model is originally developed by Schanz (Schanz, 1998; Schanz et al., 2000) based on the Double Hardening model derived by Vermeer (1978). It has been shown to provide accurate results when applied to a variety of geotechnical problems, while maintaining the input parameters of the well-established constitutive models such as Mohr-Coulomb. It is still a challenge for engineers to calibrate the HSM even though the most of its parameters hold clear physical meaning and can be determined based on basic laboratory experiments. Aiming to develop a reliable and accessible tool for scientists and engineers alike to calibrate the HSM, the authors have integrated the Hardening Soil Model into ExCalibre (Kadlicek et al., 2022a, 2022b). ExCalibre requires input of laboratory data in the form of the Excel file which contains a combination of compression and shear tests results. Templates of these input files are available on ExCalibre website. The uploaded input files are stored (by the software license agreement) for further research purposes.

In this paper, the HSM is modified by adding the Matsuoka-Nakai yielding criterion (which is defined as the limiting ratio of the average normal stress to average shear stress in the Spatial Mobilised Plane and whose outline was derived with the Mohr-Coulomb criterion) to smoothen the shear surface, together with adjusting from minor stress to mean stress dependent law for calculation of stiffness. Calibration of this model requires some modifications, especially with stiffness-related parameters. ExCalibredetermines the Mohr-Coulomb strength parameters φ_p, φ_{cs}, C and the dilatancy ψ from the triaxial data first. Later, the stiffness parameter E_{oed}^{ref}, E_{ur}^{ref}, E_{50}^{ref} and power coefficient m_p, and finally, the failure ratio R_f is evaluated. To obtain the best set of parameters, ExCalibre then optimizes selected parameters E_{50}, R_f, m_p and the dilatancy ψ together with the internal parameters $M^*$and H^*.

Calibration results of the Dobrany sand and Dortmund clay are presented. Fig. 1 illustrates the simulation of three drained triaxial and one oedometer test for the Dobrany sand. Maximum deviatoric stresses reached are slightly lower than those presented by the experiment data. Furthermore, ExCalibre provides a stiffer response than observed in data, see Fig.1a. The dilative effect and dilatancy cut-off are shown in Fig.1b. A notable discrepancy between the simulation and the oedometer data can be observed in Fig.1c.

Although the peak states are well captured the maximum deviatoric stress was not possible to reach in all cases even with increased dilatancy ψ, see Fig.2a, Fig.2b. Similarly to the previously presented simulations of the sand specimens, the stiffer response can be observed in the $q \times \varepsilon_a$ space in Fig.2a which is a result of compromises reached when calibrating both compression and triaxial shear tests simultaneously. This compromise results in a softer response of the oedometer tests in Fig.2c.

References

Kadlíček, T., Janda, T., Šejnoha, M., Mašín, D., Najser, N., Beneš, Š.: Automated calibration of advanced soil constitutive models. Part I: Hypoplastic Sand. Acta Geotechnica 17, 3421–3438 (2022a).

Kadlíček, T., Janda, T., Šejnoha, M., Mašín, D., Najser, N., Beneš, Š.: Automated calibration of advanced soil constitutive models. Part II: Hypoplastic clay and modified Cam-Clay. Acta Geotechnica 17, 3439–3462 (2022b).

Schanz, T.: Zur Modellierung des mechanischen Verhaltens von Reibungsmaterialien. Mitt. Inst. für Geotechnik 45. University of Stuttgart, Stuttgart, Germany (1998).

Schanz, T., Vermeer, P. A., Bonnier, P. G.: The Hardening Soil Model: Formulation and Verification. In: Editor, F., Editor, S. (eds.) Beyond 2000 in Computational Geotechnics, pp. 281–290. Balkema, Rotterdam (2000).

Vermeer, P. A.: A double hardening model for sand. Géotechnique 28(4), 413–433 (1978).

Figures

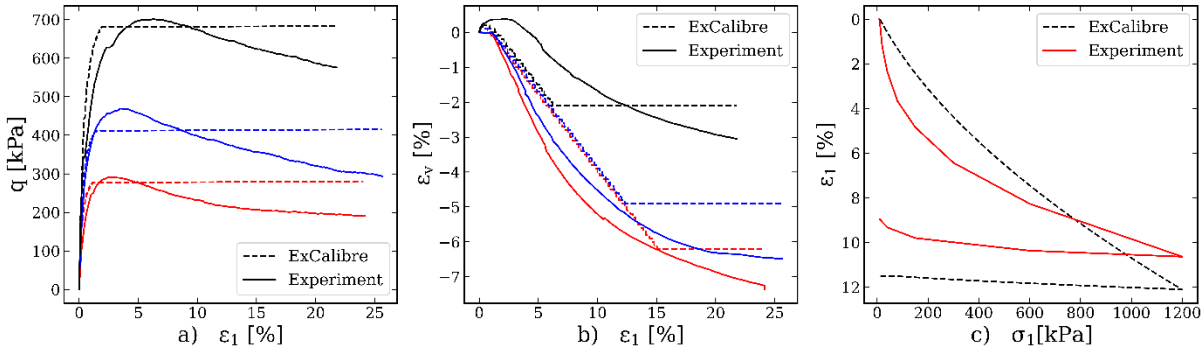

Figure 1: *Simulation for the Dobrany specimen. a) CID test in $q \times \varepsilon_1$ space; b) CID test in $\varepsilon_v \times \varepsilon_1$ space; c) OED test in $\varepsilon_1 \times \sigma_1$ space.*

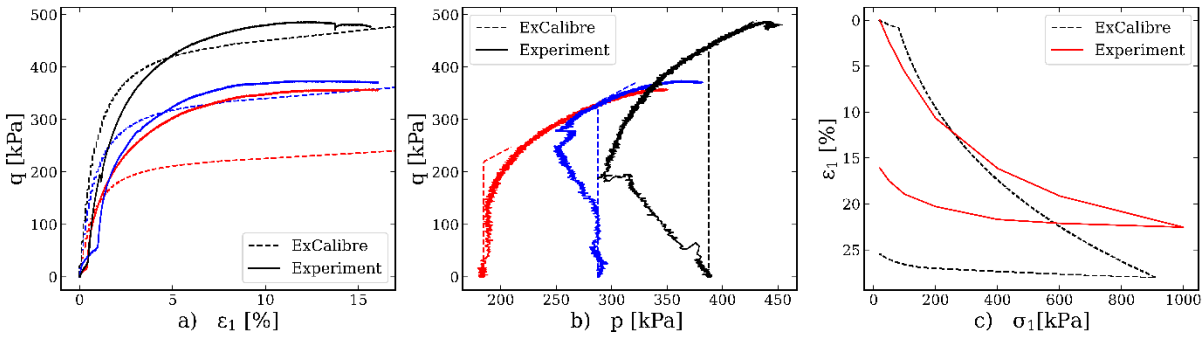

Figure 2: *Simulation for the Dortmund clay specimen. a) CIUP test in $q \times \varepsilon_1$ space; b) CIUP test in $p - q$ space; c) OED test in $\varepsilon_1 \times \sigma_1$ space.*

Compressibility Characteristics of Malaysian Kaolin Considering Different Thermo-Hydro-Mechanical Conditions

Rodrigo Polo-Mendoza, David Mašín, Jan Najser, Jakub Roháč, Jose Duque

Faculty of Science, Charles University, Prague, Czech Republic

polomenr@natur.cuni.cz, david.masin@natur.cuni.cz, jan.najser@natur.cuni.cz, jakub.rohac@natur.cuni.cz, duquefej@natur.cuni.cz

Keywords: constant rate of strain, cyclic loading, experiments, thermal effects, unsaturated soils

Abstract

The implementation of Thermo-Hydro-Mechanical (THM) constitutive models is necessary to reproduce the soil behaviour under mechanical cyclic loading coupled with temperature oscillations and changes in the degree of saturation [1]. This advanced modelling approach is essential to analyze and design geotechnical structures for high-priority applications, e.g., buried high-voltage cables, deep geological carbon sequestration systems, energy piles, nuclear waste disposal facilities, and perpetual pavements [2]. Thus, it is worth noting that developing experimental protocols to calibrate the THM models is a fundamental previous step in achieving proper numerical simulations [3]. In this regard, this research aims to perform an extensive laboratory program on the mechanical response of Malaysian kaolin (i.e., a material that seeks to represent a typical fine-grained soil) subjected to a one-dimensional constant rate of strain loading.

This experimental protocol comprises two main parts: (i) suction-controlled oedometer tests and (ii) temperature-controlled oedometer tests. On the one hand, four matric suction targets are considered, namely 0, 500, 1000, and 1500 kPa. These matric suction values were achieved by applying the axis-translation technique; specifically, a constant pore water pressure of 500 kPa was used for all suction-controlled tests, and only the pore air pressures were varied accordingly. On the other hand, four temperatures are evaluated for the thermal tests, namely 20, 50, 70, and 90 °C. For all tests, the same four-stage loading-unloading sequence is executed: (i) loading from 20 to 200 kPa, (ii) unloading from 200 to 20 kPa, (iii) loading from 20 to 2000 kPa, and (iv) unloading from 2000 to 20 kPa. It is important to highlight that these tests are strain-controlled experiments on compacted samples, maintaining a strain rate of 0.1 %/min for all the loading-unloading stages.

Figure 1 and Figure 2 show the results from the experimental program for suction-controlled and temperature-controlled oedometer tests, respectively. From these graphs, it is possible to draw the following findings: (i) the soil exhibits less compressibility at more elevated matric suction values; (ii) the differences in the mechanical response of the soil are less noticeable at higher levels of matric suction (i.e., 1000 and 1500 kPa); (iii) as the temperature increases, the soil behaves more deformable; and (iv) the influence of temperature is highly pronounced when employing the room temperature (i.e., 20 °C) as benchmark, but is attenuated when comparing higher temperatures with each other (i.e., 50, 70, and 90 °C).

As the central outcome, this experimental protocol not only validates the impact of temperature and suction on the mechanical properties of fine-grained soils but also smooths the path for its potential application in future research lines. It is anticipated that this protocol will serve as a valuable tool for calibrating THM constitutive models in the context of geotechnical analysis.

Acknowledgements

This research was supported by the Johannes Amos Comenius Programme (P JAC), project No. CZ.02.01.01/00/22_008/0004605, Natural and anthropogenic georisks.

References

[1] M. Pico and D. Mašín, "Coupled thermo-hydro-mechanical hypoplastic model for partially saturated fine-grained soils under monotonic and cyclic loading," *Comput. Geotech.*, vol. 172, no. 106447, pp. 1–19, 2024.

[2] D. Mašín, *Modelling of Soil Behaviour with Hypoplasticity: Another Approach to Soil Constitutive Modelling*. Cham, Switzerland: Springer Series in Geomechanics and Geoengineering, 2019.

[3] M. Pico, D. Mašín, and W. Fuentes, "Coupled hydro-mechanical hypoplastic model for partially saturated soils under monotonic and cyclic loading," *Acta Geotech.*, pp. 1–25, 2024.

Figures

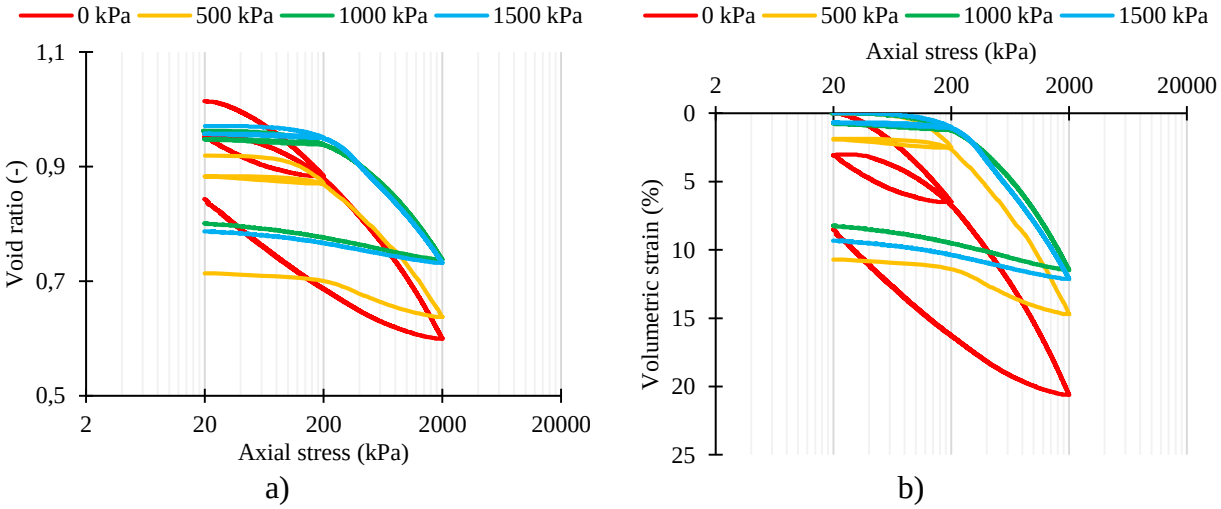

Figure 1. *Experimental results of suction-controlled oedometer tests. a) void ratio; b) volumetric strain.*

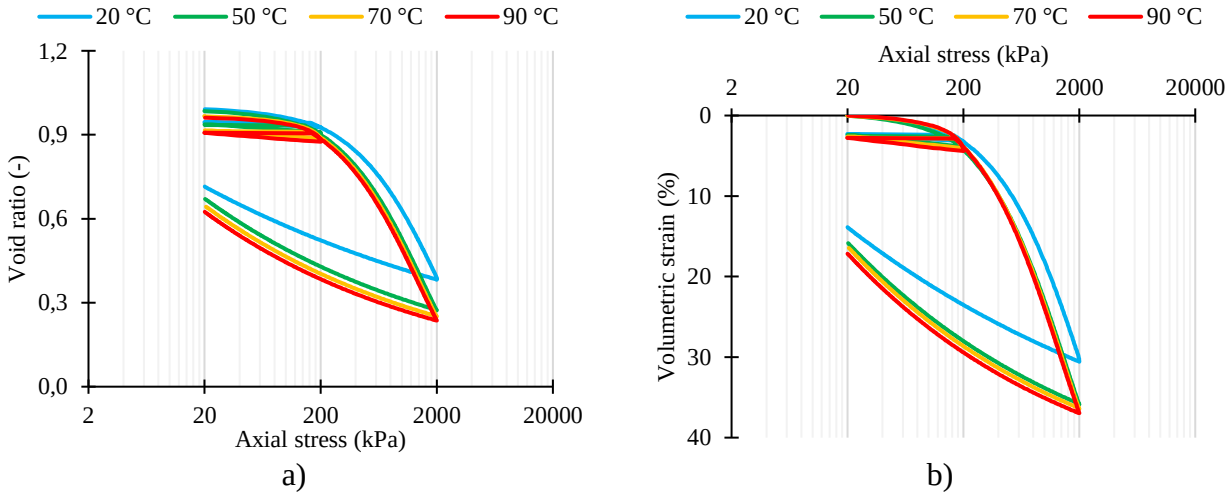

Figure 2. *Experimental results of temperature-controlled oedometer tests. a) void ratio; b) volumetric strain.*

Experimental Investigation of the Influence of Soil Plasticity on Compression and Creep Behaviour of Clayey Soils

Manh Nguyen Duy, Jan Jerman, Jan Najser

Institute of Hydrogeology, Engineering Geology and Applied Geophysics, Faculty of Science, Charles University, Albertov 6, 128 00, Prague, Czech Republic

jan.jerman@natur.cuni.cz

Keywords: creep, plasticity, viscous behaviour, secondary compression, overconsolidation ratio

Abstract

Understanding the mechanisms behind creep and identifying the factors that influence compression and creep behaviour are vital for accurately predicting long-term settlements, which are key to maintaining structural stability and safety in geotechnical engineering. Also, understanding creep deformation plays a crucial role in preventing uncontrolled settlement and unexpected structural damage during service. Some experimental studies (such as Olek et al., 2022) have observed the impact of various factors on the long-term mechanical behaviour of soil during creep, including applied stress levels, the duration of constant loading, OCR, plasticity, and soil composition. However, a comprehensive description and correlation of these factors remain limited, particularly in controlled environment. This lack of data hinders numerical modelling of long-term soil-structure interaction and soil creep. To address this shortfall, an extensive experimental program was conducted under controlled conditions, involving a series of standard and creep oedometer tests. Five reconstituted samples were prepared using different proportions of two types of clay - kaolinite and bentonite, representing low and high-plasticity clayey soils. The findings revealed that soils with higher plasticity exhibit greater creep coefficient values and experience a more significant reduction in the coefficient of secondary compression (C_α, Mesri, 1973) as stress levels increase, along with more pronounced volume changes during compression and swelling. Moreover, the influence of OCR on C_α was also observed. It has been also shown, that the initial water content (Wi) used for preparation of clay slurry significantly influences OCR of reconstituted samples, particularly at low-stress levels (10-25-50 kPa). For relatively low Wi (e.g., <130% for kaolinite), reconstituted samples show apparent overconsolidation due to soil structure, while higher Wi leads to a lower OCR. This also causes change of slope and position of NCL, with convergence occurring only at relatively high stresses.

References

Mesri, G., 1973. Coefficient of secondary compression. Journal of the soil mechanics and foundations division, 99(1), pp.123-137.

Olek, B.S., 2022. An experimental investigation of the influence of plasticity on creep degradation rate. Acta Geotechnica, 17(3), pp.803-817.

Figures

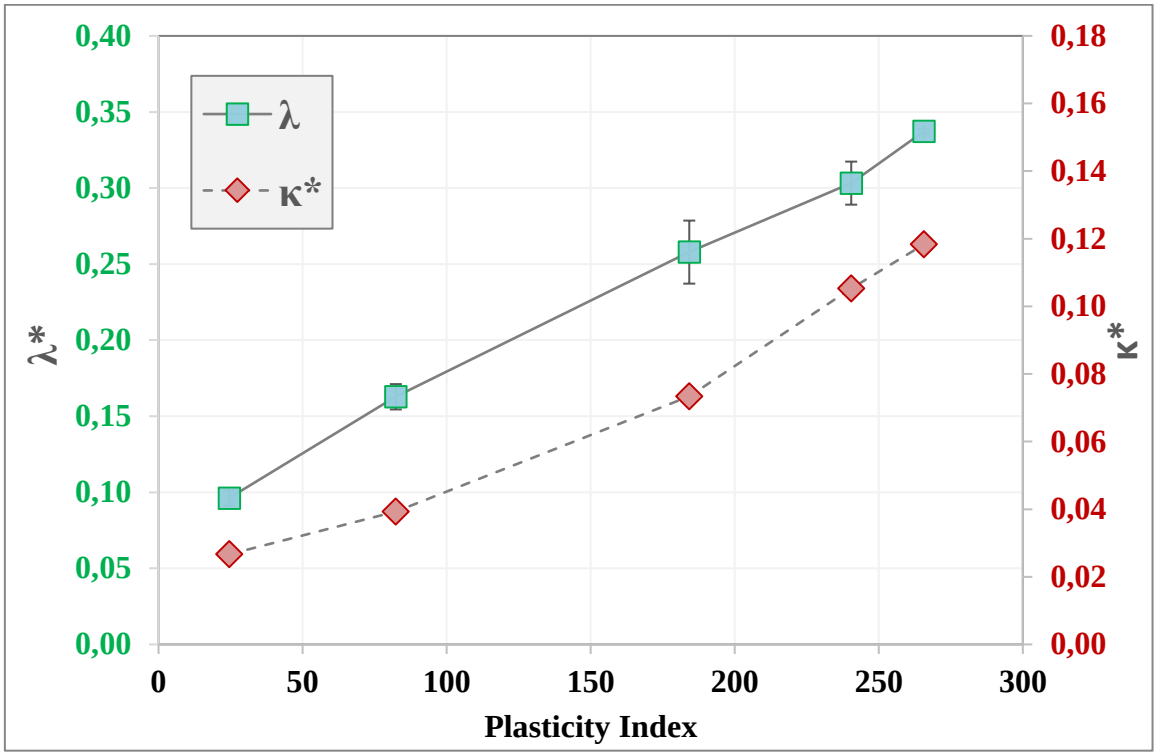

Figure 1: *Influence of plasticity on compression characteristics.*

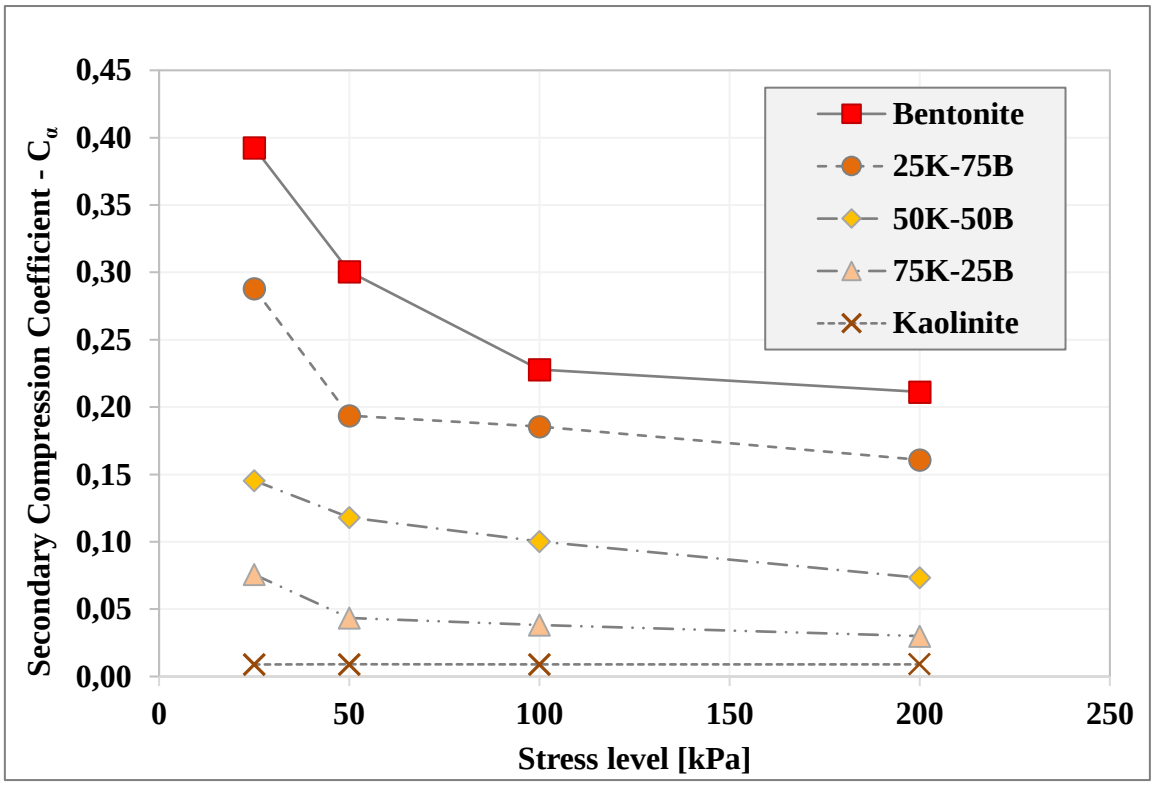

Figure 2: *Influence of plasticity on secondary coefficient (C_a) at different stress levels.*

Influence of Anisotropic Structure on the Interface Shear Strength of Fine-Grained Soil

Sabine Gehring, Hans Henning Stutz, Andrzej Niemunis

Karlsruhe Institute of Technology, Institute of Soil Mechanics and Rock Mechanics, Engler-Bunte-Ring 14, 76131 Karlsruhe, Germany

sabine.gehring@kit.edu

Keywords: interface, anisotropy, microstructure, undrained shear strength, predefined shear plane

Abstract

In geotechnical engineering, the interface shear behaviour can be crucial for the load-bearing behaviour. This holds for many geotechnical projects, as most include rigid structures like piles or walls. Therefore, the estimation of the contact shear strength is important for the design of geotechnical structures. For example, the undrained shear strength of the soil is needed to calculate the recovery force of suction buckets.

The (interface) shear strength of soil depends on many factors. For example, it is influenced by the state of the soil, the soil shear strength, the roughness of the interface and the normal stress on the interface. Whether the shear direction affects the interface shear strength, depends on the properties of the soil and the interface. If the structure of the interface is anisotropic, the maximum shear stress and dilatancy behaviour are different for different shearing directions as Stutz and Martinez (2021) presented for interface shear tests on anisotropic-shaped interfaces. The microstructure of fine-grained soil can be anisotropic too. An anisotropic microstructure can occur due to anisotropic stress states or due to the soil genesis in fine-grained soils (see Figure 1a). This effect is already incorporated in constitutive soil models by using a structure tensor, which is rendered by the loading history (Niemunis et al., 2009; Amorosi et al., 2021). As some approaches in the literature propose to derive contact models from existing soil models (e.g. Stutz et al., 2017), the question arises, how the microscopic structure of fine-grained soils influences the macroscopic interface shear strength.

In this work, triaxial tests with a predefined shear plane at a contact surface are conducted (see Figure 1b and 1c). This test method was used in (Tejchman & Wu, 1995) in a biaxial device with sand and in (Liu et al., 2024) with triaxial compression tests on clay. Here, it is used in triaxial compression and extension tests with fine-grained soil to investigate the influence of different shear directions. A Kaolin, classified as medium plastic silt, is consolidated on an inclined rigid slip surface in a triaxial device. The surface properties can be classified as smooth to ensure a failure on the contact surface. The inclination is varied and the tests are compared. Compression and extension tests with the same inclination of the rigid surface provide the same inclination of the shear plane to the sedimentation axis for different shearing directions. This test method is a contribution to the investigation of the directional dependency of the macroscopic undrained interface shear strength for soil with an anisotropic microscopic structure. In a former work, the anisotropic visco-hypoplastic model was used as a contact model and an anisotropic shear strength was found (Gehring et al., 2023). This method is used to calculate the corresponding shear strength to the experiments (see Figure 1e). The reduced friction at the contact is back-calculated from the results of the first test (see Figure 1f).

References

Amorosi, A., Rollo, F., & Dafalias, Y. F. (2021). Relating elastic and plastic fabric anisotropy of clays. *Géotechnique*, *71*(7), p. 583-593. DOI: https://doi.org/10.1680/jgeot.19.P.134

Gehring, S., Niemunis, A., & Stutz, H. H. (2023). The anisotropic preconsolidation of clay in modelling soil-structure-interface behaviour. *Proceedings 10th NUMGE 2023. Ed.: L. Zdravkovic.* DOI : https://doi.org/10.53243/NUMGE2023-120

Liu, S. A., Liao, C., Su, X., Chen, J., & Xia, X. (2024). Shear rate and roughness effect on clay-steel interface strength properties in CU and CPD drainage conditions. *Ocean Engineering*, *305*, p. 117956. DOI: https://doi.org/10.1016/j.oceaneng.2024.117956

Niemunis, A., Grandas-Tavera, C. E., & Prada-Sarmiento, L. F. (2009). Anisotropic visco-hypoplasticity. *Acta Geotechnica*, *4*, p. 293-314. DOI: https://doi.org/10.1007/s11440-009-0106-3

Stutz, H., Mašín, D., Sattari, A. S., & Wuttke, F. (2017). A general approach to model interfaces using existing soil constitutive models application to hypoplasticity. *Computers and Geotechnics*, *87*, p. 115-127. DOI: https://doi.org/10.1016/j.compgeo.2017.02.010

Stutz, H. H., & Martinez, A. (2021). Directionally dependent strength and dilatancy behavior of soil–structure interfaces. *Acta Geotechnica*, *16*(9), p. 2805-2820. DOI: https://doi.org/10.1007/s11440-021-01199-5

Tejchman, J., & Wu, W. (1995). Experimental and numerical study of sand–steel interfaces. International journal for numerical and analytical methods in geomechanics, 19(8), p. 513-536. DOI: https://doi.org/10.1002/nag.1610190803

Figures

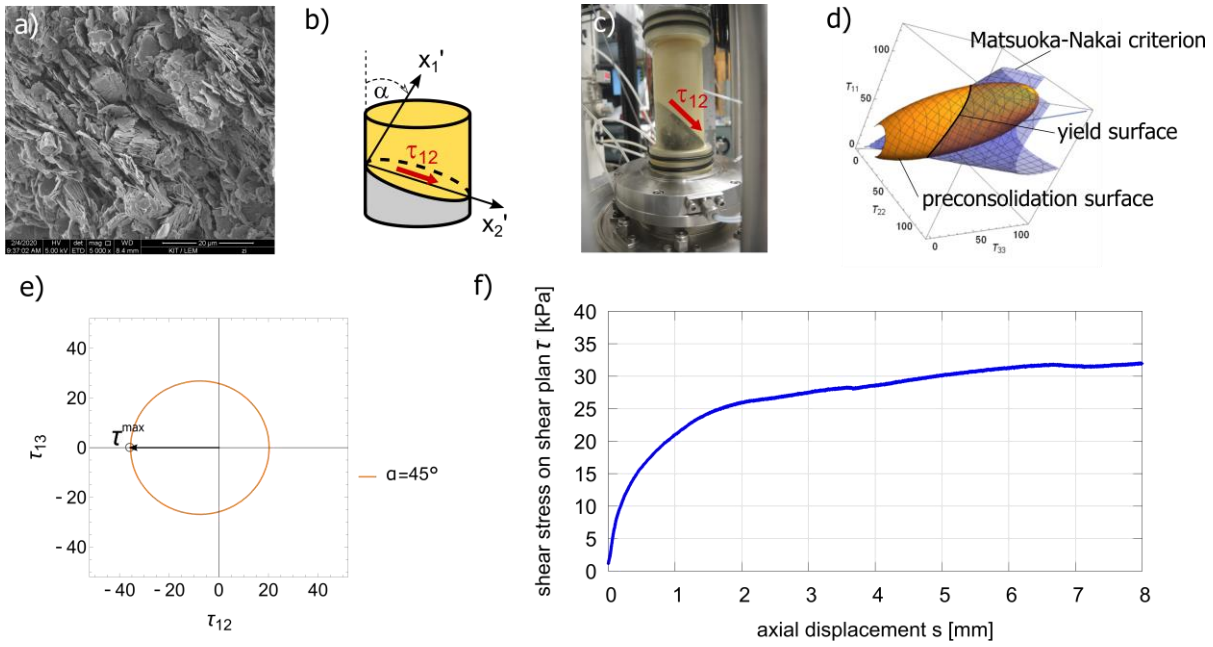

Figure 1: *a) microscopy of kaolin sample after consolidation in oedometer, b) principle of inclined predefined failure plane on contact plate, c) mounted sample on inclined predefined failure plane in triaxial device, d) preconsolidation surface and yield surface of the AVHP contact model, e) Computed undrained shear strength, f) test result for inclined failure plane with 45° inclination of 3D printed polymer surface.*

Rock Boring Process Simulation: A Coupled Approach with OpenFOAM and YADE

Manikandan Valliappan, Eleni Gerolymatou

Chair for Geomechanics and Multiphysics Systems, TU Clausthal

manikandan.valliappan@tu-clausthal.de, eleni.gerolymatou@tu-clausthal.de

Keywords: CFD-DEM, multiphase flow, rock boring, geotechnical investigations, fluid-particle interactions, borehole stability

Abstract

Coupling Computational Fluid Dynamics (CFD) with the Discrete Element Method (DEM) is essential for simulating the complex interactions between fluids and particles in geotechnical processes. This integration allows for a detailed analysis of fluid flow dynamics and particle behavior, which is critical for applications such as rock boring, where drill bits penetrate rock layers, causing intricate interactions among drilling fluids, particles, and borehole walls.

Existing coupling frameworks between OpenFOAM (CFD) and YADE (DEM) face compatibility issues with newer software versions, limiting their use in advanced simulations. This research addresses these challenges by updating the icoFoamYade and PimpleFoamYade solvers to ensure seamless operation with the latest software versions.

The updated solvers have been successfully tested for two-way point force coupling and volume fraction-based force coupling between spherical particles and fluid flow, particularly in capturing particle behavior under shear flow conditions (Figures 1, 2, and 3). Their successful operation provides a more robust and efficient platform for advanced geotechnical simulations. Additionally, the solvers will be extended to support four-way coupling, enabling more comprehensive simulations that account for the complex interactions among particles, fluids, and borehole walls.

The main focus of this research is a rock boring simulation designed to demonstrate the enhanced capabilities of the updated coupling. This simulation models the rotation of a drill bit penetrating rock particles within a cylindrical domain (Figure 4), using a four-way coupling approach to accurately capture interactions among particles, fluids, and borehole walls. The results are expected to provide valuable insights into cuttings transport and particle behavior under various flow conditions, thereby enhancing the reliability and efficiency of geotechnical simulations.

References

[1] Zakeri, Alireza, Mohammadreza Alizadeh Behjani, and Ali Hassanpour. "Fully Coupled CFD–DEM Simulation of Oil Well Hole Cleaning: Effect of Mud Hydrodynamics on Cuttings Transport." Processes 12.4 (2024): 784.

[2] Jin, L. Z., Wei Yao, and Jun Zhang. "CFD simulation of gas seepage regularity in goaf." Journal of China Coal Society 35.9 (2010): 1476-1480.

Figures

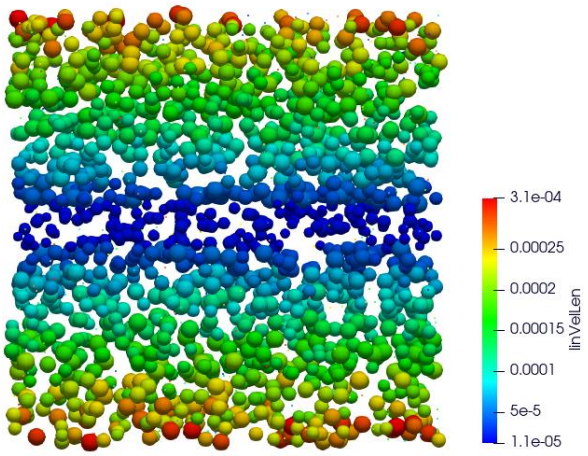

Figure 1: *Particle velocity distribution in a shear flow simulation, with colour indicating linear velocity magnitude*

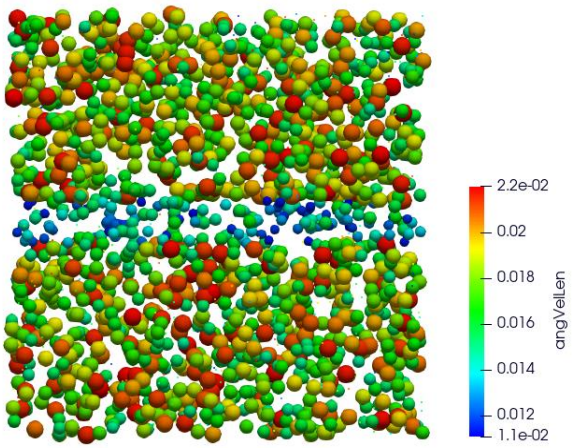

Figure 2: *Particle velocity distribution in a shear flow simulation, with colour indicating Angular velocity magnitude*

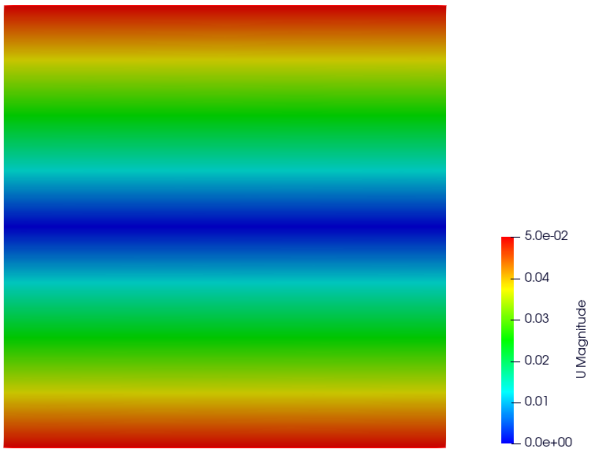

Figure 3: *Velocity distribution in a shear flow simulation of OpenFOAM results, validating the updated solver*

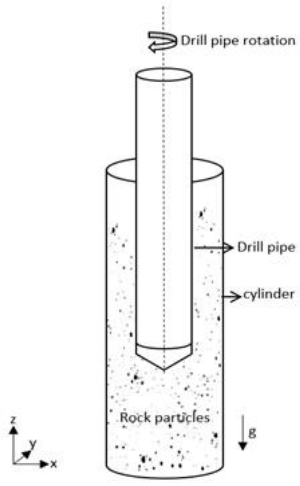

Figure 4*: Geometry: Cylinder with drill pipe containing rock particles.*

A Discrete Elements Study of Flash Heating in Fault Gouges

Hossein Shahabi, Hadrien Rattez*

Institute of Mechanics, Materials and Civil Engineering, UCLouvain, Place du Levant 1, Louvain-la-Neuve, 1348, Belgium

**Hadrien.rattez@uclouvain.be*

Keywords: flash heating, fault mechanics, frictional weakening, Discrete Element Method

Abstract

Comprehending weakening mechanisms during fault slip is necessary to understand the physics of seismic activities and for improved dynamic rupture models. These mechanisms range from formation of silica gel, flash heating at asperity contacts, to lubrication by fine-grained wear products. Flash heating is one of the primary fault weakening mechanisms that is expected to occur during sseismic slip in localized zones or discrete fault surfaces, in rocks prior to frictional melting, and is considered a crucial weakening process (Hayward et al., 2016; Yao et al., 2016).

Field studies of mature crustal faults in outcrop indicate that slip, during individual events, takes place in a thin shear band of fault gouge that is less than 1-5 mm in thickness, located within an ultracataclastic fault core filled with fine-grain materials (Rice, 2006; Scholz, 2019). At slow slip rates, the heat produced at contact points can dissipate significantly over the duration of the contact, leading to a minimal temperature increase and negligible impact on contact strength. However, at high slip rates and insufficient time to dissipate the generated heat, as intense contact stresses combined with high sliding velocities can cause intense temperature rise (Fig. 1), potentially even melting and/or leading to amorphization of the contact area, which may result in shear strengths drop (Hayward et al., 2016).

In this research, we introduce a particulate DEM model for fault frictional weakening that captures the phase changes occurring at asperity contacts due to flash heating. The model also takes diverse ranges of PSD into account due to the presence of finer grained materials in natural fault gouges and lubrication caused by those. The model considers several combinations of slip rates and overburden pressures, essential for investigation of various seismogenic conditions, deepening our knowledge of fault frictional behavior and the mechanisms that lead to rupture and the propagation of earthquakes.

References

[1] Goldsby, D., & Tullis, T. (2011). *Earthquake Slip Rates*. *334*(October), 216–219.

[2] Hayward, K. S., Cox, S. F., Gerald, J. D. F., Slagmolen, B. J. J., Shaddock, D. A., Forsyth, P. W. F., Salmon, M. L., & Hawkins, R. P. (2016). Mechanical amorphization, flash heating, and frictional melting: Dramatic changes to fault surfaces during the first millisecond of earthquake slip. *Geology*, *44*(12), 1043–1046. https://doi.org/10.1130/G38242.1

[3] Rice, J. R. (2006). Heating and weakening of faults during earthquake slip. *Journal of Geophysical Research: Solid Earth*, *111*(5). https://doi.org/10.1029/2005JB004006

[4] Scholz, C. H. (2019). *The Mechanics of Earthquakes and Faulting 2nd Edition*.

[5] Yao, L., Ma, S., Platt, J. D., Niemeijer, A. R., & Shimamoto, T. (2016). The crucial role of temperature in high-velocity weakening of faults: Experiments on gouge using host blocks with different thermal conductivities. *Geology*, *44*(1), 63–66. https://doi.org/10.1130/G37310.1

Figures

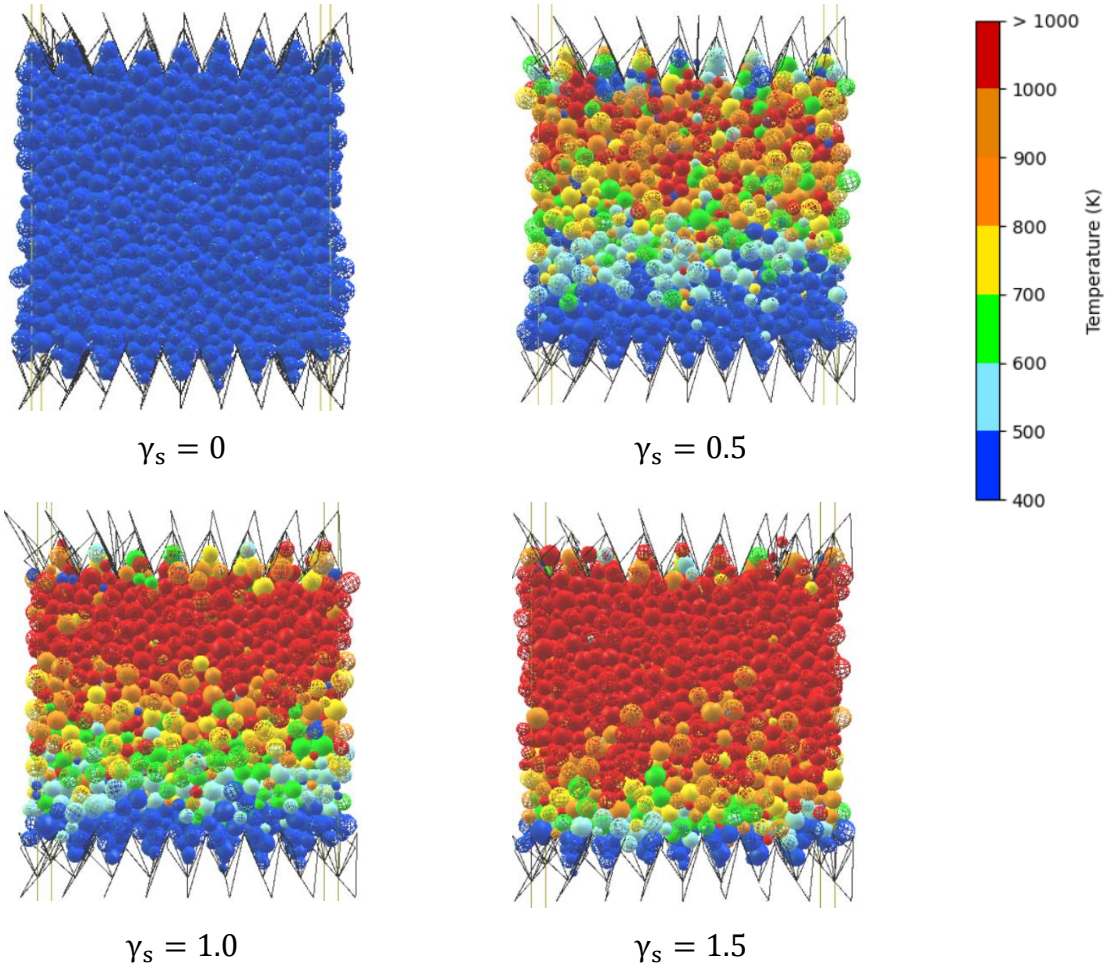

***Figure 1**: The evolution of temperature rise in particles*

Considering the Ductile Behavior of Altered Volcanic Rocks in the Flank Stability of Volcanoes and Their Response to Earthquakes

Jens Niclaes[1], Pierre Delmelle[2], Hadrien Rattez[1]

[1]Institute of Mechanics, Materials and Civil Engineering , Civil and environmental engineering, Université catholique de Louvain, Louvain-la-Neuve, Belgium

[2]Earth and Life Institute , Environmental Sciences, Université catholique de Louvain, Louvain-la-Neuve, Belgium

jens.niclaes@uclouvain.be

Keywords: volcano, FEM, numerical simulation, flank instability, brittle-ductile transition, earthquakes

Abstract

Volcanic flank collapses are among the most destructive natural hazards, with the potential to cause widespread devastation and trigger catastrophic events such as tsunamis [1]. Understanding the factors contributing to their instability is crucial. These large flank collapses occur cyclically throughout the life of a volcano. One potential cause is hydrothermal alteration, where reactive fluids and heat interact with the host rocks, altering their mechanical properties [2]. In most volcanoes, this process negatively impacts the brittle-ductile transition of volcanic rocks, leading to a more ductile failure behavior instead of a brittle one. The mechanisms behind large volcanic flank collapses remain unclear, particularly when hydrothermal alteration is involved [3]. The impact of the transition in mechanical behavior is rarely considered in volcanic stability assessments.

We performed Finite Element Method simulations under both dry and wet conditions on 2D and 3D models of the Tutupaca volcano as it existed before its collapse in the late 18th century. To assess stability, we applied the strength reduction method to each configuration, allowing us to determine the factor of safety and identify the most critical failure mechanism. The collapse was most accurately reproduced when the volcanic rocks were modeled as a Mohr-Coulomb material with a compressive cap. This compressive cap accounts for the low brittle-ductile transition observed in previous experimental studies of altered volcanic rocks. Importantly, incorporating the compressive cap significantly enhances the model's ability to predict volcanic stability against earthquake-induced ground acceleration.

Our results highlight that hydrothermal alteration affects volcanic stability by altering the brittle-ductile transition. This research provides a foundation for understanding volcanic instabilities influenced by hydrothermal alteration and suggests that incorporating variations in the brittle-ductile transition could enhance future volcanic hazard assessments.

References

[1]L. Siebert, “Large volcanic debris avalanches: Characteristics of source areas, deposits, and associated eruptions,” Journal of Volcanology and Geothermal Research, vol. 22, no. 3–4, pp. 163–197, Oct. 1984, doi: 10.1016/0377-0273(84)90002-7.

[2] M. Detienne, “Unravelling the role of hydrothermal alteration in volcanic flank and sector collapses using combined mineralogical, experimental, and numerical modelling studies,” Université catholique de Louvain, Louvain-la-Neuve, 2016.

[3] M. J. Heap and M. E. S. Violay, “The mechanical behaviour and failure modes of volcanic rocks: a review,” Bull Volcanol, vol. 83, no. 5, p. 33, May 2021, doi: 10.1007/s00445-021-01447-2.

Accelerated Implicit Cyclic Loading

Kadlíček Tomáš, Mašín David

Faculty of Science, Charles University, Czech Republic

Tomas.kadlicek@natur.cuni.cz

Keywords: cyclic loading, finite element analysis, acceleration

Abstract

In general, numerical simulations of cyclic loading can be performed by two distinct approaches. First, called the implicit cyclic loading, simulates each individual cycle in its full length. Second, designated as the explicit cyclic loading, determines only the average values of each cycle. Due to the nature of the implicit cyclic loading, any numerical simulation of the cyclic loading is significantly computationally demanding, and its use is typically restrained to the span of tens or hundreds of loading cycles. Simulating hundreds of thousands of cycles is thus computationally unfeasible. In addition, results of the implicit cyclic loading are solely dependent on the reliability and precision of the implicit constitutive model. The hight cycle accumulation model (HCA) (Niemunis, 2005) is a typical representation of the explicit constitutive model, however, the model still requires the implicit cyclic loading to be performed first to calculate the magnitude and direction of the cyclic loading. This model was derived from the thorough experimental investigation of soil behaviour under the cyclic loading. In its nature, the HCA model is a version of a creep model and thus it can produce a pseudo-relaxation or a pseudo-creep depending on boundary conditions of a finite element. The model predicts well the displacements and strains, however, evolution of stress components and prediction of the failure conditions do not have to be reliable.

To remedy the main obstacle of the implicit cyclic simulation, that is, the significant computational time, the method of the accelerated implicit cyclic loading was developed. The attribute "accelerated" conveys the fact that the method significantly increases the speed of the numerical calculations while preserving the capabilities of the implicit constitutive models. This method is proceeded on two levels: global and local. On the global level, the displacements $\boldsymbol{u}$ are recorded in the designated cycle and extrapolated in all nodal points by the predefined number of cycles. On the local level, the strains $\boldsymbol{\varepsilon}$, stresses $\boldsymbol{\sigma}$ and other state variables are extrapolated by the predefined number of cycles. The core principle is thus extrapolation the recorded of recorded quantities. In addition, the method presented does not require composition and inversion of the global stiffness matrix since all nodal points are simultaneously loaded during the acceleration (extrapolation) and thus no free points remain. Moreover, the whole process of acceleration is performed in one step with no iterations. Unifying all the described characteristics of the accelerated implicit cyclic loading significantly speeds up the numerical calculation.

The first numerical calculations were performed with the hypoplastic sand model (Von Wolffersdorff, 1996) with the intergranular strain concept (Niemunis, 1997) on the numerical model of the laterally loaded monopile. The diameter of the model is 200 m and 100 m in height. The pile, modelled with linear elastic model, is 68 m long, embedded 60 m below the surface, and m 6 m in diameter. The model is composed of 59,666 tetrahedral elements and loaded with the harmonic force $\tilde{F}_x = 50$ kN at the top of the pile for 100 implicit cycles. Two accelerated implicit cyclic loading were performed to test the method developed. First, 10 implicit cycles

were followed with 10 accelerated cycles. Second, 10 implicit cycles were followed with 20 accelerated cycles. The results are displayed in Fig. 1, which shows evolution of the measured displacements, stresses and void ratios in the soil near the pile. The qualitative results are show in Fig. 2 in the form of the filled contours of the shear stress σ_{xz}. Although the linear extrapolation was used to accelerate the measured quantities in the presented calculations, the results show remarkable agreements between the implicit and accelerated implicit cyclic loading.

References

Niemunis, A., Wichtmann, T., & Triantafyllidis, T. (2005). A high-cycle accumulation model for sand. *Computers and geotechnics*, *32*(4), 245-263.

Von Wolffersdorff, P. A. (1996). A hypoplastic relation for granular materials with a predefined limit state surface. *Mechanics of Cohesive-frictional Materials: An International Journal on Experiments, Modelling and Computation of Materials and Structures*, *1*(3), 251-271.

Niemunis, A., & Herle, I. (1997). Hypoplastic model for cohesionless soils with elastic strain range. *Mechanics of Cohesive-frictional Materials: An International Journal on Experiments, Modelling and Computation of Materials and Structures*, *2*(4), 279-299.

Figures

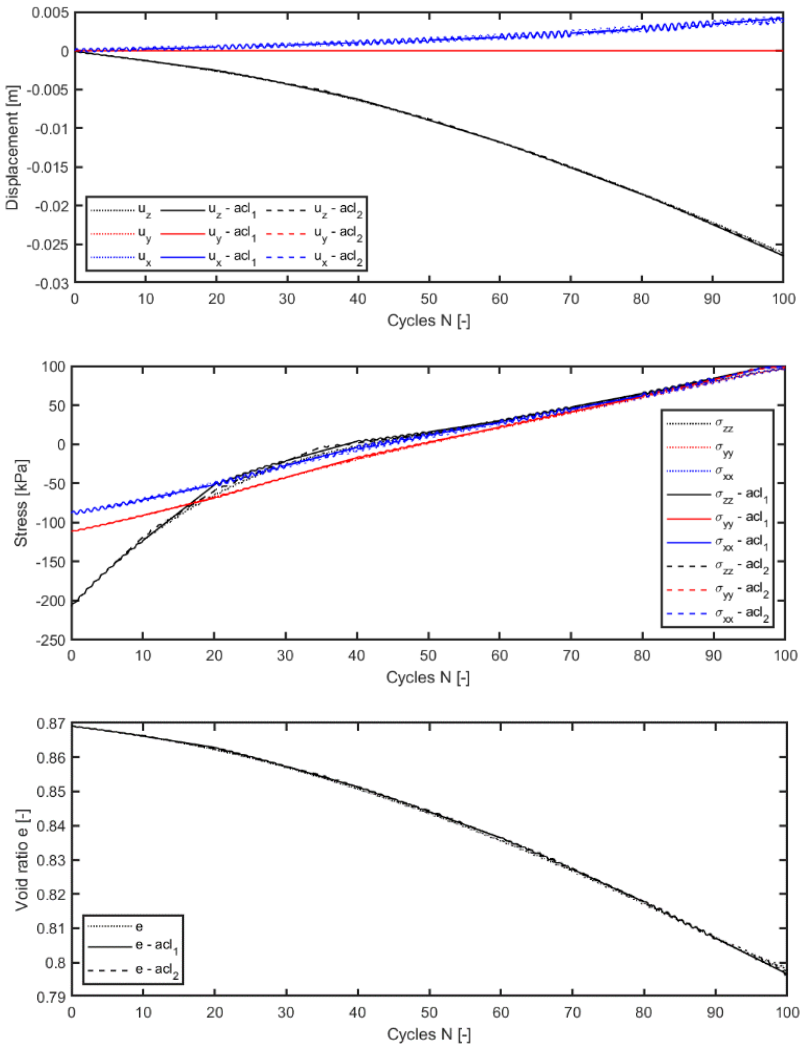

Figure 1: *Display of measured quantities: displacements, stresses, void ratios.*

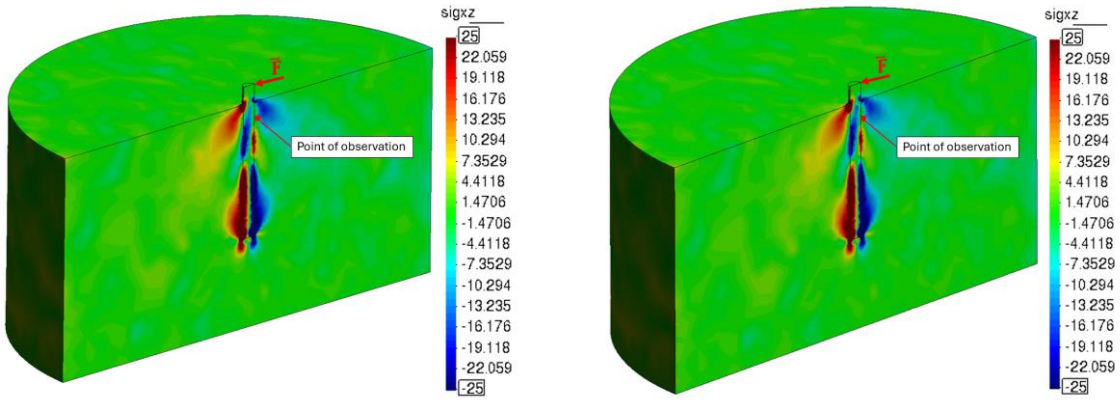

a) Implicit cyclic loading b) Accelerated implicit cyclic loading

Figure 2: *Filed isolines of the shear stress component* σ_{xz}.

A Rheological Model for Ice

Faranak Sahragard, Mehdi Pouragha, Mohammad Rayhani

Department of Civil and Environmental Engineering, Carleton University, Ottawa, CA

Faranaksahragardjun@cmail.carleton.ca

Keywords: constitutive modeling, ice mechanics, rheology, damage, healing

Abstract

The sensitivity of frozen soil to temperature variations and its complex ice-related behavior present significant challenges for construction and design in cold regions. To ensure safe infrastructure development in such environments, a reliable model for frozen soil is essential. This relies in turn on the accuracy of the ice model since the thermomechanical behaviour of frozen soil is governed primarily by ice. In this study, we develop a constitutive model for ice that can capture its behavior across a range of strain rates, temperatures, and confining pressures with an acceptable accuracy.

The model developed in this study builds upon a rheological model proposed by Danserau et al. (2016) for sea ice. We adopt a similar Maxwell framework incorporating damage and healing mechanisms. Nonlinear viscosity is defined by Glen's law (1955), which is both stress and temperature dependent. Damage initiation is determined using a teardrop-shaped criterion developed by Nadreau et al. (1986), which accounts for the effects of strain rate and confining pressure on ice strength, as well as pressure melting at very high confining pressures. The evolution of damage is described through a thermodynamics framework, where a damage evolution rule—akin to the flow rule in plasticity—is established based on the principle of maximizing energy dissipation. Moreover, a viscous healing mechanism, as observed in magma and glass (Kanchika & Wakai, 2019; Lamur et al., 2019), is integrated into the model, with the assumption that healing is directly proportional to viscous dissipation. The model is calibrated using triaxial test results from Rist and Murrell (1994) where a complex transition between ductile and brittle responses are observed for different strain rates. Figure 1 (left) demonstrates the performance of the model in plausibly capturing the effect of strain rate on ice behavior, showing increased ultimate strength and a shift towards brittle behavior at higher strain rates. Furthermore, the model also captures the transition from ductile to brittle failure at high strain rates as confining pressure increases, as shown in Figure 1 (right).

References

Dansereau, V., Weiss, J., Saramito, P., & Lattes, P. (2016). A Maxwell elasto-brittle rheology for sea ice modelling. The Cryosphere, 10(3), 1339-1359.

Glen, J. W. (1955). The creep of polycrystalline ice. Proceedings of the Royal Society of London. Series A. Mathematical and Physical Sciences, 228(1175), 519-538.

Jones, S. J. (1982). The confined compressive strength of polycrystalline ice. Journal of Glaciology, 28(98), 171-178.

Kanchika, S., & Wakai, F. (2019). A model of crack healing of glass by viscous flow at elevated temperatures. Journal of the American Ceramic Society, 102(3), 1373-1378.

Lamur, A., Kendrick, J. E., Wadsworth, F. B., & Lavallée, Y. (2019). Fracture healing and strength recovery in magmatic liquids. Geology, 47(3), 195-198.

Murrell, S. A. F., Sammonds, P. R., & Rist, M. A. (1991). Strength and failure modes of pure ice and multi-year sea ice under triaxial loading. In Ice-Structure Interaction: IUTAM/IAHR Symposium St. John's, Newfoundland Canada 1989 (pp. 339-361). Berlin, Heidelberg: Springer Berlin Heidelberg.

Nadreau, J. P., & Michel, B. (1986). Yield and failure envelope for ice under multiaxial compressive stresses. Cold Regions Science and Technology, 13(1), 75-82.

Rist, M. A., & Murrell, S. A. F. (1994). Ice triaxial deformation and fracture. Journal of Glaciology, 40(135), 305-318.

Figures

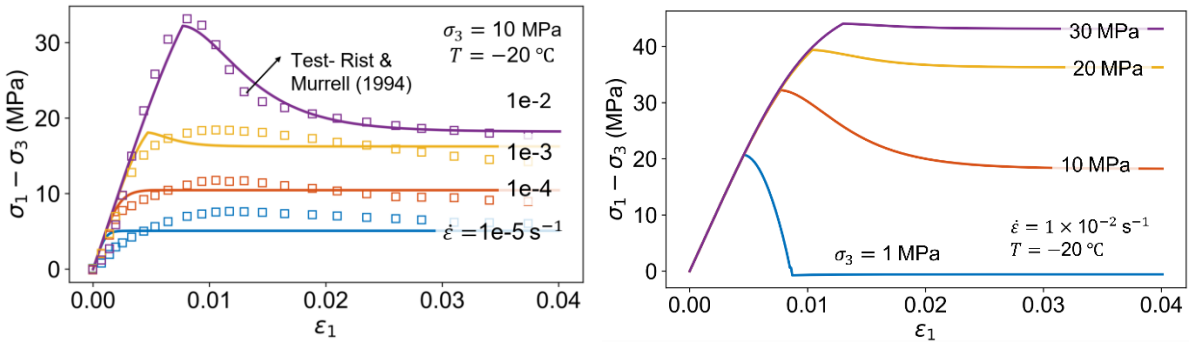

Figure 1: *(left): Comparison between the experimental data and model predictions, effect of strain rates; (right) Effect of Confining pressure.*

Experimental Approaches to Evaluate Temperature and Time-Dependent Effects in Sheared Soil

Tomáš Mladý, Om Prasad Dhaka, Bhargavi Chowdepalli

Charles University, Institute of Hydrogeology, Engineering Geology and Applied Geophysics

mladyt@natur.cuni.cz

Keywords: experimental soil mechanics, temperature, creep

Abstract

The goal of this project was to design and modify a direct shear apparatus to be able to study the impact of temperature on time-dependent effects, namely creep. The modifications were made on a decommissioned VJ-tech shear box device. Contrary to the traditional constant shearing rate mode, the device was modified to be able to apply a constant shear stress on the sample. It was shown that the device is capable of imposing the constant shear stress and above that to control the temperature and to run the creep test. This can be done for prolonged periods of time. The modifications were done using of the shelf components, 3D printed parts and custom software. The device was refitted with an arm and pulley system to substitute the original motor and induce constant stress with a dead weight. The tests were performed on pre-sheared soil sample. The pre-shearing done with only the pulley was not sufficient because of many repetitions needed. This led to the motor in the device being replaced with a new custom motor assembly, that was built around an Arduino micro controller. This enables easy control of the pre-shearing step and makes it much.

References

Garcia, L. M., Pinyol, N. M., Lloret, A., and Soncco, E. A. (2023). Influence of temperature on residual strength of clayey soils. Engineering geology, 323:1–19.

Scaringi, G. and Loche, M. (2022). A thermo-hydro-mechanical approach to soil slope stability under climate change. Geomorphology, 401:1–7.

Shibasaki, T., Matsuura, S., and Okamoto, T. (2016). Experimental evidence for shallow, slow- moving landslides activated by a decrease in ground temperature. Geophysical research letters, 43:6975–6984.

Figures

Figure 1: *Constant shear force shear box device.*

Geotechnical Clay Core Characterisation for Deep Geological Disposal of Radioactive Waste in the Netherlands

Vidushi Toshniwal[1*], Ties de Jong[1], Hemmo Abels[1], Wout Broere[1], Ana Maria Fernández[2], Michael A. Hicks[1], Dirk Munsterman[3], Erika Neeft[4], Philip J. Vardon[1], Anne-Catherine Dieudonné[1]

[1] Delft University of Technology, Delft, The Netherlands, [2] CIEMAT, Madrid, Spain, [3] TNO, Geological Survey of the Netherlands, Utrecht, The Netherlands, [4] COVRA, Nieuwdorp, The Netherlands

V.T.Toshniwal@tudelft.nl

Keywords: geological disposal, paleogene clays, intact cores, lithostratigraphy, geophysical logs, X-ray CT scan, core quality assessment, clay characterisation

Abstract

Poorly indurated Paleogene clays are viewed as potential host formations for the geological disposal of radioactive waste in the Netherlands. The considered disposal depth ranges between 200 and 1000 m for High Level Waste. Core samples are very rare in this stratigraphic interval [1]. Therefore, the lithostratigraphy and properties of these clay layers are poorly characterised, and currently largely inferred from the material at much shallower depths in Belgium (e.g. 220 m in the HADES Underground Research Laboratory). Extrapolating the data induces large technical uncertainties due to variations in lithology [2], stress history [3], in situ stress level, and pore water chemistry [4].

The SECUUR (Safe Environment for Clay Underground Repository) research project intends to enhance the understanding of the behaviour of Dutch Paleogene clay formations by providing a comprehensive dataset from the deep subsurface, including intact cores extracted for the first time at appropriate disposal depths. Recently, high-quality cores and sediment samples were obtained from the multi-purpose research borehole DAPGEO-02 [5]. The Smet Coring System (SCS), previously applied in Belgium, was employed to extract cores of adequate mechanical quality. 64 cores were extracted at depths between 362 and 415 m beneath Delft, in either PVC or Shelby tube core barrels. The cores were air/light-tight sealed in aluminium bags, and then stored at 4°C in a temperature-controlled room at TU Delft. The cores were further scanned using a medical X-Ray CT scanner to assess their integrity and visualise lithology changes. Finally, the coring programme was coupled with investigations of formation properties from samples taken during the drilling at every metre depth [1] and down-hole geophysical logging [5]. The initial borehole dataset and the CT scan data are published via the 4TU.ResearchData repository to ensure data are accessible.

This dataset is complemented by an extensive characterisation of the core material, pore water composition and core integrity. More specifically:

- **Reconstitution of lithological sequence** through palynological study on samples taken during drilling coupled with logging and X-ray CT scans to precisely determine the formation transitions [1, 5]. Lithostratigraphy fits with 4 formations: Diessen (364.1-382.95 m), Groote Heide (382.95-390.5 m), Dongen: Ieper Member (390.5-394.0 m); Oosteind Member (394.0-402.0 m), and Landen: Liessel Member (402.0-414.0 m). Hence, up to 390.5 m samples belong

to the lower Neogene period and from 390.5 to 414.0 m to the Paleogene period. Transition between the two periods is also indicated by changes in logs.

- **Core quality assessment** by identifying fissured zones, crack patterns, and heterogeneity within cores by reconstructing material profiles from medical X-ray CT scan images. Fig. 1 shows a CT scan of a PVC core (382.1-382.95 m), CT number profile (capturing pore spaces and density variations) and corresponding sample taken during the drilling.
- **Clay characterisation** is being done for samples from different formations and includes mineralogical analysis, physico-chemical properties, and pore water composition. The experimental findings are correlated with the logs.

This research provides a comprehensive dataset for the considered host formation corresponding to the Dutch disposal depths. The correlations between coring, downhole logging, CT scans, and experimental findings enhance understanding of sub-surface geology.

Acknowledgement

This work is part of the Safe Environment for Clay Underground Repository (SECUUR) project (no. 19986), which is financed by the Dutch Research Council (NWO). The project used samples provided by COVRA and EPOS-NL (European Plate Observing System – Netherlands), which is partly financed by NWO.

References

[1] D.K. Munsterman, "The results of the palynological analysis from core-shoe samples in borehole DAPGEO-02 (Delft), interval: 364.10-414.64 m," TNO report 2023 R10164, Utrecht, The Netherlands, pp. 1-33, Jan. 2023.

[2] H. Verweij, G.J. Vis and E. Imberechts, "Spatial variation in porosity and permeability of the Rupel Clay member in the Netherlands," Netherlands Journal of Geosciences, vol. 95, pp. 253–268, Aug. 2016.

[3] B. Dehandschutter, S. Vandycke, M. Sintubin, N. Vandenberghe and L. Wouters, "Brittle fractures and ductile shear bands in argillaceous sediments: inferences from Oligocene Boom Clay (Belgium) ," Journal of Structural Geology, vol. 27, pp. 1095–1112, Jun. 2005.

[4] J. Griffioen, "The composition of deep groundwater in the Netherlands in relation to disposal of radioactive waste," COVRA NV, OPERA-PU-TNO521-2, Utrecht, The Netherlands, Apr. 2015.

[5] P. Vardon et al., "Geothermal Project on TU Delft Campus - DAPGEO-02 Drilling Report," TU Delft, Delft, The Netherlands, Nov. 2022, doi: 10.4233/uuid:fde70c00-cf65-4174-9cd3-89585a5e61bd.

Figures

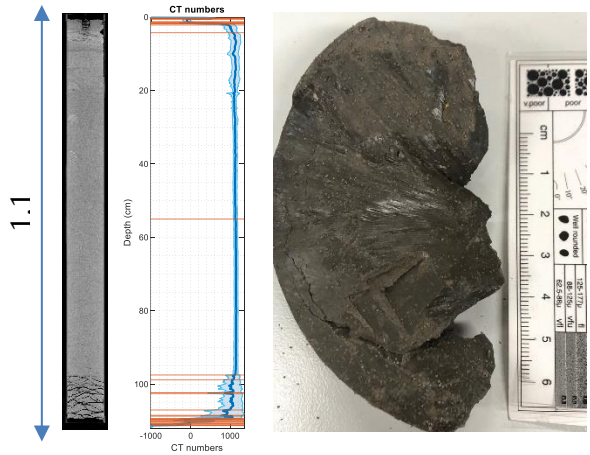

***Figure 1**: X-ray CT scan, CT number profile of core (382.1-382.95 m) and sample taken during the drilling.*

Evolution of Clay Microstructure Under 1-D Consolidation

Rishabh Tiwari[1], Béatrice Baudet[1], Matthew Richard Coop[1], Jean-Michel Pereira[2], Pierre Delage[2]

[1]University College London, U.K.

[2]Ecole des Ponts Paris Tech, France

Rishabh.tiwari.21@ucl.ac.uk

Keywords: clay, micropore, Mercury Intrusion Porosimetry, Scanning Electron Microscopy

Abstract

Micro and meso-structural studies are increasingly used to improve understanding of the macroscopic behaviour and physical properties of compacted and natural soils, micropores are pores of size below 2 nm; mesopores have sizes between 2nm and 50nm and macropores have sizes greater than 50 nm. These microstructural studies involve the use of techniques at particle aggregation scale (<100 μm) to analyse the arrangement and distribution of particles, particle assemblies, micropores-macropores and their contacts and connectivity in different soils (Collins and McGowan 1974; Delage and Lefebvre 1984; Mitchell and Soga 2005).

The microstructure of soil is the fundamental key to resolving many unexplained behaviours of soil, but it is challenging to examine during loading. Typically, microstructure analyses are done at specific states, on samples retrieved from the loading tests (Delage and Lefebvre, 1984). The mechanical testing typically involves the specimen consolidation with or without shearing in oedometer and triaxial testing system. After test completion, the specimen is carefully unmounted and preserved small soil samples (about 1 cm^3) are then freeze-dried to retain the soil structure as scanning electron microscopy (SEM) and the mercury intrusion porosimetry (MIP) are some of the techniques that require the use of thoroughly dried samples. A standard air or oven-drying is not convenient for high water content clays due to significant volume shrinkage. Therefore, other methods like critical-point-drying and freeze-drying are used. The freeze-drying method, also known as lyophilization, introduced by (Delage *et al*., 1984), is applied to dehydrate samples. The microscopic testing can involve the analysis on SEM, gas adsorption technique, MIP, transmission electron microscopy (TEM) and X-ray microtomography (XR-μCT). The visual observations of these micro pores are carried out to analyse particles and micropore arrangement and variation using the SEM monographs. This project focuses on evolution of these micropores using image digitization. The pores or voids are classified as interparticle and interlayer voids. The size and orientation of the pores are extracted by processing the digitized SEM monograph to analyse the variation and correlation in parameters like: pore size distribution, pore orientation, aspect ratio, coefficient of compression, void ratio and coefficient of uniformity and specific volume subjected to different stress path and initial state as shown in figure.1.

The scanning electron microscope, SEM is a direct method for observing soil microstructures from aggregate scales down to particle scales or even smaller. Images of a soil sample are obtained by scanning the surface with a focused electron beam. Combined with the image processing method, this technique allows for quantitatively characterizing pore morphology, void ratio, and soil pore size distribution. The SEM-based image analysis method can measure soil pores of size 0.005–100 μm. In MIP analysis a non-wetting fluid is forced to ingress porous

medium placed into a vacuum by being submitted to increasing pressure. During this test, mercury pressure is very progressively increased by steps to let mercury intrude each pore that correspond to the applied pressure step. The equation Eq.(1). (Washburn 1921) applies to pores of cylindrical shape and parallel infinite plates (fissure-like microstructure).

$$p = -\frac{n\sigma_{\mathrm{Hg}} \cos \theta_{\mathrm{nwx}}}{x} \quad (1)$$

Here σ_{Hg} is the surface tension of mercury, θ_{nw} the contact angle between mercury and the pore wall, (σ_{Hg} = 0.484 N/m at 25°C and θ_{nw} = 147°) (Diamond, 1970) and x the entrance pore diameter.

Observations from variations of PSD and orientation with stress state of soil can provide an insight in the physical laws governing micro-macro relationships. Different machine learning model like Ensemble learning and neural networks are trained on the labelled data set of correlations of pore shape descriptors as shown in figure.1 to predict the stress strain states of soils from their SEM monographs with reasonable accuracy.

References

Collins, K. and A. McGown (1974). The form and function of microfabric features in a variety of natural soils. Géotechnique. 24(2): 223-254.

Delage, P. and G. Lefebvre (1984). Study of the structure of a sensitive Champlain clay and of its evolution during consolidation. Canadian Geotechnical Journal. 21(1): 21-35.

Diamond, S. (1970). Pore Size Distributions in Clays. Clays and Clay Minerals. 18(1): 7-23.

Mitchell, J.K. and K. Soga (2005). Fundamentals of soil behavior. Vol. 3.: John Wiley & Sons New York.

Washburn, E.W. (1921). The Dynamics of Capillary Flow. Physical Review. 17(3): 273-283.

Figures

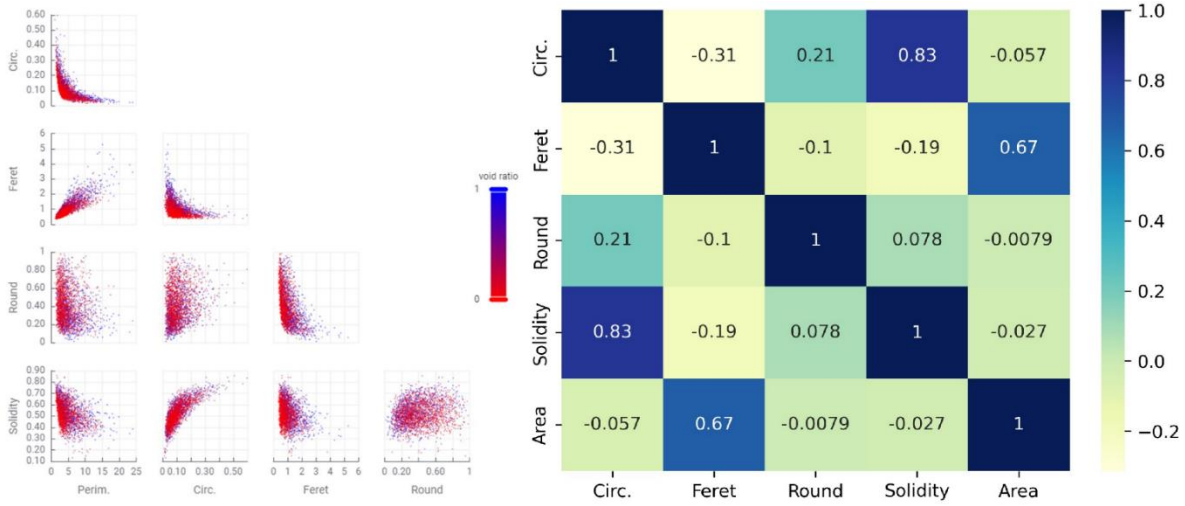

Figure 1: *Evolution of correlation in pore shape descriptors.*

Hydromechanical Coupling in the Rupture of Saturated Geomaterials

Antoine Guggisberg[1], Mehana Allache[2], Philipp Braun[2], Marie Violay[1], Mathias Lebihain[2]

[1]LEMR, EPFL, Lausanne, Switzerland

[2]Laboratoire Navier, École Nationale des Ponts et Chaussées, Champs-sur-Marne, France

antoine.guggisberg@epfl.ch

Keywords: tensile cracks, fracture propagation, poromechanics, geomaterials

Abstract

Understanding crack development in porous rocks is crucial for geomechanical applications such as permeability enhancement and leakage prevention in reservoir engineering. The interaction between surrounding water in rock pores and the advancing crack front introduces complex physical phenomena, including lubrication, chemical reactions, and mechanical effects. Theoretical models [Ruina, 1978] suggest a significant coupling between fluid flow and matrix deformation, indicating that rapid crack propagation can generate an underpressurized zone ahead of the crack tip, thereby critically influencing crack growth.

Using a novel testing setup (Fig. 1a), we investigate these induced poromechanical effects that have remained unexplored experimentally. We employ a controlled crack propagation test, the wedge splitting test (WST), within a triaxial cell. This setup allows for measuring fracture energy, the resistance to crack propagation, while observing pore pressure fluctuations in a cement-based rock analogue during rupture. Our tests reveal that pore pressure fluctuations are highly dependent on the crack propagation velocity (Fig. 1b), showing a transition from fully drained to nearly undrained conditions. Indeed, we observe that the faster the crack advances, the more localized and stronger is the underpressurized zone. This directly affects the measured fracture energy, as the pore pressure drop has a significant toughening effect; fracture energy under undrained conditions is doubled compared to drained conditions (Fig. 1c). We postulate that changes in pore pressure may critically influence the micromechanisms at stake during material breakdown at the crack tip, highlighting the crucial role of surrounding water on the dynamics of crack propagation.

References

Ruina, Andy. "Influence of coupled deformation-diffusion effects on the retardation of hydraulic fracture." *ARMA US Rock Mechanics/Geomechanics Symposium*. ARMA, 1978.

Figures

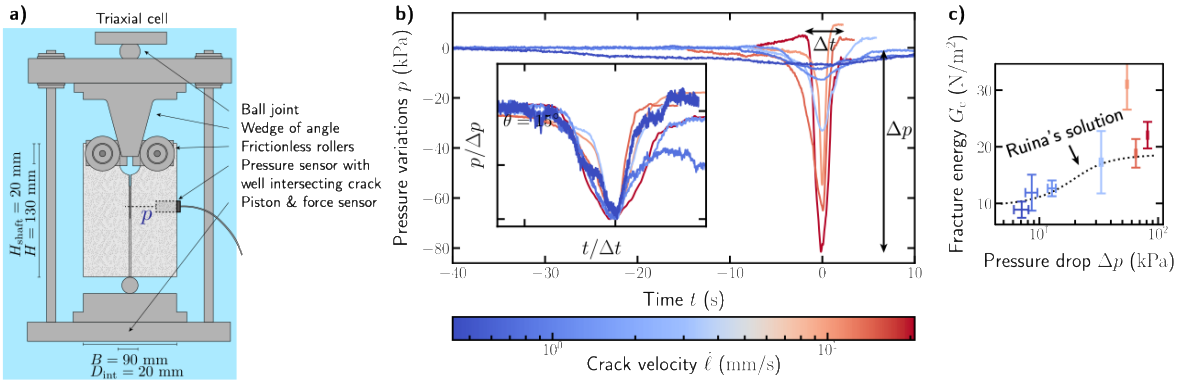

Figure1: *a) Experimental setup to measure b) pore pressure fluctuations at a fixed position during crack propagation. The pore pressure drop is self-similar and scales with crack velocity. c) This may cause a change in propagation mechanisms inducing an increase of the measured fracture energy.*

Influence of the Sample Preparation Method on the Monotonic and Cyclic Response of Malaysian Kaolin

Elvis Covilla[1]*, David Mašín[1], Jose Duque[1,2], Jakub Roháč[1], Jan Najser[1]

[1]Faculty of Science, Charles University in Prague, Czech Republic

[2]Universidad de la Costa, Barranquilla, Colombia

**covillae@natur.cuni.cz*

Keywords: cyclic loading, triaxial, kaolin, inherent anisotropy.

Abstract

This poster presents key findings from an experimental study on Malaysian kaolin (liquid limit (LL) of 65%, a plastic limit (PL) of 40%, and a plasticity index (PI) of 25% [1]). The investigation was focused on the material's behaviour under cyclic triaxial loading using two different sample preparation methods: slurry consolidation (with maximum axial stress during the pre-consolidation of $\sigma^{tot}_{1,max-p}$=100 kPa) and moist compaction ($\sigma^{tot}_{1,max-p}$=100 kPa and $\sigma^{tot}_{1,max-p}$=1250 kPa). All undrained cyclic triaxial tests were performed on samples isotropically consolidated (p_0 = 200 kPa, q_0 = 0) and then subjected to undrained cyclic shearing considering a sinusoidal waveform and a loading frequency f = 0.1 Hz. The experimental results revealed significant qualitative differences depending on how the samples were prepared, including variations in the inclination of effective stress paths, linked to the inherent anisotropy in the sample's microstructure [2], the number of cycles to failure and the amount of asymmetry in the accumulation of vertical strain in the stress-strain space.

References

[1] E. Covilla, D. Mašín, J. Duque, J. Najser, and J. Roháč. On the influence of the shearing rate on the monotonic and cyclic response of Malaysian kaolin. Géotechnique, pages 1–30, 2024.

[2] W. Fuentes, D. Mašín, and J. Duque. Constitutive model for monotonic and cyclic loading on anisotropic clays. Géotechnique, 71(8):657–673, 2021.

Acknowledgements

The authors appreciate the financial support given by the grant No. 21-35764J of the Czech Science Foundation. The first author appreciates the financial support given by the Charles University Grant Agency (GAUK) with project number 245223.

Figures

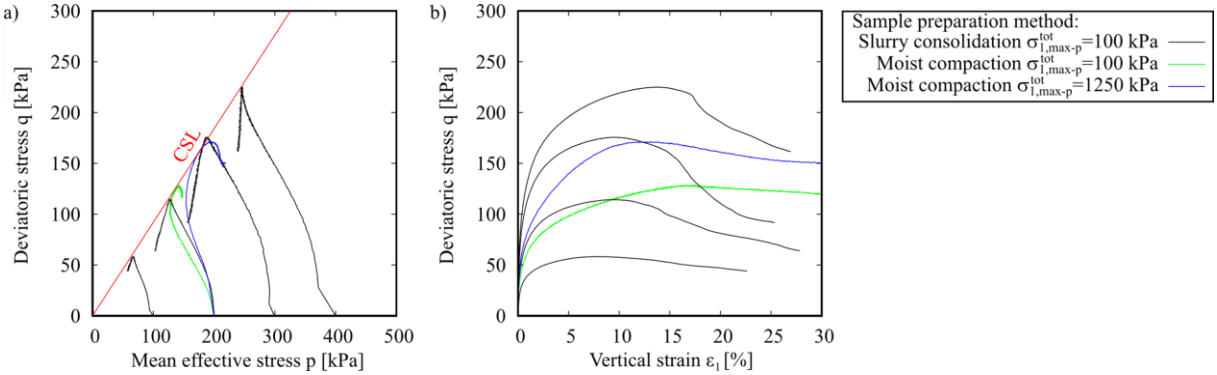

Figure 1: *Undrained monotonic triaxial tests on samples with different preparation methods*

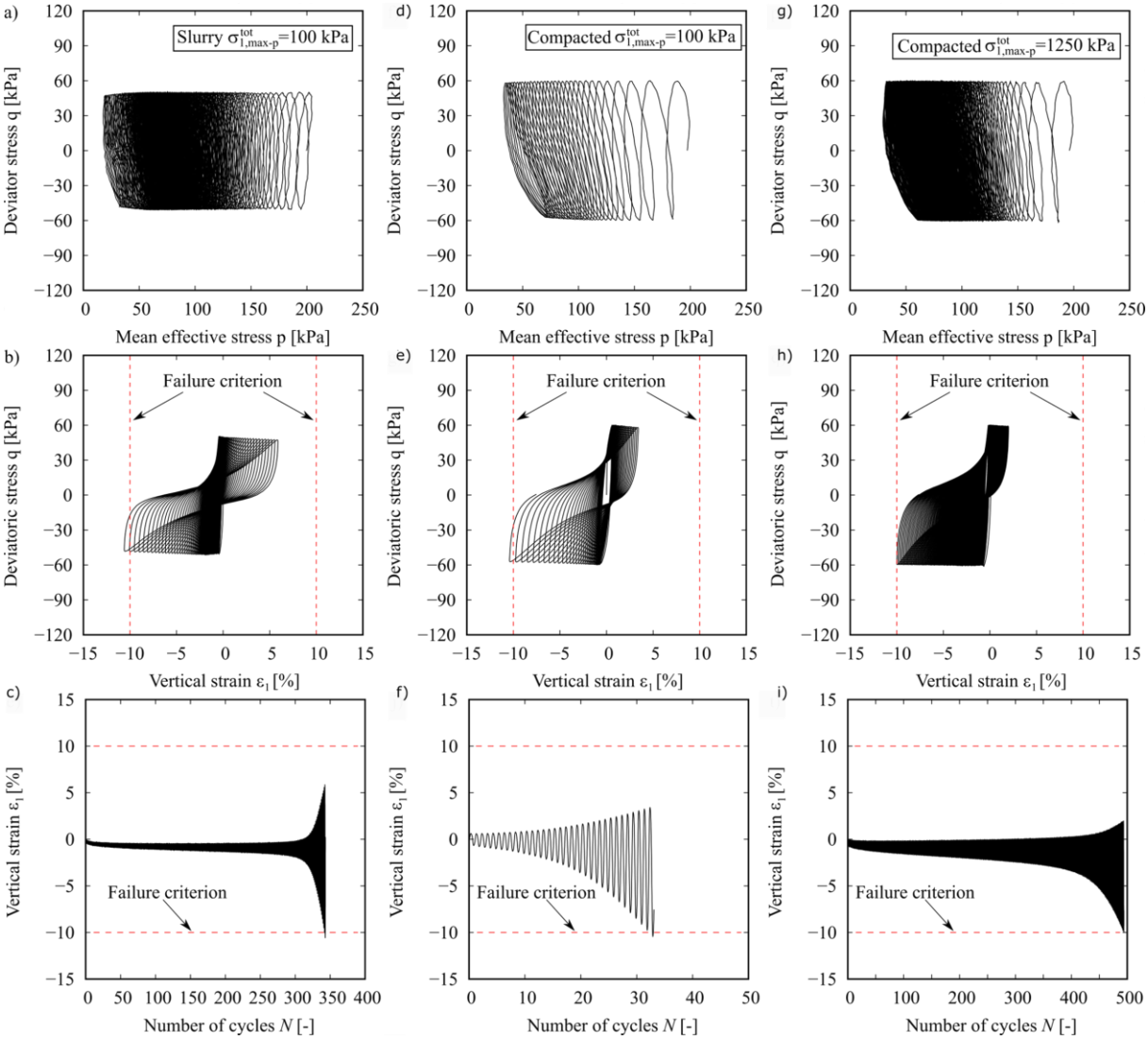

Figure 2: *Sample preparation method:* ***a-c)*** *Slurry consolidation with* q^{amp} *= 50 kPa;* ***d-f)*** *moist compaction with* q^{amp} *= 60 kPa and* $\sigma_{1,max-p}^{tot}$ *= 100 kPa;* ***g-i)*** *moist compaction with* q^{amp} *= 60 kPa and* $\sigma_{1,max-p}^{tot}$ *= 1250 kPa.*

A Constitutive Model for Predicting Soil Strength and Compressibility Under Grain Crushing

David León-Vanegas[1], Lluís Monforte, Marcos Arroyo, Antonio Gens

[1]Universitat Politècnica de Catalunya –Department of Civil and Environmental Engineering

david.eduardo.leon@upc.edu

Keywords: constitutive modelling, grain crushing, critical state line, grading state index

Abstract

Particle crushing holds significant importance in numerous geotechnical applications, such as pile foundations, rockfill dams and ballasted railways, as it has a substantial impact on the mechanical behaviour of granular materials, affecting soil strength and compressibility. In this work, a new constitutive model was formulated to incorporate the effect of grain crushing on the mechanical response of soil. The model is based on the crushing surface developed by Kikumoto et al. [1], which considers that the evolution of crushing is linked with stress history, ensuring that crushing stops if the stress level remains constant, even if plastic strain from shearing occurs. An important aspect of the constitutive model is the existence of a critical state plane in the e-p'-I_G (void ratio – mean effective stress – grading state index) space, that reflects the shift downward of the critical state line (CSL) on the compression plane as grain crushing develops, as evidenced in different experimental and numerical test [2].

Modifications were made to CSL, hardening law, and shape of the crushing surface to ensure a better match with various experimental and discrete element simulations for a Fontainebleau sand as it depicted in Figure 1 and Figure 2. Furthermore, the crushing surface is used alongside the shear yield surface developed by Hu et al. [3], where the mobilized strength and dilatancy are function of the critical state slope, and the Been and Jeffries [4] state parameter. The use of these two yield surfaces allows for capturing the change in strength and dilatancy that occurs during crushing. This effect is clearly demonstrated in Figure 3, wherein a drained triaxial test conducted on an initial denser than critical sand is presented. In this simulation, as grain crushing is produced, the CSL moves downward, resulting in a material that exhibits a looser than critical behaviour.

Acknowledgement

This work has received funding from the European Union's Horizon Europe Programme under the Marie Sklodowska-Curie actions HORIZON-MSCA-2021-DN-01 call (Grant agreement ID: 101072360).

References

[1] Kikumoto, M., Wood, D. M., & Russell, A. (2010). Particle Crushing and Deformation Behaviour. *Soils and Foundations*, *50*(4), 547–563.

[2] Ciantia, M. O., Arroyo, M., O'Sullivan, C., Gens, A., & Liu, T. (2019). Grading evolution and critical state in a discrete numerical model of Fontainebleau sand. Géotechnique, 69(1), 1–15

[3] Hu, W., Yin, Z., Dano, C., & Hicher, P.-Y. (2011). A constitutive model for granular materials considering grain breakage. Science China Technological Sciences, 54(8), 2188–2196

[4] Been, K., & Jefferies, M. G. (1985). A state parameter for sands. Géotechnique, 35(2)

Figures

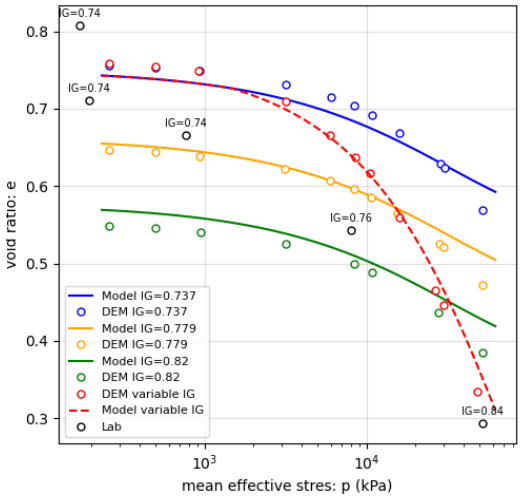

Figure 1: *Critical state lines for different grading state index IG. Comparison of DEM experiment [2] and constitutive model.*

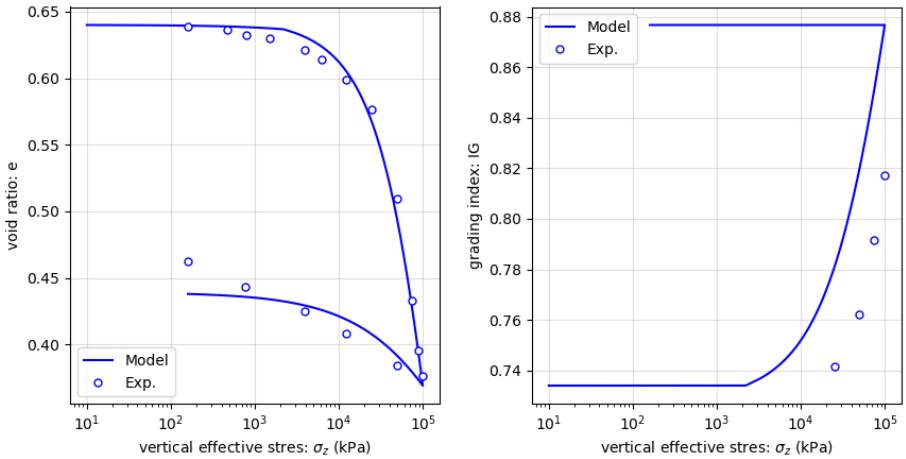

Figure 2: *Variation of void ratio and grading state index for a high-pressure oedometric compression test. Comparison of experimental experiment [2] and constitutive model.*

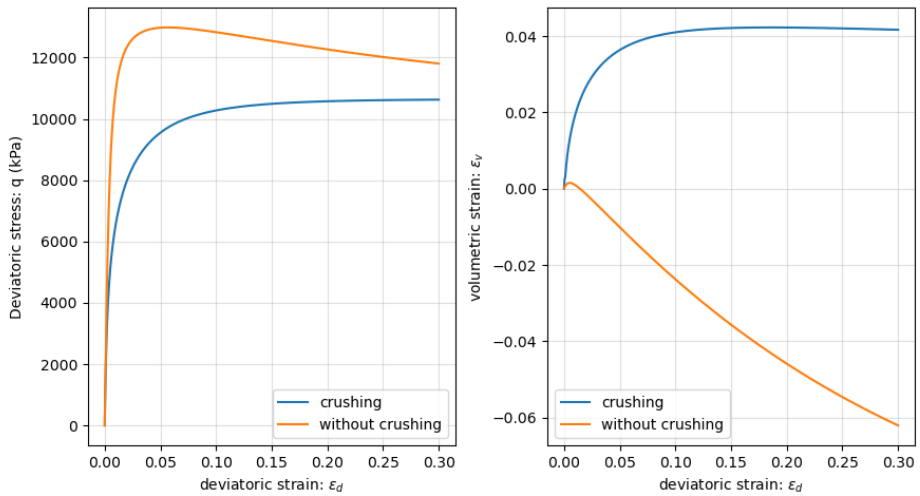

Figure 3: *Simulation of a drained triaxial test for an initially denser than critical sand ($\sigma_c = 5000\ kPa$) considering the mechanical effect of grain crushing.*

Coupled Thermo-Hydro-Mechanical Behavior of Clays: From Constitutive Modelling with Hypoplasticity to Finite Element Simulations

Pico Maria, Mašín, David

Charles University, Prague, Czech Republic

picoduam@natur.cuni.cz

Keywords: hypoplasticity, temperature, suction, cyclic loading, intergranular strain

Abstract

The popularity of energy piles has increased due to the need to find new alternative energy sources. This type of structures not only work as foundations for buildings, but also they take advantage of the soil's geothermal properties as a primary source of energy for heating and cooling buildings. As a result, the foundations are subjected to coupled-thermo-mechanical loading and water content changes, which can vary cyclically every year depending on the season. Although the great advantages of this technology, robust constitutive models able to account for these effects are still needed to predict the soil response when subjected to thermo-hydro-mechanical variations. In this line, a new coupled-thermo-hydro-mechanical hypoplastic constitutive for fine-grained soils model is proposed.

The constitutive model developed in this work is based on the previous formulation by and Wong and Mašín (2014). It captures Thermo-Hydro-Mechanical (THM) effects at large strains by defining an Asymptotic State Boundary Surface (SBS), depending on temperature and suction. Additionally, the model incorporates a temperature dependent Water Retention Curve (WRC) to capture the effects of temperature on soil retention capacity. In terms of small strains, the Improvement of the Intergranular Strain (ISI) by Duque, Mašín, and Fuentes (2020) is further extended to account for the effects of suction and temperature. The model can also predict the soil response due to heating and cooling cycles in normally consolidated (NC) and over-consolidated conditions (OC).

The constitutive model was implemented in the single-element program Triax (Mašín, 2023) using the "Generalmod" interface and validated against monotonic and cyclic laboratory tests conducted at various temperatures and suctions on two different materials (Di Donna and Laloui, 2015; Ng and Zhou, 2014). Subsequently, the constitutive model was integrated into the Finite Element software "OpenGeoSys" using the MFront tool. A key advantage of this tool is that it allows a direct and user-friendly integration of constitutive THM models in the "Generalmod" format. Currently, the finite element implementation of the constitutive model is under validation against experimental results of centrifuge tests on energy piles.

References

Di Donna, A., and Laloui, L. (2015). Response of soil subjected to thermal cyclic loading: Experimental and constitutive study. *Engineering Geology*, *190*, 65–76. https://doi.org/10.1016/j.enggeo.2015.03.003

Duque, J., Mašín, D., and Fuentes, W. (2020). Improvement to the intergranular strain model for larger numbers of repetitive cycles. *Acta Geotechnica*, *15*(12), 3593–3604. https://doi.org/10.1007/s11440-020-01073-w

Mašín, D. (2023). Triax. *TRIAX User's Manual*. Prague, Czech Republic. Retrieved from https://soilmodels.com/triax/

Ng, C. W. W., and Zhou, C. (2014). Cyclic behaviour of an unsaturated silt at various suctions and temperatures. *Geotechnique*, *64*(9), 709–720. https://doi.org/10.1680/geot.14.P.015

Wong, K. S., and Mašín, D. (2014). Coupled hydro-mechanical model for partially saturated soils predicting small strain stiffness. *Computers and Geotechnics*, *61*, 355–369. https://doi.org/10.1016/j.compgeo.2014.06.008

Figures

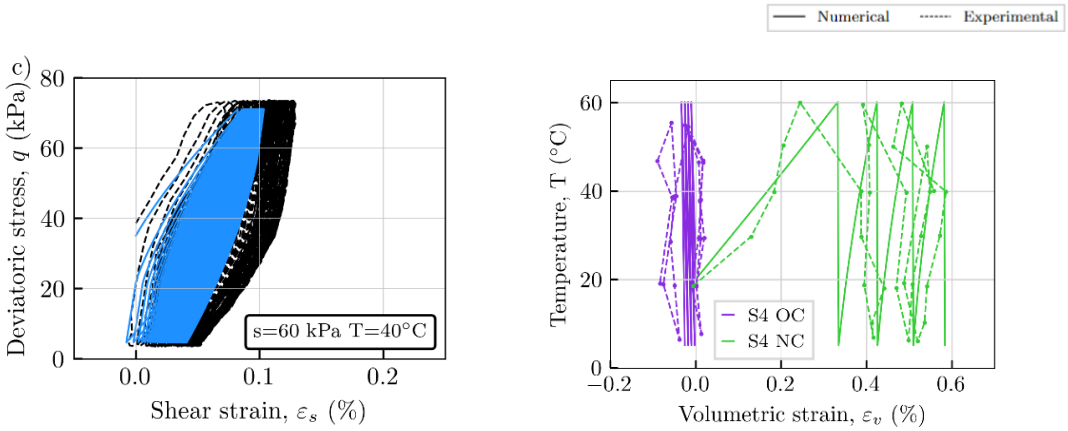

Figure 1: *Single-Element simulations vs. Experimental results of a) Constant water content triaxial tests b) Heating-cooling cycles at constant vertical stress. (Experimental results from (Di Donna and Laloui, 2015; Ng and Zhou, 2014)*

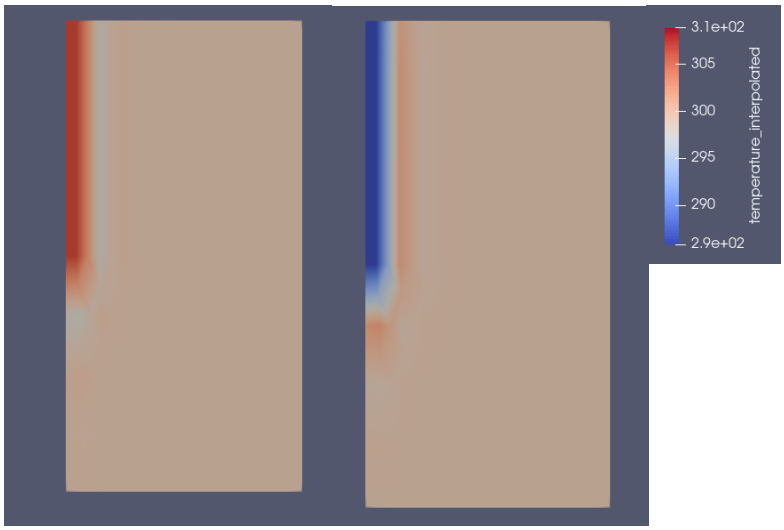

Figure 2: *Heating-cooling cycle of an Energy Pile in OpenGeoSys using the newly developed coupled thermo-hydro-mechanical hypoplastic model.*

Influence of Suction and Saturation on Accumulated Axial Strain and Post-Cyclic Strength of Unsaturated Soils

Bhargavi Chowdepalli[1,2], Kenji Watanabe[2]

[1]Faculty of Science, Charles University, Albertov 6, 128 43 Prague 2, Czech Republic

[2]Department of Civil Engineering, University of Tokyo, Bunkyo City, Tokyo, 113-8654

chowdepb@natur.cuni.cz

Keywords: accumulated axial strain, post-cyclic strength, Unsaturated conditions, non-Plastic fines content, suction, saturation

Abstract

This research addresses the increased importance of understanding the deformation characteristics of sandy soil materials used in the construction of railway embankments. As infrastructure expands in developing Asian countries, the scarcity of natural or high-quality sands (soils with less fines content) near construction sites escalates project costs. The lack of proper guidelines for compaction when utilizing various soil types further adds to the challenges. This highlights the critical need to explore effective compaction methods for utilizing different cost-effective geomaterial alternatives (Chowdepalli et al. 2022), particularly soils with different fines content. The general compaction method occurs in unsaturated conditions and compacted soil in the embankment experiences vehicle loading along with the fluctuations in saturation levels over its lifespan. Moreover, even small changes in density and moisture levels, influenced by fines content, can greatly impact the mechanical properties and stability of unsaturated soils (Chowdepalli et al. 2024). Therefore, a comprehensive series of tests were conducted on three soil types varying fines content – namely Katori sand with 18% (F18) and 30% (F30) fines contents.

A specially manufactured linkage double-cell triaxial apparatus (as seen in Figure 1a) was employed to conduct tests on unsaturated soil specimens. It involves suction-controlled drained cyclic and post-cyclic monotonic loading tests in unsaturated conditions, as well as drained cyclic and post-cyclic monotonic loading tests in soaked conditions. These tests were carried out to evaluate the accumulated axial strain ($\boldsymbol{\varepsilon_a}$) under high-frequency cyclic compressive loading (1 Hz and CSR =0.4) and, to evaluate the post-cyclic strength q_{max}under low strain rate (0.1%/min). These tests aimed to elucidate the mechanical characteristics of different soil types with varying fines content in unsaturated conditions, focusing on the soaking behaviour, post-cyclic strength, and accumulated axial strain.

Figure 1b shows the determination of the parameters using experimental data obtained by cyclic (ε_a) and post-cyclic monotonic loading tests (q_{max}). The accumulated axial strain ε_a at 50,000 loading cycles represents the strain accumulation up to the 50,000th loading cycle (shown in Figure 1b). Figure 2 and Figure 3 (a), (b) and (c) demonstrate the accumulation of axial strain at 50000 loading cycles and post cyclic strength for F18 and F30, respectively with varying compaction levels at different saturations. The results indicate that there is a reduction in accumulated axial strain, particularly in unsaturated conditions. Notably, when the compaction is performed on the drier side or at low saturations, a lesser amount of accumulated axial strain was recorded during cyclic loading. In unsaturated states, an increase in compaction results in

an increasing trend for both post-cyclic peak strength and stiffness. Simultaneously, there is a growing trend in these factors as saturation decreases, with the increased suction at low saturations strengthening the soil and enhancing its ability to resist loading. However, beyond a specific saturation point i.e., at drier side, peak strength decreases despite the increased stiffness. Interestingly, accumulated axial strain consistently decreases, indicating its independence from strength behaviour.

Moreover, the increase of fines particles increases peak strength while concurrently increasing strain accumulation during cyclic loading in unsaturated conditions. This behaviour is more pronounced when soil is compacted on the drier side, indicating that an increase in fines particles improves the positive effects of suction in unsaturated conditions. It is important to highlight that soils with higher fines content compacted at low saturations exhibit higher initial suction and stiffness in the unsaturated state, which may mislead field practitioners. In other words, "Higher stiffness immediately after the compaction" does not always correspond to "Effective compaction" when utilizing the soil with higher fines content. In summary, this research provides insights on strength and deformation characteristics of soils considering the influence of suction and saturation for different fines content.

References

Chowdepalli, B., B. K. Karnamprabhakara, and B. Umashankar. 2022. "Mechanical and environmental characteristics of geogrid-reinforced waste foundry sand beds." *Proc. Inst. Civ. Eng. Gr. Improv., (2016): 1–11.* https://doi.org/10.1680/jgrim.21.00022.

Chowdepalli, B., A. Singh Rathore, and K. Watanabe. 2024. "Effect of compaction and moisture content on the deformation characteristics of unsaturated sandy soils varying fines content*." Int. J. Geotech. Eng., 00 (00): 1–10. Taylor & Francis.* https://doi.org/10.1080/19386362.2024.2362467.

Figures

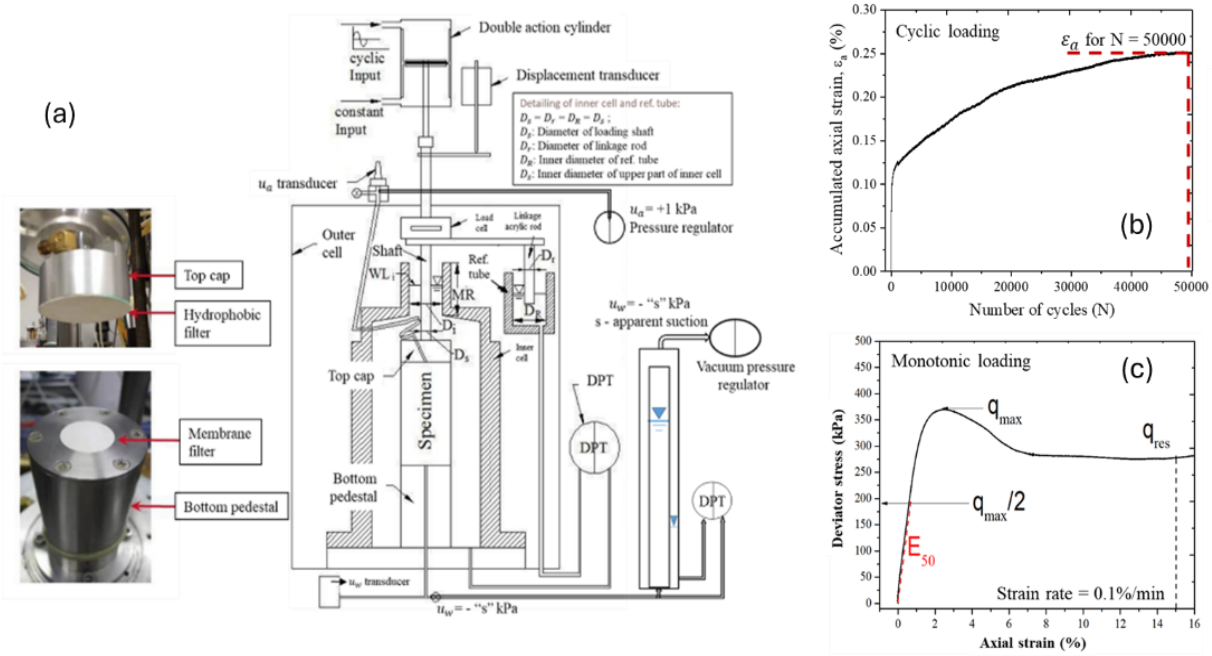

Figure 1*: (a) Schematic diagram of linkage double cell triaxial apparatus (right); Top cap and bottom pedestal (left). (b) Determination of parameters from the experimental data obtained by cyclic (top) and (c) monotonic (bottom) loading tests.*

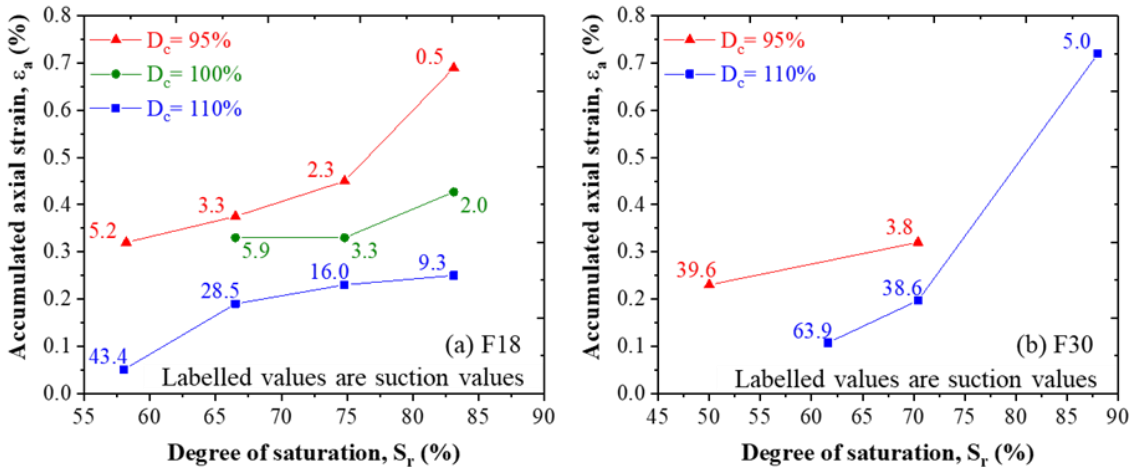

***Figure 2**: Variation of accumulated axial strain at 50,000 loading cycles with the apparent suction values varying the degree of saturation. (a) Inagi sand (b) Katori sand-F18 (c) Katori sand-F30.*

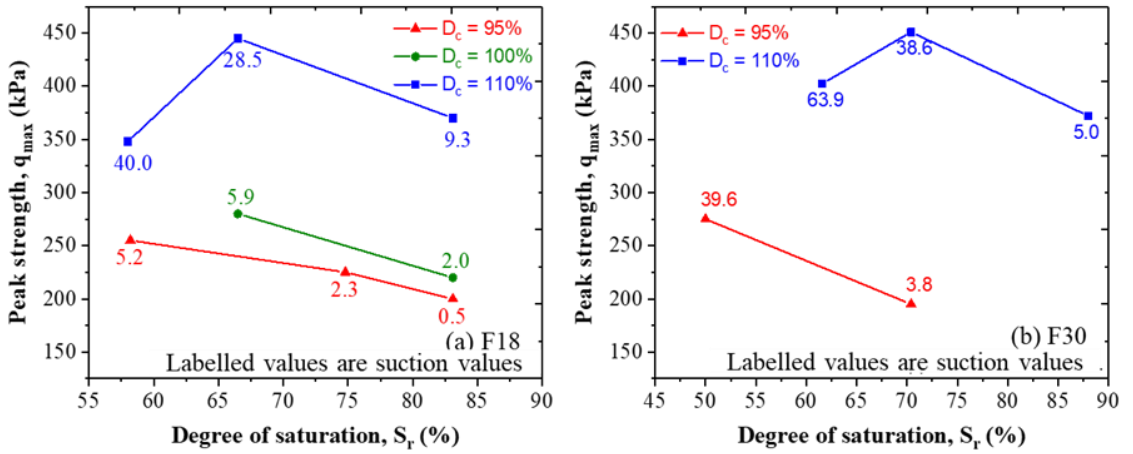

***Figure 3**: Variation of post-cyclic peak strength with the saturation. (a) Inagi sand (b) Katori sand-F18 (c) Katori sand-F30.*

Widgets for Teaching in Geomechanics

Eleni Gerolymatou, Erik Bruer, Maryam Zali, Yousef Al-Hadhrami, Franck Andy Dzoupet Yimtchi, Farzaneh Rajabi Monfared

TU Clausthal

eleni.gerolymatou@tu-clausthal.de

Keywords: teaching, geomechanics, interactive tools, self-study

Abstract

Promoting deep understanding and critical thinking is an important part of higher education and a prerequisite for teaching engineering. Geomechanics and Geotechnics are no exception. Currently, the opportunity to develop such skills is limited by the limited interaction time between lecturers and students and the lack of opportunities for students to gain their own experience. Lectures and exercises are important tools, but provide limited opportunities for experimentation on the side of the students.

With this in mind, the group for Geomechanics and Multiphysics Systems at the Clausthal University of Technology has developed a series of widgets for use by students in geotechnical engineering and geomechanics in connection with teaching. Widgets in the specific context are small online apps. They consist of visualizing the solution of various problems, including explanation, methodology and calculation, as well as a series of sliders and input fields where students can change the input parameters and observe the impact on the results. In a typical widget of the collection the theory is explained first in the form typical of a textbook. The interactive part follows.

For the development of the majority of the widgets Python on Jupyter Notebook (Kluyver et al. 2016) has been used in combination with the Bokeh library (Bokeh Development Team, 2018). This allows for easy formatting of the text and figures, while the interactive part of the resulting exported webpage uses Java, thus not requiring a server running Python. The time required to load the widget is also very reasonable, It is hoped that with the help of such apps, students have the opportunity to understand typical concepts and methods by visualizing the influence of various factors and parameters. The project is in progress and new widgets are uploaded continuously. First examples can be found here: https://geomechanics.eu/widgets/ The poster presents the method used for the creation of the widgets and introduces several examples. It is hoped that the widgets developed as part of this project will be used in the future by lecturers and students outside of Clausthal University of Technology.

References

Kluyver, T., Ragan-Kelley, B., Fernando Perez, Granger, B., Bussonnier, M., Frederic, J. et al. (2016). Jupyter Notebooks – a publishing format for reproducible computational workflows. In F. Loizides & B. Schmidt (Eds.), Positioning and Power in Academic Publishing: Players, Agents and Agendas (pp. 87–90).

Bokeh Development Team (2018). Bokeh: Python library for interactive visualization, URL http://www.bokeh.pydata.org.

Microstructural Insights Into the Failure Mechanism of Lightweight Cemented Soils Coupling In-Situ X-Ray Microtomography and Digital Image Correlation

Laura Perrotta[1], Enza Vitale[2], Emmanuel Roubin[3], Alessandro Tengattini[4], Giacomo Russo[5], Gioacchino Viggiani[6]

[1]Scuola Superiore Meridionale, Naples, Italy, [2,5]Department of Earth Sciences, Environment and Resources, University of Naples Federico II, Naples, Italy, [3,4,6]3SR, Université Grenoble Alpes, Grenoble, France ,[4]Institut Laue Langevin, Grenoble, France

laura.perrotta@unina.it, enza.vitale@unina.it, emmanuel.roubin@3sr-grenoble.fr, alessandro.tengattini@3sr-grenoble.fr, cino.viggiani@3sr-grenoble.fr

Keywords: Soil treatment, foam, lightweight, microstructure, mechanical behaviour, x-ray microtomography, digital image correlation

Abstract

Lightweight Cemented Soils (LWCS), made by mixing natural soil, water and cement with air foam are heterogeneous materials characterised by a complex microstructure consisting of large foam-induced voids immersed in a cemented small-porous matrix (*i.e.*, soil + cement). The use of cement as binder allows for improving the mechanical strength of the material, whereas the addition of surfactants, which incorporate air as voids remaining stable during the mixing process, guarantees its reduced volume weight. These characteristics, coupled with a high workability, make LWCS suitable for several geotechnical applications [1-5].

From a chemo-mineralogical point of view, LWCS undergo a very complex evolution over curing time due to the hydration of cement, the interaction of the hydrated phases with the clay fraction of the soil and the presence of the surfactant. Although Vitale *et al.*, (2020) [6] highlights that the foaming agent does not alter the cementing reactions of the binder, the initial porosity induced by foam rules the hydro-mechanical behaviour of LWCS, changing the initial void ratio of the material. The foam-induced quasi-spherical pores range between 50 μm to 600 μm and can be observed by means of x-ray microtomography [7].

Herein, a novel experimental investigation on the mechanical response of LWCS under triaxial loading paths using in-situ x-ray microtomography is presented, in order to reach a deep understanding of LWCS mechanical behavoiur and failure mechanisms and of their dependence on foam-induced porosity. The microtomographies are acquired during the shear phase of multiple triaxial compression tests performed on samples with two contents of foam, *i.e.*, 20% and 40%, and at different confining mean effective stresses, *i.e.*, 50 kPa, 150 kPa. The macroscopic behaviour obtained by the performed tests is shown in Figure 1a and Figure 1b.

Image analysis is employed for obtaining 3D incremental strain fields developed inside samples. For samples having 20% foam content, at the lowest mean confining stress, the deformation essentially consists in the progressive opening of sub-vertical dilatant fractures connecting the foam-induced voids (Figure 2). At higher confining stress, *i.e.*, 150 kPa, localised compactions develop in the cemented matrix along the directions coherent with the deviatoric loading path, determining the development of a shear band. For samples exhibiting a foam content equal to 40%, the shear band is detectable since the lowest mean confining stress

whereas, by increasing the confinement level up to 150 kPa, diffuse pore collapses determining the densification of the material are clearly visible. The initial content of foam determines a shift of the confining threshold needed to observe the transition from a brittle to a ductile behavoiur. The test results highlight that the deformation and failure mechanisms of LWCS strongly depend on the confining mean stress level, on the initial foam-induced porosity and on the microstructural heterogeneities, *i.e.*, shrinkage fractures.

References

1. Satoh, T., Tsuchida, T., Mitsukuri, K., Hong, Z. (2001). Field placing test of lightweight treated soil under seawater in Kumamoto port. Soils and Foundations, 41(4), 145–154.
2. Tsuchida, T., & Egashira, K. (2004). The lightweight treated soil method: new geomaterials for soft ground engineering in coastal areas. CRC Press.
3. Watabe, Y., Itou, Y., Kang, MS., Tsuchida, T., (2004). One-dimensional compression of air-foam treated lightweight geo-material in microscopic point of view. Soils and Foundations, 44(6), 53–67.
4. Jamnongpipatkul, P., Dechasakulsom, M., Sukolrat, J. (2009). Application of air foam stabilized soil for bridge-embankment transition zone in Thailand. In: Geotechnical special publication no. 190, ASCE, Reston, VA, pp 181–193.
5. Miki, H., Mori, M., Chida, S. (2003). Trial embankment on softground using lightweight-foam-mixed in situ surface soil. In: Proceedings of the 22nd permanent international association of road congresses (PIARC) world road congress. World RoadAssociation, La Defense Cedex.
6. Vitale, E., Deneele, D., Russo, G., De Sarno, D., Nicotera, M. V., Papa, R., & Urciuoli, G. (2020). Chemo-mechanical behaviour of lightweight cemented soils. Acta Geotechnica, 15(4), 933-945.
7. Perrotta, L., Vitale, E., Arciero, M., Roubin, E., Tengattini, A., Russo, G., & Viggiani, G. (2024). Microstructural insights into the mechanical behaviour of Lightweight Cemented Soils using X-ray microtomography. Géotechnique Letters, 1-21.

Figures

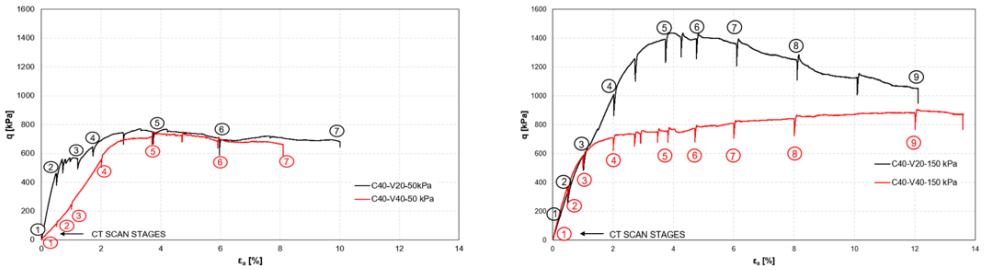

Figure 1: *(a) triaxial tests results of C40-V20 p' = 50 kPa and C40-V40 p' = 50 samples, (b) triaxial tests results of C40-V20 p' = 150 kPa and C40-V40 p' = 150 samples.*

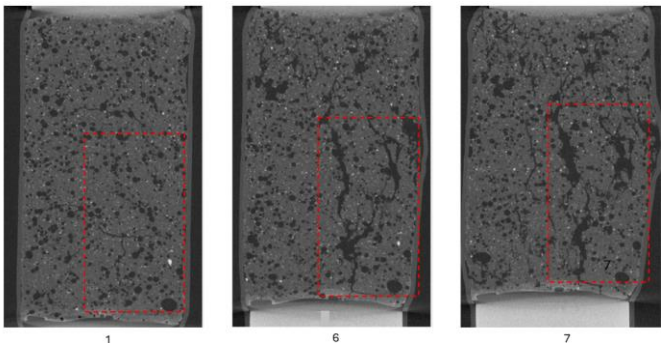

Figure 2: *Details of vertical slices of the reconstructed tomographies for LWCS sample C40-V20, p' = 50 kPa.*

Multiscale Modeling of Granular Materials: A Statistical Homogenization Strategy Relying on Mesoscale DEM Simulations

Aoxin Li[1], Antoine Wautier[1], François Nicot[2], Mehdi Pouragha[3], Claudio Carvajal[1]

[1]Aix Marseille Univ., INRAE, UMR RECOVER, Aix-en-Provence, France

[2]Université Savoie Mont Blanc, ISTerre, Le Bourget-du-lac, France

[3]Carleton University, Dept. of Civil and Environmental Engineering, Ottawa, Canada

aoxin.li@inrae.fr

Keywords: multi-scale models, H-model, DEM, mesostructures, statistical homogenization

Abstract

Multi-scale modelling of the constitutive behavior of geomaterials may be seen as a legacy of the multislip, multilaminate or microplane models introduced Taylor [1], Zienkiewicz and Pande [2] and Bazant [3]. Following their approach, the overall material response is derived by averaging constitutive properties attributed to independent planes of various orientations. Proposed by Nicot and Darve [2], the H-model is a multi-scale model for granular material that has the particularity to account explicitly for local arrangement of grains (i.e. mesostructures). Therefore, the model predicts the material response as the average response of a collection of mesostructures formed of six grains in 2D and ten grains in 3D. To propose an analytical formulation of the constitutive law, the original H-model assumes that the mesostructures (the H-cells) form regular hexagons in both the 2D and 3D versions of the model. In this study, we extend the framework of the H-model by relying on mesoscale discrete element simulations to consider widely graded material idealized as binary mixtures of fine and coarse grains. We construct enriched H-cells corresponding to hexagonal coarse grains patterns filled with fine grains, as shown in Figure 1 for both 2D and 3D conditions.

The enriched version of the H-model extends the class of materials that can be modeled with the H-model, and in particular, it allows for the straightforward simulation of internal erosion by changing the internal fine content. Preliminary results shown in Figure 2 for 2D conditions illustrate the mechanical response of binary mixtures with different fine grain contents, while subjected to constant volume biaxial compression. We observe that a higher fine content results in lower deviatoric stresses for the same mean stress, leading to a lower residual friction angle. This is consistent with the results obtained from direct DEM simulations at the representative volume element scale [3]. This finding highlights that the enriched version of the H-model can capture the influence of fine grains through changes in the internal structure.

References

[1] Taylor, G. I. (1938). Plastic strain in metals. J. Inst. Metals, 62, 307–324.

[2] Zienkiewicz, O. and Pande, G. (1977). Time-dependent multilaminate model of rocks—a numerical study of deformation and failure of rock masses. International Journal for Numerical and Analytical Methods in Geomechanics, 1, 219–247.

[3] Bazant, Z. P. (1984). Microplane model for strain-controlled inelastic behaviour. Mechanic of Engineering Materials, edited by C. S. Desai and R. H. Gallagher, pp. 45–59, John Wiley & Sons.

[4] Nicot, F., & Darve, F. (2011). The H-microdirectional model: accounting for a mesoscopic scale. Mechanics of Materials, 43, 918–929.

[5] Peter A, Antoine W., and Nadia B. (2024). A Micromechanics-Based Classification of the Regimes Delineating the Behaviour of Gap-Graded Soils. Computers and Geotechnics, 168, 106-165.

Figures

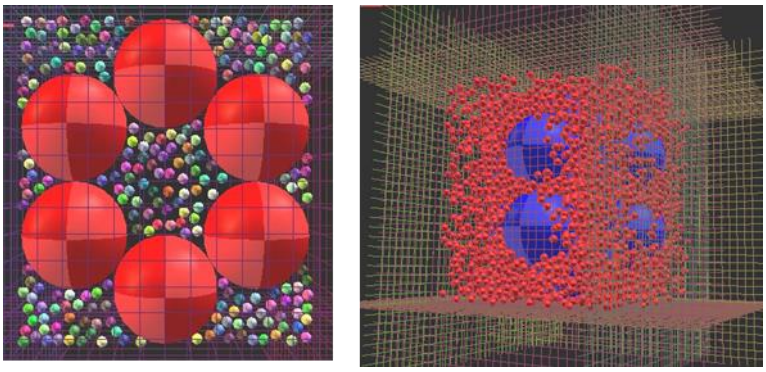

Figure 1: *Enriched H-cells with fine number fn = 229 in 2D (left) and fn = 3990 in 3D (right). The size ratio between coarse and fine grains is 10 in both cases.*

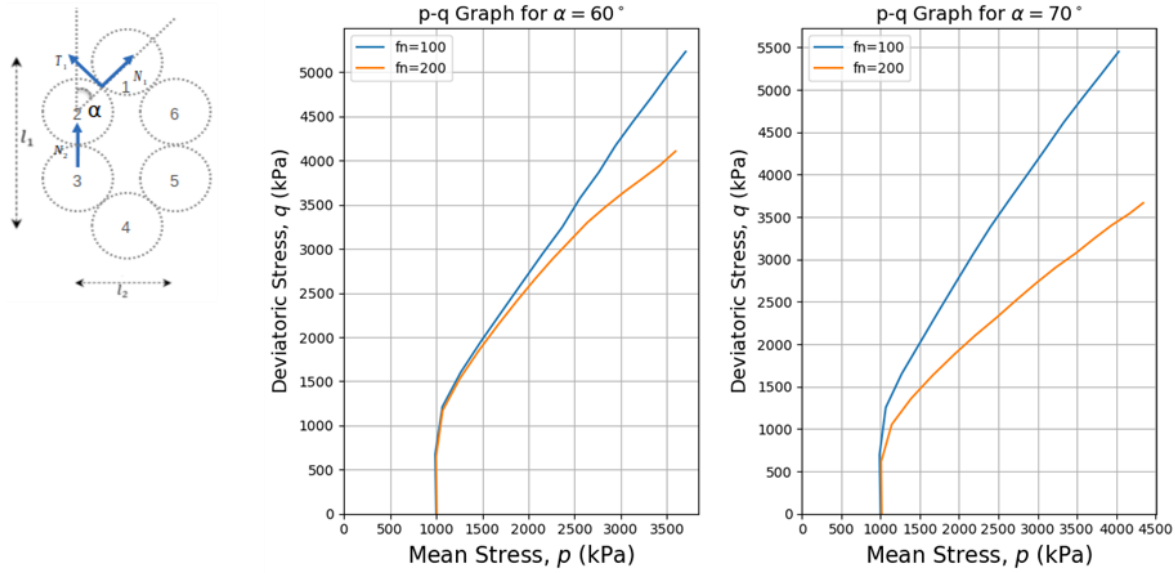

Figure 2: *p-q graphs for two initial opening angle (controlling relative density) and for two fine numbers (fn). The material is subjected to constant volume biaxial compression tests. Isotropic collections of 18 H-cells are uses in all cases.*

Behaviour of Reservoir Rocks Under Hydrostatic Cyclic Loading for Hydrogen Storage Application

Zhaochen Xu, Philipp Braun, Jean Sulem

Laboratoire Navier, École des Ponts, Univ Gustave Eiffel, CNRS, Marne-la-Vallée, France

zhaochen.xu@enpc.fr

Keywords: hydrostatic cyclic loading, porous reservoir rock, mechanical response, permeability change

Abstract

Hydrogen, as a clean energy carrier, can alleviate the seasonal supply-demand mismatch of renewable sources like solar and wind power (Heinemann et al., 2018). Geological storage is regarded as the optimal solution for hydrogen's large-scale and long-term storage, in which the high porosity and permeability of porous reservoir rocks make it promising (Thiyagarajan et al., 2022). Due to seasonal injection and recovery of gas, the rocks are subjected to cyclic pressure changes, which could potentially provoke subsidence, uplift, loss of volume or loss of permeability. Given that cyclic loading on rocks has received less attention in experimental characterization studies (Naderloo et al., 2023), this work investigates the macroscopic geomechanical behavior of Saint-Maximin limestone (SML), a typical reservoir rock.

Rock samples were tested under hydrostatic stress and pore pressure through various loading paths in a triaxial cell. A constant pore pressure gradient allowed continuous permeability recording, accompanied by acoustic wave velocity measurements.

The results of multi-level cyclic loading (Figure 1) show that the damage progression manifests as limited property changes in the elastic region (zone 1), substantial deformation increases and stiffness reductions above the elastic-plastic threshold in zone 2, followed by a decreasing deformation rate coupled with a stiffness rise in zone 3. Stiffness changes are corroborated by acoustic velocity measurements. Importantly, comparison with monotonic and creep loading results indicates that the historical maximum stress dictates the activation of damage processes, while the cycling intensifies existing damage accumulation without altering the intrinsic damage characteristics.

Results from constant amplitude cyclic loading tests (Figure 2) within the elastic zone indicate only minor irreversible cyclic deformations, while permeability and stiffness of SML remain relatively stable. However, beyond the onset of plastic deformation, even minimal excursions past this threshold lead to a noticeable deterioration in the properties of the SML over subsequent cycles. Consequently, controlling the maximum stress level within the reservoir rock emerges as a pivotal parameter in the engineering design of hydrogen storage reservoirs. Moreover, while it can be anticipated that the reservoir rock will maintain stable properties in the elastic zone during long-term service, the presence of irreversible deformation in this zone, as observed in the experiments, warrants further investigation.

References

Heinemann, N., Booth, M.G., Haszeldine, R.S., Wilkinson, M., Scafidi, J., Edlmann, K., 2018. Hydrogen storage in porous geological formations – onshore play opportunities in the midland valley (Scotland, UK). International Journal of Hydrogen Energy 43, 20861–20874.

Thiyagarajan, S.R., Emadi, H., Hussain, A., Patange, P., Watson, M., 2022. A comprehensive review of the mechanisms and efficiency of underground hydrogen storage. Journal of Energy Storage 51, 104490.

Naderloo, M., Ramesh Kumar, K., Hernandez, E., Hajibeygi, H., Barnhoorn, A., 2023. Experimental and numerical investigation of sandstone deformation under cycling loading relevant for underground energy storage A R T I C L E I N F O. The Journal of Energy Storage 64, 107198.

Figures

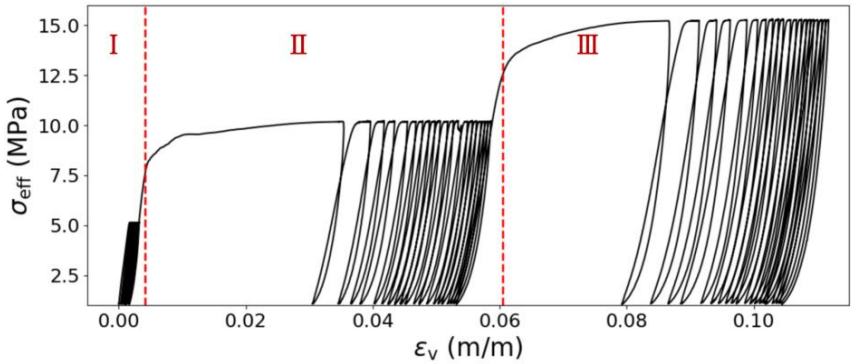

Figure 1: *Stress-volumetric strain curve under multi-level cyclic loading.*

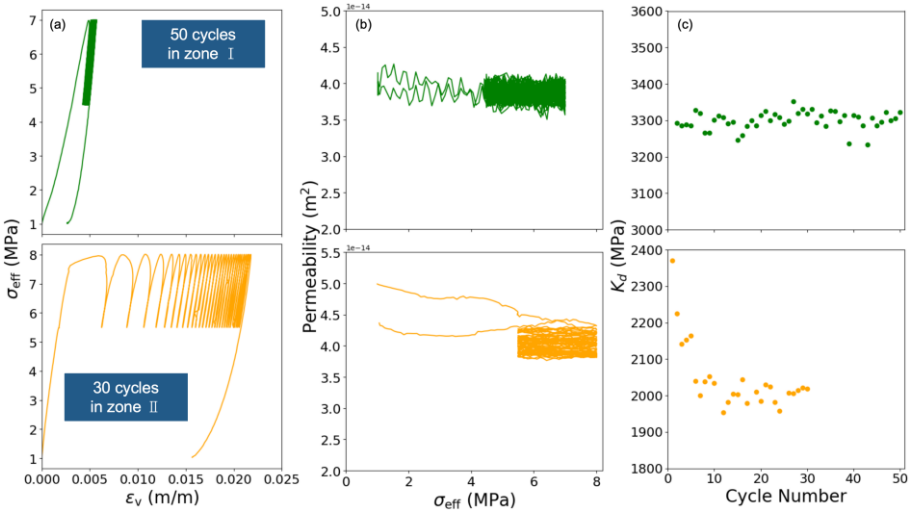

Figure 2: *Deformation and property change under constant amplitude cyclic loading in zone Ⅰ and Ⅱ : (a) Stress-volumetric strain curve, (b) permeability evolution and (c) drained bulk modulus evolution.*

Microscale Precursors of Failure in Fine Grained Porous Sandstone under Cyclic Thermo-Mechanical Coupling: A Grain Based Model (GBM) Study

Jinci Chen[1,3], Elli-Maria Charalampidou[1], Ali Ozel[2], Audrey Ougier-Simonin[3]

[1]Institute of Geoenergy Engineering, School of Energy, Geoscience, Infrastructure and Society, Heriot-Watt University, UK

[2]School of Engineering and Physical Sciences, Heriot-Watt University, UK

[3]British Geological Survey, Keyworth, UK

jc2138@hw.ac.uk

Keywords: subsurface rock stability, Discrete Element Method, Voronoi tessellation, damage evolution, microscale spatial analysis

Abstract

The cyclical injection and withdrawal operations for geoenergy storage and/or extraction in subsurface rock induce localised thermo-mechanical (TM) stress fluctuations, which may alter the long-term integrity of the targeted lithologies. Accurate prediction of the behaviour of subsurface rock formations subjected to these stress fluctuations is therefore essential for sustainable energy applications but remains a scientific challenge. This study aims to address this challenge by employing Discrete Element Method (DEM) to simulate the behaviour of rock materials under cyclic TM coupling conditions. A two-dimensional, particle-based numerical model has been constructed to explore microscale precursors, such as mineral deformation, pre-existing microcracks and microstructure damage, that could contribute to rock failure. Particle motion and force-displacement relationships follow linear elastic behaviour. Each particle is connected by cement, with each cement entity represented as a bond (see Fig. 1). These bonds are assigned tensile and shear strengths to resist external stress applied at the particle contact points. If the stress on a bond exceeds its corresponding strength, the bond breaks, triggering a microcrack event. Voronoi tessellation, an effective method for simulating microstructure of rocks, is introduced to mimic the rock mineral shape, with particles filling each tessellated region while maintaining uniform properties (see Fig. 2). First, we calibrate and validate our model using previously published laboratory data (Woodman et al., 2021), achieving a good agreement between the simulated and experimental global response (see Fig. 3). Next, we define microstructural damage as the breaking of bonds, with microcrack events occurring as a direct result during the heating and mechanical cyclic loading stages. Furthermore, to correlate damage with the microstructural evolution, we conduct a spatial analysis of particle rotation angles, porosity distribution, and contact force orientation. Our simulation indicates that the linear contact model seems incapable of reproducing the crack closure stage during compression, the stress-strain curve typically remains linear up to the peak strength. However, introducing particle separation or breaking some bonds before running the model helps produce a gradual, nonlinear compaction (Ji, Zhang and Zhang, 2018). Spatial damage distribution is influenced by Voronoi tessellation geometry because, in GBM, grain boundaries typically have lower strength than grain themselves. As a result, bond breaking occurs preferentially along the grain boundaries. Therefore, the grain size effect needs to be considered to determine a reasonable GBM. Particle rotation evolution before failure can be divided into three stages:

initially random directions, followed by local concentrations, and finally aligning along the macroscopic fracture plane.

References

[1] Woodman, J. et al. (2021) 'Laboratory Experiments and Grain Based Discrete Element Numerical Simulations Investigating the Thermo-Mechanical Behaviour of Sandstone', Geotechnical and Geological Engineering, 39(7), pp. 4795–4815. Available at: https://doi.org/10.1007/s10706-021-01794-z.

[2] Linear Parallel Bond Model — PFC 7.0 documentation (2023). Available at: https://docs.itascacg.com/pfc700/common/contactmodel/linearpbond/doc/manual/cmlinearpbond.html?node2560 (Accessed: 6 August 2024).

[3] Ji, P.-Q., Zhang, X.-P. and Zhang, Q. (2018) 'A new method to model the non-linear crack closure behavior of rocks under uniaxial compression', International Journal of Rock Mechanics and Mining Sciences, 112, pp. 171–183. Available at: https://doi.org/10.1016/j.ijrmms.2018.10.015.

[4] Zhang, Y. and Wong, L.N.Y. (2018) 'A review of numerical techniques approaching microstructures of crystalline rocks', Computers & Geosciences, 115, pp. 167–187. Available at: https://doi.org/10.1016/j.cageo.2018.03.012.

Figures

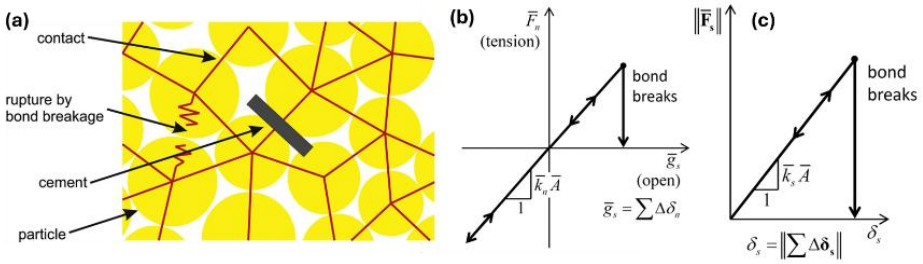

Figure 1: *(a) Particles as elements and the bond connecting them (Zhang and Wong, 2018); (b) normal force vs relative normal displacement; (c) shear force vs relative shear displacement (PFC 7.0 documentation, 2023).*

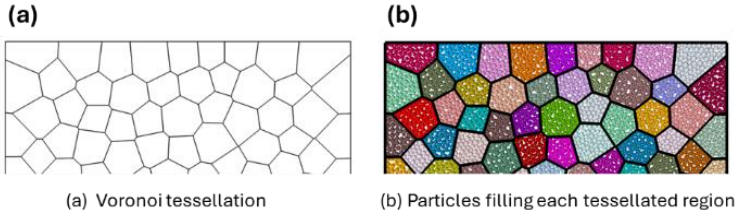

Figure 2: *(a) Voronoi cells; (b) each region maintains a group of particles with uniform properties.*

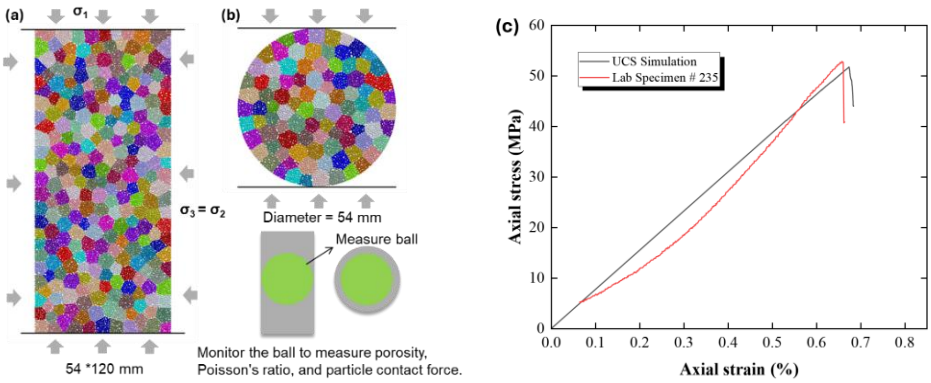

Figure 3: *(a) Uniaxial and triaxial compression simulations; (b) indirect tension (Brazilian disc) simulations; (c) axial stress-strain curve: comparison between laboratory results and simulation.*

Thermal Effect on the Residual Shear Strength and its Correlation to the Available Clay Fraction

Om Prasad Dhakal, Bhargavi Chowdepalli, Tomas Mlady, Marco Loche, Gianvito Scaringi

Charles University, Czech Republic

dhakalo@natur.cuni.cz

Keywords: residual shear strength, clay fraction, climate change, thermal weakening

Abstract

Shearing resistance in soil is affected by temperature changes (Loche & Scaringi, 2023), and the magnitude of these effects depends on the shearing rate and the mineralogy of the tested materials. Generally, heating high-plasticity clays at a residual state tends to strengthen at slower shear rates (Shibasaki et al., 2017) and weaken as the shear rate increases (Garcia et al., 2023). However, further testing is required to fully understand the impact of temperature on soil shear resistance, including the role of initial conditions.

Regarding the impact of climate change on landslide occurrence, it is crucial to comprehend the fundamental behaviour of soil (Scaringi & Loche, 2022). This involves conducting experiments on soils in a residual state across various shearing rates, initial conditions, and mineral compositions. Additionally, uncertainties such as thermal propagation to landslide depth, landslide velocity, and initial stress state need further investigation.

As an overview to access thermal effects on a landslide-prone catchment in Melamchi, central Nepal, we conducted ring-shear experiments using remoulded low-plasticity soil samples. These experiments were carried out in water-saturated conditions under representative normal stress values (50-100-150 kPa) with a constant shearing rate of 0.1 mm/min. During each test, we controlled the temperature and performed a heating-cooling cycle (20- 50-20°C) while shearing continued. To assess the role of the clay fraction (grain size <0.002 mm), we prepared specimens from the same soil samples, retaining the finest portion under three different cutoff grain sizes (0.125, 0.063, and 0.020 mm). The aim is to establish a relationship between the available clay fraction and the observed thermal effect, which can then be extrapolated to a broader study area as shown in Figure 2. The effect of temperature was assumed to increase linearly. This relationship would be useful for assessing landslide reactivation and runoff modelling using physically-based models.

The collected data were analysed statistically using variance and skewness to evaluate the robustness of the interpretations as shown in Figure1. A t-test was also applied to exclude data points close to experimental uncertainty, determining the experiment's significance at a 68% confidence interval (1 sigma). Our results indicated a decrease in residual shear strength upon heating (thermal weakening) (Dhakal et al., 2024 *Preprint*), with the extent of this weakening being correlated with the specimen's clay fraction, as shown in Figure 2. Notably, a response to heating was only observed in specimens with a clay fraction of at least 10%, and higher clay fractions and normal stresses led to greater weakening.

However, the observed effect was relatively minor, corresponding to a decrease in friction angle of <0.6° to 4.9^{0}C heating (corresponding to RCP 8.5 towards the end of the century). This suggests that temperature has a limited role in influencing the shear behaviour of low-plasticity

soils. Nonetheless, further experiments covering a wide range of soil mineral compositions are needed to fully understand the role of temperature in the shearing process and to develop empirical laws for quantifying thermal effects.

References

Dhakal, O. P., Loche, M., Dahal, R. K., & Scaringi, G. (2024). *Influence of temperature on the residual shear strength of landslide soil: role of the clay fraction*. EarthArXiv. https://doi.org/10.31223/X5HH6H

Garcia, L. M., Pinyol, N. M., Lloret, A., & Soncco, E. A. (2023). Influence of temperature on residual strength of clayey soils. *Engineering Geology*, *323*, 107220. https://doi.org/10.1016/j.enggeo.2023.107220

Loche, M., & Scaringi, G. (2023). Temperature and shear-rate effects in two pure clays: Possible implications for clay landslides. *Results in Engineering*, *20*, 101647. https://doi.org/10.1016/J.RINENG.2023.101647

Scaringi, G., & Loche, M. (2022). A thermo-hydro-mechanical approach to soil slope stability under climate change. *Geomorphology*, *401*, 108108. https://doi.org/10.1016/J.GEOMORPH.2022.108108

Shibasaki, T., Matsuura, S., & Hasegawa, Y. (2017). Temperature-dependent residual shear strength characteristics of smectite-bearing landslide soils. *Journal of Geophysical Research: Solid Earth*, *122*(2), 1449–1469. https://doi.org/10.1002/2016JB013241

Figures

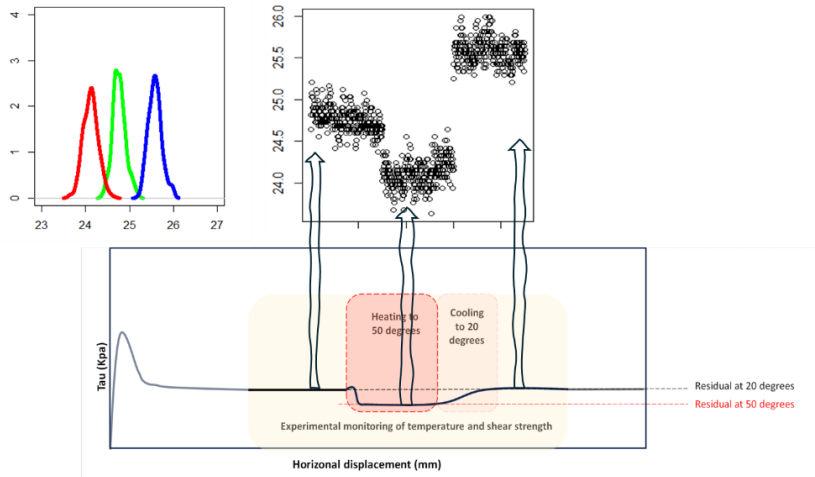

Figure 1: *Data analysis in the form of the probability density function of the measured data points and further into the test of statisical significance.*

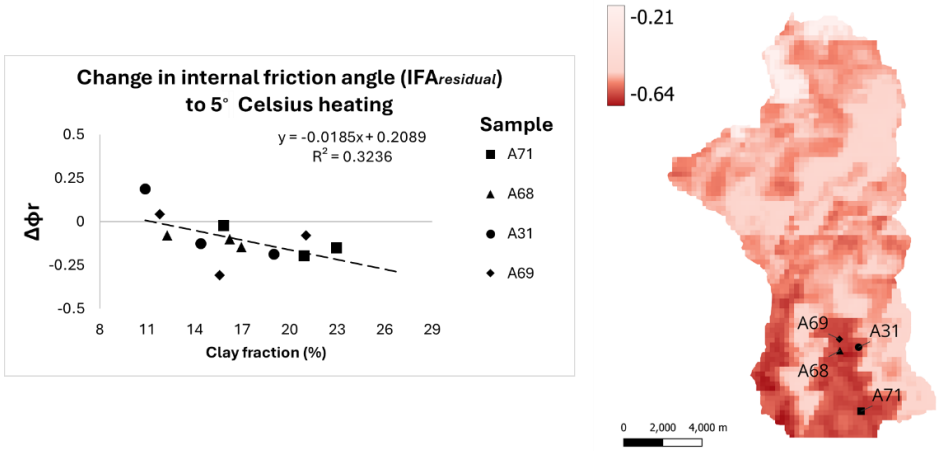

Figure 2: *Left - Thermal weakening coorelated with the clay fraction present within the tested sample. Right - Linear relationship established with teh clay fraction and extrapolated into a broader study area (Melamchi catchment) showing four points where the soil was sampled. Clay fraction(%) of the study area obtained from Soilgrids.org for the top 2 meters.*

Strategies for Extending Saturated Constitutive Soil Models to Unsaturated Tailings

Mina Mofrad, Mehdi Pouragha, Paul H. Simms

Carleton University, Ottawa, ON, Canada

minamofrad@cmail.carleton.ca, mehdi.pouragha@carleton.ca, paul.simms@carleton.ca

Keywords: tailings, unsaturated soil, constitutive model, hydromechanic

Abstract

Constitutive modelling of tailing materials poses specific questions that can potentially go beyond the traditional soil mechanics; the presence of a wide range of particle sizes together with their hydromechanical loading history of wetting/drying cycles during self-weight consolidation necessitates a careful revisiting of models adopted to represent their response. The strength and deformation of hard rock tailings are strongly impacted by their hydromechanical history, including recurrent cycles of desiccation and subsequent re-saturation often due to their stratified deposition methodology, which prevents the conventional simplification of behaviors solely to effective stress parameters. Earlier studies have effectively established the foundational principles for integrating the influence of matric suction into classical continuum soil mechanics. This has led to the development of various constitutive models for unsaturated soils, including the Barcelona Basic Model [1] and the Glasgow Coupled Model [2, 3], developed based on the Cam Clay theory. Compared to granular materials, the wide particle size distribution in hard rock tailings leads to a relatively wide water retention curve and a notable capacity for hydraulic hysteresis.

In this study, we explore how previously developed framework by Glasgow Coupled Model can be adopted for extending existing saturated constitutive models to unsaturated tailings. In particular, a simple double hardening model based on Mohr-Coulomb criterion and a modified Rowe's stress-dilatancy relationship is used for reference [5]. The model is extended by; (1) considering suitable hydraulic energy conjugates including the effect of matric suction, (2) adding two hydraulic yield surfaces, and (3) including proper hydro-mechanical coupling terms in the hardening laws. Figure 1 shows the schematics of the extended 3D yield surface in $(p^* - q - s^*)$. The study addresses different strategies for incorporating hydromechanical effects into the hardening of the yield surfaces. The trends predicted based on these strategies have been compared to triaxial tests performed on unsaturated Stava silt tailing undergoing hydro-mechanical stress path [7]. The comparison between model predictions and experimental results helps in identifying effective strategies for developing unsaturated constitutive models for partially saturated tailing materials.

References

[1] Alonso, E. E., Gens, A. & Josa, A. (1990). A constitutive model for partially saturated soils. G´eotechnique 40 (3) 405–430.

[2] Wheeler, S., Sharma, R. & Buisson, M. (2003). Coupling of hydraulic hysteresis and stress– strain behaviour in unsaturated soils. G´eotechnique 53 (1) 41–54.

[3] Lloret-Cabot, M., S´anchez, M., & Wheeler, S. J. (2013). Formulation of a three-dimensional constitutive model for unsaturated soils incorporating mechanical–water retention couplings. International Journal for Numerical and Analytical Methods in Geomechanics 37 (17) 3008- 3035.

[5] Wan, R. & Guo, P. (1998). A simple constitutive model for granular soils: modified stress dilatancy approach, Computers and Geotechnics 22 (2) 109–133.

[6] Mofrad, M., Pouragha, M. and Simms, P., 2023. Constitutive modelling of unsaturated gold tailings subjected to drying and wetting cycles. International Journal for Numerical and Analytical Methods in Geomechanics, 47(10), pp.1936-1949.

[7] Bella, G., 2017. Hydro-mechanical behaviour of tailings in unsaturated conditions.

Figures

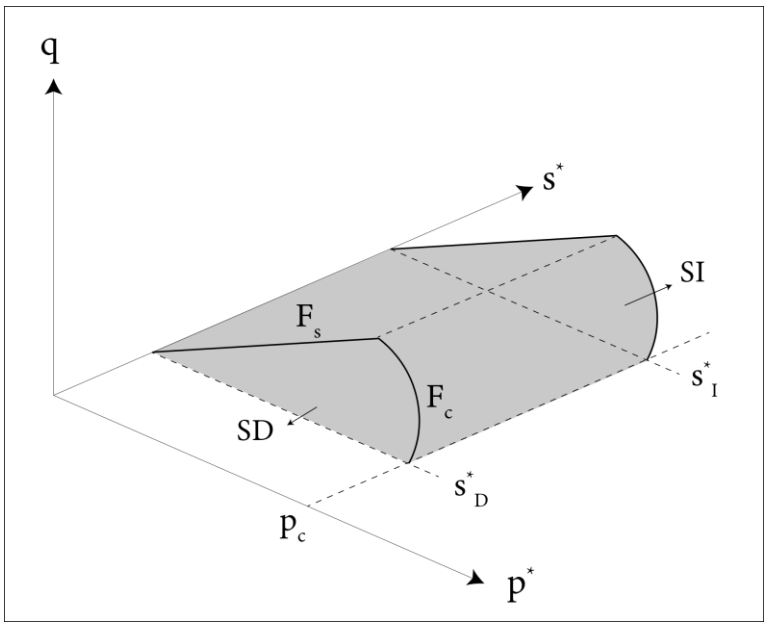

Figure 1: *Yield surface of modified WG model in* $(p^* - q - s^*)$ *stress space*

Terracotta: A Simple Hydrodynamic Model for Clays

Max Wiebicke, Itai Einav

Sydney Centre in Geomechanics and Mining Materials, School of Civil Engineering, The University of Sydney, 2006, Sydney, Australia

max.wiebicke@sydney.edu.au

Keywords: hydrodynamics, clay, rate dependency, constitutive model

Abstract

When describing the behaviour of clay, it is necessary to distinguish the crucial spatial scales of interest, which at the very least allow to separate atoms from clay particles and aggregates and finally the continuum. In Terracotta (Wiebicke and Einav, 2024) we have introduced a simple constitutive model that considers this scale separation. Following the hydrodynamic procedure (Landau and Lifshitz, 1987) and aspects from Granular Solid Hydrodynamics (Jiang and Liu, 2009), the model is build on a rigorous physical basis involving not only the first two laws of thermodynamics, but most importantly also the reciprocity of irreversible thermodynamic fluxes (Onsager, 1931). Despite the rigorous physics and thanks to some novel developments, the final model is surprisingly simple as shown in Figure 1, which is a complete representation of all model equations that are necessary for integration in a triaxial invariant form.

One novel development regarding clay models is the introduction of a meso-related temperature T_m to address the scale separation. This temperature accounts for the non-affine motion of meso-structures such as clay particles and aggregates. To describe the energy flow within the material, we employ the principle of two-stage irreversibility by Jiang and Liu (2009): the energy either flows directly to the micro-scale to increase the thermal temperature T or flows to the meso-scale where it increases T_m before sinking to the micro-scale. Following Onsager (1931), we describe the dissipative flows, that are the plastic strain rate and the viscous stress in the case of Terracotta, by linear relation to their thermodynamic driving forces. To identify the coefficients in these relations (commonly called transport coefficients) we proposed a novel scheme based on conventional steady-state observations.

The above choices lead to the surprising simplicity and predictability of Terracotta, which successfully captures a plethora of clay behaviours. By coupling the transport coefficients with the meso-related temperature, driven by viscous heating, the model also accounts for various rate-dependent phenomena during transient loading, as well as creep and relaxation processes. This is demonstrated in Figure 2, which presents an oedometer test on highly organic Gyttja, as reported by Niemunis and Krieg (1996). The experiment, which included a strain rate jump, served to study the behaviour during different creep stages following unloading, primary loading, or relaxation. The figure highlights how well the simple model captures the volumetric response in this complex test.

References

Jiang, Y. and Liu, M. (2009). Granular solid hydrodynamics. Granular Matter, 11, 139–156

Landau, L. D. and Lifshitz, E. M. (1987). Fluid Mechanics. Butterworth

Niemunis, A. and Krieg, S. (1996). Viscous behaviour of soil under oedometric conditions. Canadian Geotechnical Journal, 33, 159–168

Onsager, L. (1931). Reciprocal relations in irreversible processes I. Phys. Rev. 37 (4), 405

Wiebicke, M. and Einav, I. (2024). A simple hydrodynamic model for clay. Journal of the Mechanics and Physics of Solids, 192.

Figures

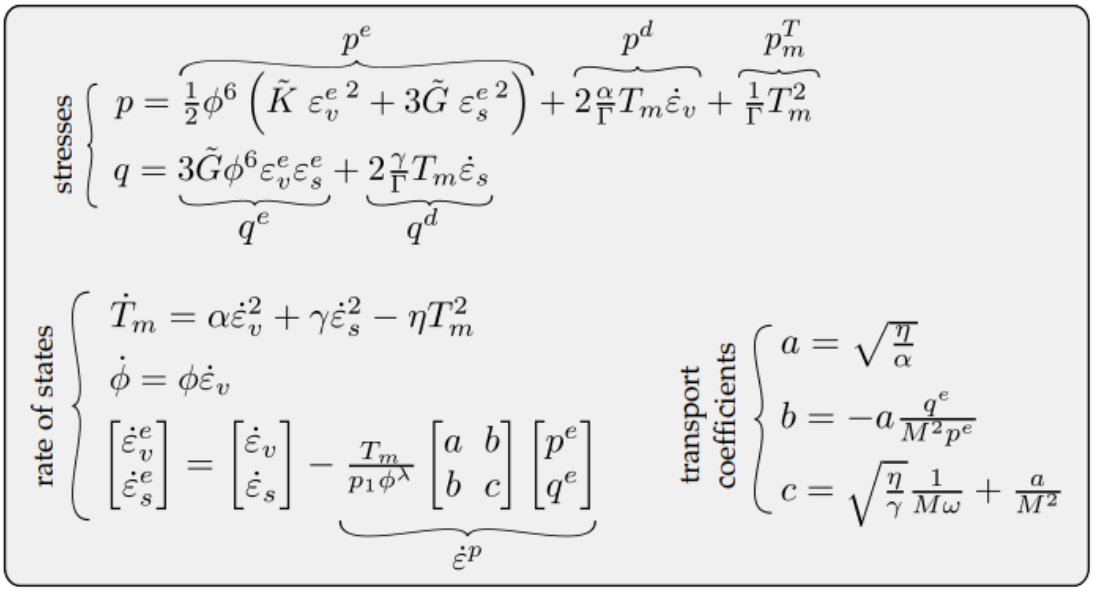

Figure 1*: The `Terracotta' model -- all the required equations. In the above, p and q denote the volumetric and deviatoric stress invariants; ε_v and ε_s the volumetric and deviatoric strain invariants; ϕ the solid fraction; T_m the meso-related temperature; superscripts e, d, T, p refer to the elastic, dissipative (or viscous), thermodynamic and plastic contributions; $\tilde{K}, \tilde{G}, M, \omega, p_1, \lambda$ are material constants; α, γ, η are coefficients, chosen to be constant in this paper, while Γ is a fixed coefficient that sets the unit of the meso-related temperature. (Wiebicke and Einav, 2024).*

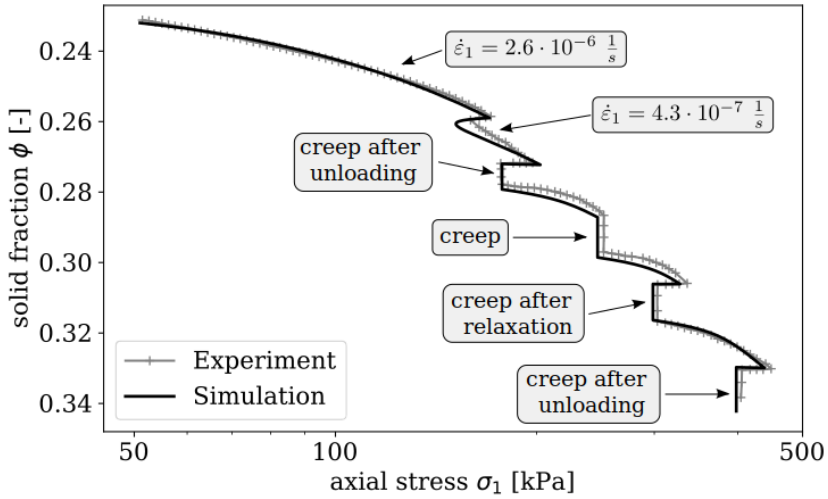

Figure 2: *Comprehensive oedometer test with one change in loading rate and different stages of unloading, relaxation and creep reported in Niemunis and Krieg (1996). (Wiebicke and Einav, 2024).*

Multiphysics Modelling of Slope Instability of a Large-Scale Physical Model

Maria Lazari, Matteo Camporese, Lorenzo Sanavia

Department of Civil, Environmental and Architectural Engineering, University of Padova, Padova, Italy

maria.lazari@unipd.it, matteo.camporese@unipd.it, lorenzo.sanavia@unipd.it

Keywords: multiphase porous media, rainfall-triggered shallow landslide, physical model, second-order work criterion, finite element modelling

Abstract

In this work, a rainfall-triggered landslide of a large-scale physical model is numerically simulated as a coupled variably saturated thermo-hydro-mechanical problem. The experimental slope consisted of a shallow layer of loose sand overlying a less permeable sandy clay (Figure 1a) and was equipped with TDR and WCR sensors to monitor the pore water pressure and moisture content response to the artificial rainfall, and with optical fibres to measure the landslide-induced strains and temperatures [1-2].

For the numerical simulation the geometrically linear finite element code Comes-Geo [3-4], enhanced with Taylor-Hood finite elements [5], is used. An advanced constitutive model for non-isothermal partially saturated soil [6] is adopted and the material parameters are calibrated based on available experimental data (more details can be found in [7]). In addition, the effective failure of the slope is described using the global (normalised) second-order work stability criterion [8].

It is shown that the numerical model can predict the experimental observations very well both in terms of hydraulic and mechanical behaviour (Fig. 2 and Fig. 3), and describes the triggering mechanism during the progressive failure of the physical slope. The numerical model also reproduces successfully the strain distribution obtained from the optical fibre elements in the experiment and that the failure process occurs in isothermal conditions (as novel contributions in the existing literature), emphasizing the importance of the multiphase and multiphysics modelling of landslides.

References

[1] Lora, M., Camporese, M., Troch, P.A. and Salandin, P. 2016. “Rainfall-triggered shallow landslides: infiltration dynamics in a physical hillslope model.” Hydrological Processes 30, 3239–3251.

[2] Schenato, L., Palmieri, L., Camporese, M., Bersan, S., Cola, S., Pasuto, A., Galtarossa, A., Salandin, P. and Simonini, P. 2017. “Distributed optical fibre sensing for early detection of shallow landslides triggering.” Scientific Reports, 7, 14686.

[3] Lewis, R.W. and Schrefler, B.A. 1998. The Finite Element Method in the Static and Dynamic Deformation and Consolidation of Porous Media. John Wiley, New York.

[4] Sanavia, L., Pesavento, F. and Schrefler, B.A. 2006. “Finite element analysis of non-isothermal multiphase geomaterials with application to strain localisation simulation.” Computational Mechanics, 37 (4), 331-348.

[5] Sanavia, L. and Cao, D.T. 2017. Modelling multiphase geomaterials at high temperatures in dynamics with application to strain localization and rapid catastrophic landslides. *Poromechanics VI: Proceedings of the Sixth Biot Conference on Poromechanics*. July 9-13, 2017, Paris, (F). Edited by Matthieu Vandamme; Patrick Dangla; Jean-Michel Pereira and Siavash Ghabezloo. 1866-1875.

[6] Bolzon, G. and Schrefler, B.A. 2005. "Thermal effects in partially saturated soils: a constitutive model." International Journal for Numerical and Analytical Methods in Geomechanics, 29(9), 861-877.

[7] Lazari, M., Camporese, M. and Sanavia, L. "Multphase and multiphysics modelling of a rainfall induced failure in an experimental hillslope." (under review)

[8] Lignon, S., Laouafa, F., Prunier, F., Khoa, H.D.V. and Darve, F. 2009. "Hydro-mechanical modelling of landslides with a material instability criterion." Géotechnique, 59(6), 513-524.

Figures

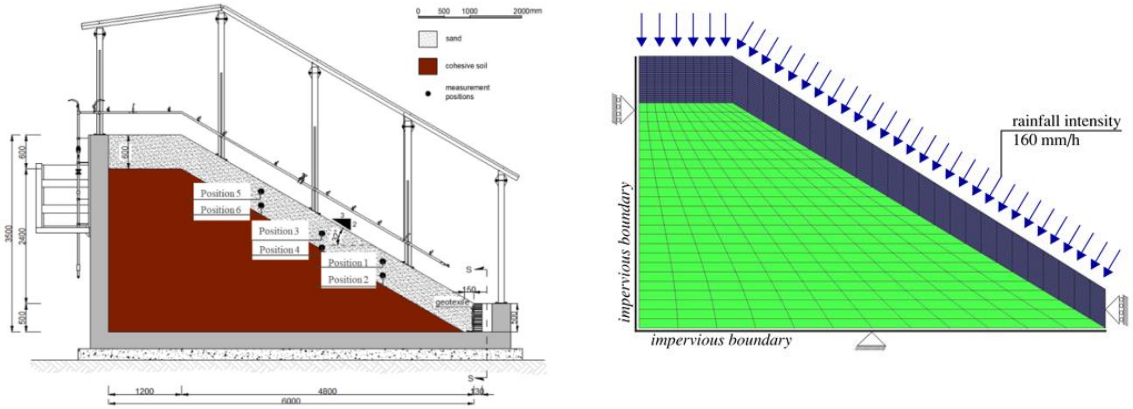

(a) (b)

Figure 1: *(a) Geometry, soil layers and monitoring points of the physical model [1] and (b) finite element mesh of the numerical model and boundary conditions.*

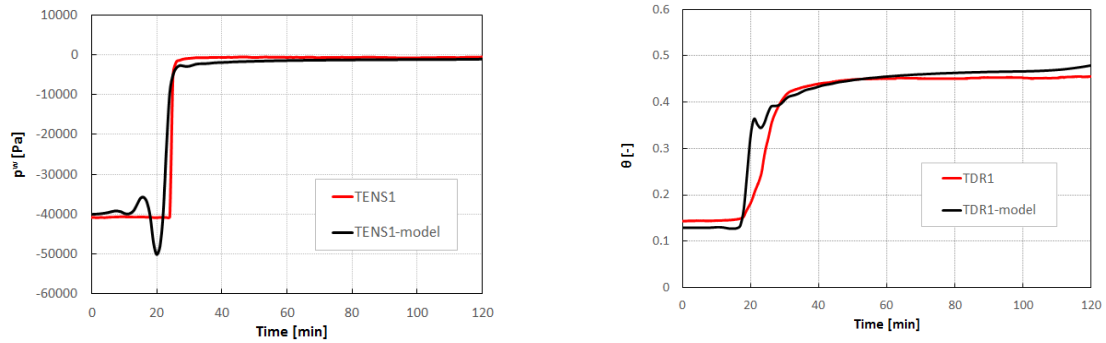

(a) (b)

Figure 2: *Comparison between the numerical and experimental (a) pore water pressure, p^w and volumetric water content, θ, at downslope position 1*

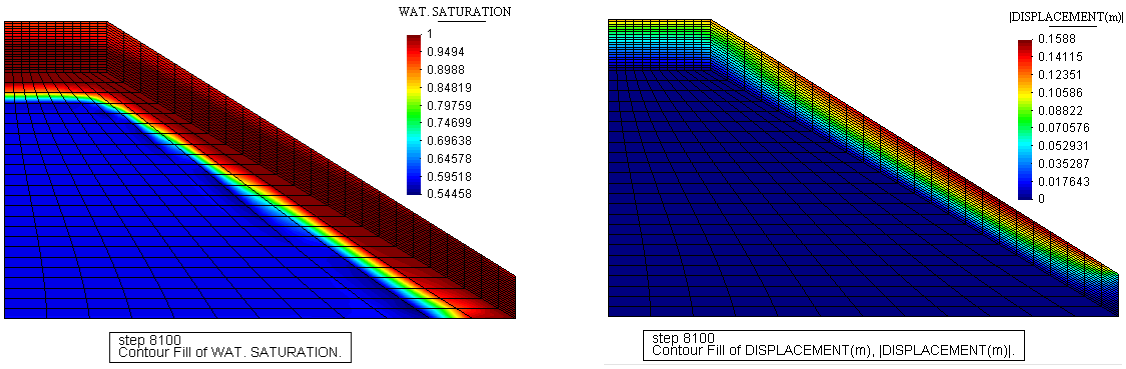

(a) (b)

Figure 3: *Contours of (a) water degree of saturation and (b) displacements at failure.*

Multiphysics Modelling of Desaturation Cracks in Non-Isothermal Multiphase Porous Media

Zechao Chen[1], Laura De Lorenzis[2], Lorenzo Sanavia[3]

[1]Center of Studies and Activities for Space (CISAS) - "G. Colombo", University of Padova, Italy

[2]Department of Mechanical and Process Engineering, ETH Zurich, Switzerland

[3]Department of Civil, Environmental and Architectural Engineering, University of Padova, Italy

zechao.chen@phd.unipd.it, ldelorenzis@ethz.ch, lorenzo.sanavia@unipd.it

Keywords: crack phase field approach, thermo-hydro-mechanical coupled model, Hybrid Mixture Theory, coupled finite element model

Abstract

The presented work aims at the development and validation of a general Thermo-Hydro-Mechanical crack phase-field numerical model able to study the nucleation and propagation of cracks induced by thermo-hydro-mechanical effects in multiphase porous materials. Earlier research ([1], [2], [3]) proposed a computational u-p_w-d model (displacements, u; water pressure, p_w; crack phase-field, d) for the simulation of liquid water flow, deformation and cracking in isothermal variably saturated porous media. That model assumed the passive gas phase assumption. However, a gaseous phase can play a role in the development of deforming porous materials, e.g. [5], as well as the non-isothermal processes, needing also to consider the phase change of the liquid water in water vapour and vice versa [5]. Hence, a non-isothermal multiphase and multiphysics porous media model including a gas phase composed by dry air and water vapour needs to be formulated and coupled with a fracture model for the solid skeleton. In this work, a new model to describe cracking in variably saturated deformable porous media including heat flow, flows of liquid water and gas and water evaporation/condensation is developed. The porous media model is based on the Hybrid Mixture Theory developed in [5] implemented in [4]. This model is sequentially coupled with the brittle crack phase-field model developed in [1], [2], [3] and is named as u-p_c-p_g-T-d model in the following (with p_c and p_g the capillary and gas pressure). The staggered algorithm adopted is summarised in Figure 1.

This model is validated by simulating test cases from the literature, including two numerical benchmark tests: (i) a free desaturation test and (ii) the corresponding restrained desaturation one [1], whose results are now presented. (i) is a u-p_c-p_g problem, known in literature as Liakopoulos test, which is the desaturation of an initially water saturated vertical column of sand. Figure 2(a) presents the comparison between the vertical displacements obtained with the Comes-Geo u-p_c-p_g-T finite element code [5], [4] and the u-p_c-p_g-T-d model of Figure 1. The coincidence of the two numerical solutions is displayed. The numerical results obtained by solving the corresponding restrained desaturation test (ii) are presented in Figures 2(b) and 2(c). In this case the vertical displacement of the upper horizonal surface is prevented, to induce traction in the desaturating upper part of the column [1]. Figure 2(b) shows the development of cracks in the upper part of the column within the zone where capillary pressures are formed, Figure 2(c).

The u-p_c-p_g-T-d model of Figure 1 is going to be applied to the simulation of a restrained desiccation test of an initially water saturated clay sample applying a convective thermal boundary condition [4], to simulate more realistically the experimental desiccation test solved in [1] (in which an outgoing water flux boundary condition was applied to simulate the evaporation of the liquid water from the clay sample).

References

[1] Cajuhi, T., Sanavia, L., De Lorenzis, L. (2017). Phase-field modeling of fracture in variably saturated porous media. Computational Mechanics, 61(3), 299-318.

[2] Gavagnin, C., Sanavia, L., De Lorenzis, L. (2020). Stabilized mixed formulation for phase-field computation of deviatoric fracture in elastic and poroelastic materials. Computational Mechanics. 65, 1447–1465.

[3] Chenyi, L., Sanavia L., De Lorenzis L. (2023). Phase-field modeling of drying-induced cracks: choice of coupling and study of homogeneous and localized damage. Comput. Methods Appl. Mech. Engrg.410, 115962, https://doi.org/10.1016/j.cma.2023.115962

[4] Sanavia, L., Pesavento F., Schrefler, B.A. (2006). Finite element analysis of non-isothermal multiphase geomaterials with application to strain localisation simulation, Computational Mechanics, 37(4), 331-348.

[5] Lewis, R. W., Schrefler, B. A. (1998). The Finite Element Method in the Static and Dynamic Deformation and Consolidation of Porous Media (Second). Chichester, UK: John Wiley & Sons.

Figures

Initialization $(t = t_0 = 0)$: $\bar{\mathbf{u}}, \bar{\mathbf{t}}, \bar{p}, \bar{q}, \bar{d}, \mathcal{H}, \mathrm{T} = 0$;
for $n = 0 : N - 1$ *do*
  compute $\Psi^+(t = t_{n+1})$
  if $\Psi^+ > \mathcal{H}_n$ **then**
    $\mathcal{H}_{n+1} \leftarrow \Psi^+(t = t_{n+1})$;
  else
    $\mathcal{H}_{n+1} = \mathcal{H}_n$;
  end
  solve $d_{n+1}(\mathcal{H}_{n+1})$;
  solve $\mathrm{u}-p_c-p_g-\mathrm{T} := \mathbf{U}_{n+1}(d_{n+1})$;
end

Figure 1: *Algorithmic solution procedure for solving the u-p_c-p_g-T-d system of finite element equations (see [1] for the meaning of the terms of this figure).*

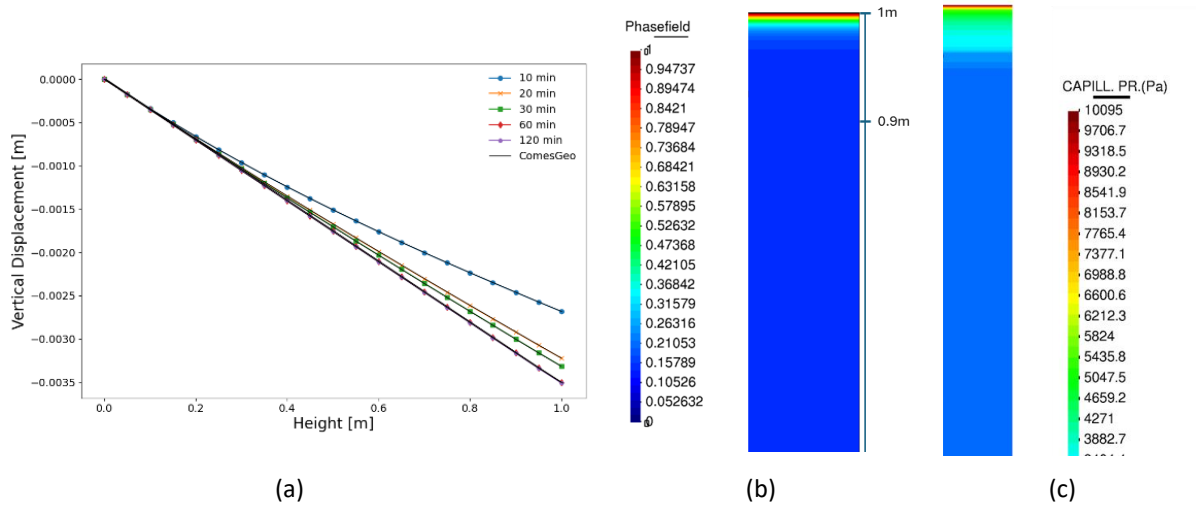

(a) (b) (c)

Figure 2: *(a) Vertical displacements along the column in the free desaturation test (Liakopoulos test), (b) Phase-field and (c) Capillary pressure (Pa) in the upper part of the column of the restrained desaturation test (ii).*

Three-Dimensional Numerical Study on the Internal Erosion Mechanism of the Agly Dike

Zezhi Deng[1,2], Nadia Benahmed[2], Laurence Girolami[2,3], Pierre Philippe[2], Stephane Bonelli[2], Gang Wang[1]

[1]School of Civil Engineering, Chongqing University, Chongqing, China

[2]INRAE, Aix-Marseille Université, UMR RECOVER, Aix-en-Provence, France

[3]GéHCO, Campus Grandmont, Université de Tours, Tours, France

zezhi.deng@inrae.fr

Keywords: suffusion, internal erosion; geophysical investigation; finite element analysis

Abstract

In this study, a large-scale three-dimensional (3D) numerical simulation was conducted to explore the mechanisms responsible for the observed erosion signatures (sinkholes, leaks, and sand-boils) at the Agly dike. A numerical model with dimensions of 1400 m × 400 m × 100 m (Fig. 1) was developed based on the stratigraphic structures revealed by geophysical measurements (EMI and ERT) and geotechnical investigations [1]. Notably, this model captures the variations in stratigraphic structures from upstream to downstream. A multi-species transport finite element method (FEM) was employed to simulate the seepage in the entire field and the suffusion process [2] in the erodible sandy gravel sediments. The numerical description of suffusion was formulated within a continuum four-constituent mixture framework, and the erosion process was quantified by a novel erosion model for sandy gravels [3]. The governing equations were solved using the Multiphysics FEM program COMSOL Multiphysics. Seepage and suffusion dynamics were investigated under the periodic flood events with monitored water level. The simulation results indicate that, during the peak flood, there is a high-velocity zone at the constrictions where paleo-valley tapering into paleo-channel, which can lead to intense suffusion and potential contact erosion. The comparison between the erosion zones and the on-site distribution of sinkholes (Fig. 2) suggests that this mechanism could be responsible for the occurence of sinkholes. In addition, the high pore pressure acting on the bottom of the silty sand surface layer during the peak flood were found to potentially cause the leaks and sand-boils, as the artesian and uplift boundaries in the surface layer aligning with the on-site distributions of these erosion signatures. (Fig. 2). This study emphasizes the pivotal role of stratigraphic features on internal erosion, and demonstrate the effectiveness of integrating geophysical investigations with numerical simulation in analyzing erosion behaviors in practical engineering.

References

[1] Girolami, L., Bonelli, S., Valois, R., Chaouch, N., Burgat, J. On Internal Erosion of the Pervious Foundation of Flood Protection Dikes. Water. 2023, 15: 3747.

[2] Nguyen, C. D., Benahmed, N., Ando`, E., Sibille, L., and Philippe, P. (2019). Experimental in- vestigation of microstructural changes in soils eroded by suffusion using x-ray tomography. *Acta Geotechnica*, **14**, 749–765.

[3] Deng, Z., Wang, G., Jin, W., Tang, N., Ren, H., Chen, X. Characteristics and quantification of fine particle loss in internally unstable sandy gravels induced by seepage flow. Engineering Geology, 2023, 321: 107150.

Figures

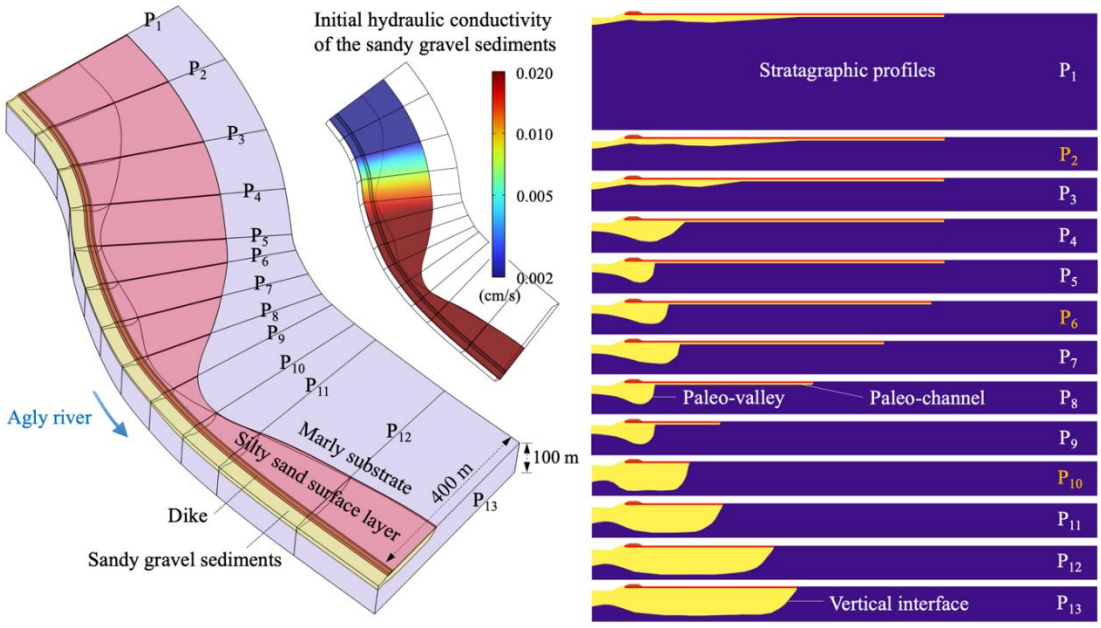

Figure 1: *Idealized model used for FEM simulation.*

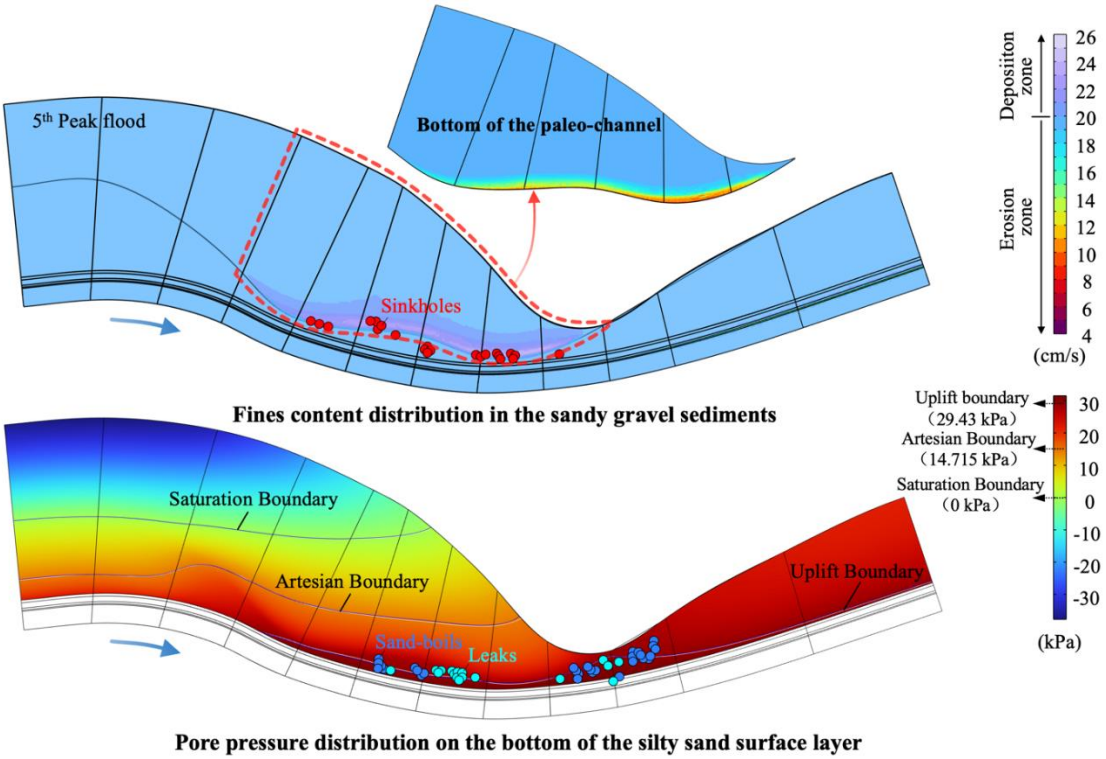

Figure 2*: Fines content and pore pressure fields at the peak flood and the on-site distribution of erosion signatures.*

A Novel Testing System for Particle-Scale Investigation of Clay in Nano-X-Ray Imaging Instruments

Angela Casarella[1], Anders Karlsson[1], Gustave Pinzón[2], Olga Stamati[2], Julie Villanova[2], Jelke Dijkstra[1]

[1]Chalmers University of Technology, Department of Architecture and Civil Engineering

[2]ESRF – The European Synchrotron Radiation Facility

angela.casarella@chalmers.se

Keywords: X-ray tomography, digital volume correlation, in-situ testing, clay micromechanics

Abstract

The mechanical behaviour of geomaterials is fundamentally governed by the interactions between individual particles. Understanding these interactions is crucial in soil mechanics, as it allows researchers to interpret experimental data, elucidate fundamental behavioural mechanisms, inform the development of continuum-based constitutive models, and advance simulations using the discrete-element method (DEM).

Significant strides have been made in the micromechanics of granular materials, particularly through the use of X-ray computed (micro-)tomography (XCT/XμCT). This technology has been instrumental in characterizing the internal deformation of coarse-grained materials, such as sand, during hydro-mechanical testing, with pixel size reaching just a few micrometres (Lenoir et al., 2007; Matsushima et al., 2010; Hall et al., 2010; Andò et al., 2012).

In contrast, progress in the micromechanical study of fine-grained soils, such as clay, has been slower due to the complexities involved in observing the structural evolution of clay particles and their assemblies under mechanical and environmental loading. This challenge has resulted in a scarcity of experimental data that directly links particle-scale mechanisms to the macroscopic engineering properties of these soils.

Recent advancements in Nano-X-ray Computed Tomography (nano-XCT), particularly with the advent of 4th generation synchrotron sources, have opened new avenues for research. These instruments provide the submicron spatial resolution necessary to study the four-dimensional (3D spatial + time) evolution of soil fabric at the particle level in fine-grained soils, allowing observations in their natural in-situ state.

This study introduces a novel testing system (Figure 1) specifically designed to investigate the kinematics of individual clay particles and clusters under one-dimensional (1D) compression. The system accommodates samples with diameters as small as 300 μm, enabling the capture of high-resolution images with voxel sizes down to 50 nm. This setup allows for displacement-controlled loading under both drained and undrained conditions, all within a simple and efficient assembly that positions samples close to the detector.

An example application of this system is presented, showcasing the monitoring of the three-dimensional (3D) fabric evolution in saturated samples of calcined Speswhite kaolin clay under 1D compression. The study also discusses potential improvements to the system for future research, aiming to enhance our understanding of the behaviour of fine-grained soils under various initial and loading conditions.

References

Lenoir, N., Bornert, M., Desrues, J., Bésuelle, P. & Viggiani, G. (2007). Volumetric digital image correlation applied to X-ray microtomography images from triaxial compression tests on argillaceous rock. Strain 43, No. 3, 193–205.

Matsushima, T., Uesugi, K., Nakano, T. & Tsuchiyama, A. (2010). Visualization of grain motion inside a triaxial specimen by micro X-ray CT at SPring-8. In Advances in X-ray tomography for geomaterials (eds J. Desrues, G. Viggiani and P. Bésuelle), pp. 255–261. London, UK: John Wiley & Sons, Ltd.

Hall, S. A., Bornert, M., Desrues, J., Pannier, Y., Lenoir, N., Viggiani, G. & Bésuelle, P. (2010). Discrete and continuum analysis of localised deformation in sand using X-ray CT and volumetric digital image correlation. Géotechnique 60, No. 5,315–322.

Andó, E., Viggiani, S. H. G., Desrues, D. & Bésuelle, P. (2012). Grain-scale experimental investigation of localised deformation in sand: a discrete particle tracking approach. Acta Geotech. 7, No. 1, 1–13.

Figures

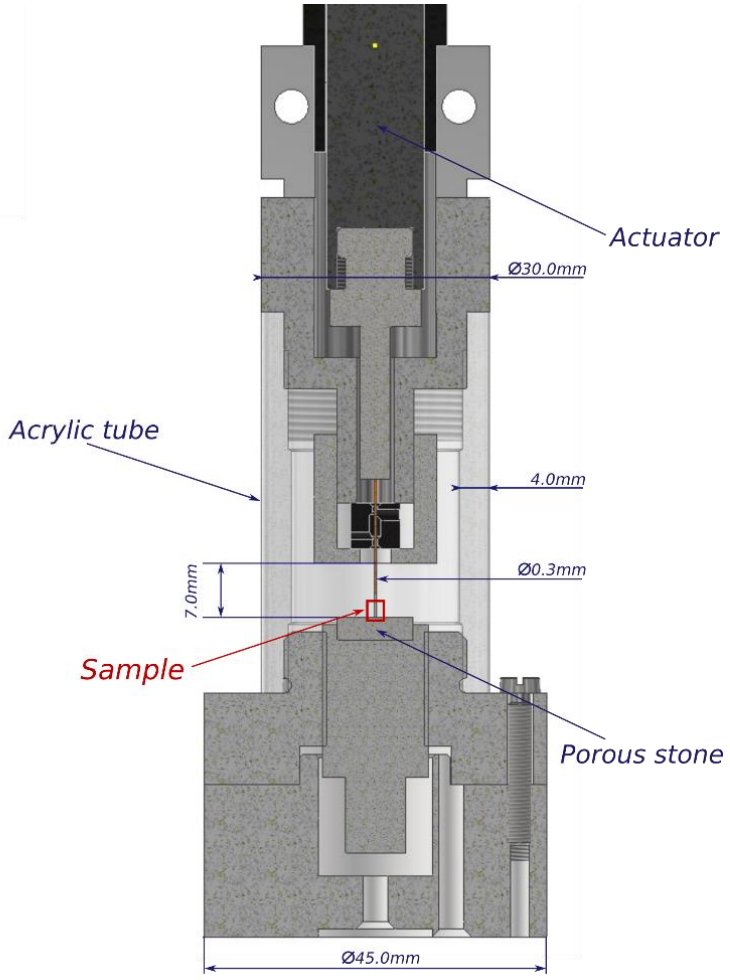

Figure 1: *Schematic diagram of the 1D compression cell key components.*

DEM-Based Model of PVC Geomembranes to Understand the Mechanical Behavior

Nesrin Akel[1], Antoine Wautier[1], François Nicot[3], Guillaume Stoltz[1], Nathalie Touze-Foltz[2]

[1]INRAE, Aix Marseille Univ, RECOVER, Aix-en-Provence, France

[2]Université Paris-Saclay, INRAE, SDAR, Jouy-en-Josas, France

[3]Université Savoie Mont-Blanc, ISTerre, Le Bourget-du-Lac, France

nesrin.akel@inrae.fr

Keywords: PVC Geomembrane, mesoscale analysis, Discrete Element Method (DEM), tensile properties

Abstract

Over the decades, geomembranes have become indispensable in modern engineering, specifically as hydraulic barriers in a wide range of hydraulic and geotechnical structures. PVC geomembrane, a type of geomembranes, is preferred over other barrier materials for their flexibility and ability to withstand significant deformation. However, they face challenges from unexpected mechanical actions (e.g., earthquake, rocks falling, animals; displacement by wind wave action), which can induce tensile stress, leading to indentations, or even holes and tears (Abdelaal et al. 2014; David Frost et al. 2012; Hornsey and Wishaw 2012; Luciani and Peila 2019; Müller and Wöhlecke 2019; Rowe et al. 2019).

Understanding the mechanisms behind this macroscopic behavior remains challenging, necessitating further investigation at the microstructural level. Specifically, Such research could provide deeper insights into the complex behavior (i.e., ultimate strength, strain, stiffness) of PVC geomembranes under different tensile rates that may occur under in-situ condition, as noted by Akel et al. (2024).

To address this challenge, a 3D micromechanical model has been developed in this study, accounting for the nanoscale morphological structure of PVC geomembranes. This innovative approach models the geomembrane as a semi-crystalline assembly of polymers embedded in a matrix of plasticizers, using the Discrete Element Method (DEM) to track the elementary mechanisms at the mesoscale. By bridging the gap between microscopic deformation and macroscopic behavior, this study paves the way for a deeper investigation into how microstructural features influence the mechanical behavior of geomembranes.

References

Abdelaal, F. B., R. K. Rowe, and R. W. I. Brachman. 2014. "Brittle rupture of an aged HPDE geomembrane at local gravel indentations under simulated field conditions." *Geosynthetics International*, 21 (1): 1–23. https://doi.org/10.1680/gein.13.00031.

Akel, N., A. Wautier, G. Stoltz, N. Touze-Foltz, and F. Nicot.2024 "Rate-Dependent Tensile Response of Polyvinyl Chloride Geomembranes."*Geotextiles and Geomembranes Journal*. (Under review).

David Frost, J., D. Kim, and S.-W. Lee. 2012. "Microscale geomembrane-granular material interactions." *KSCE J Civ Eng*, 16 (1): 79–92. https://doi.org/10.1007/s12205-012-1476-x.

Hornsey, W. P., and D. M. Wishaw. 2012. "Development of a methodology for the evaluation of geomembrane strain and relative performance of cushion geotextiles." *Geotextiles and Geomembranes*, 35: 87–99. https://doi.org/10.1016/j.geotexmem.2012.05.002.

Luciani, A., and D. Peila. 2019. "Tunnel Waterproofing: Available Technologies and Evaluation Through Risk Analysis." *Int J Civ Eng*, 17 (1): 45–59. https://doi.org/10.1007/s40999-018-0328-6.

Müller, W. W., and A. Wöhlecke. 2019. "Zero leakage? Landfill liner and capping systems in Germany." *Environmental Geotechnics*, 6 (3): 162–170. https://doi.org/10.1680/jenge.16.00031.

Rowe, R. K., M. S. Morsy, and A. M. R. Ewais. 2019. "Representative stress crack resistance of polyolefin geomembranes used in waste management." *Waste Management*, 100: 18–27. https://doi.org/10.1016/j.wasman.2019.08.028.

Figures

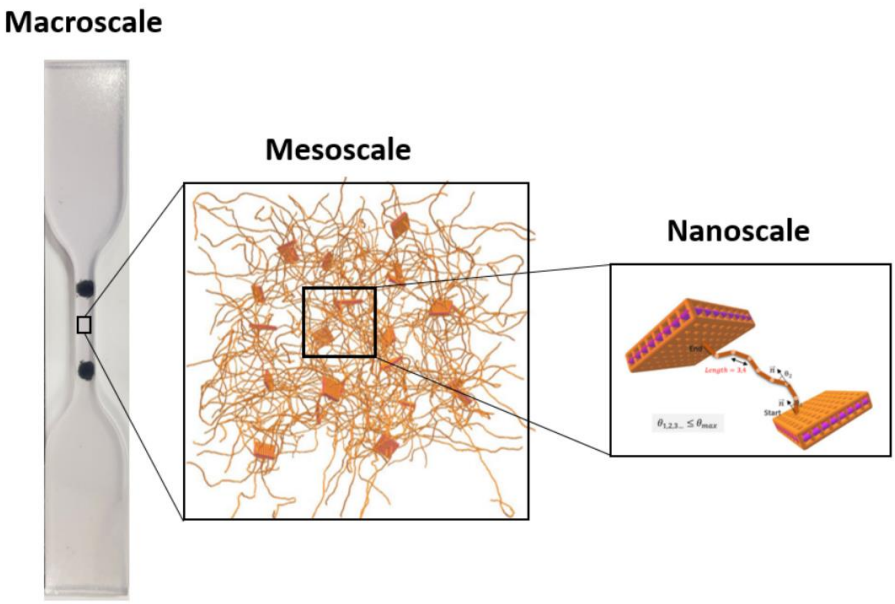

Figure 1: *DEM-based model of PVC geomembrane, incorporating its semi-crystalline microstructure, including crystallites, the amorphous regions, and the plasticizer.*

The Sand Atlas

Ilija Vego, Benjy Marks

School of Civil Engineering, The University of Sydney, Sydney, NSW, 2006, Australia

ilija.vego@sydney.edu.au

Keywords: granular materials, imaging, numerical simulation, DEM, mesh, open source

Abstract

The Sand Atlas is a recently launched open-access digital repository that provides researchers with image-based data on the shape and morphology of various particles and grains. This initiative aims to address the potential need for detailed grain shape descriptors, which are essential for accurately simulating the behaviour and response of granular materials [1].

The creation of the Sand Atlas originates from the extensive application of imaging techniques, such as tomography, MRI, and structured light scanning, to explore and understand the shape and morphology of geomaterials. X-ray tomography in particular enables exploration of the microstructure of grains at relatively high resolutions, either at synchrotron facilities [2] or in laboratory scanners, which have seen recent advances in resolution and speed [3]. Following the image acquisition, each grain within the assemblies is labelled using a combination of image processing and machine learning techniques [4-6]. This step is crucial for enabling the accurate identification and isolation of individual grains within the dataset. The Sand Atlas relies on the expertise of its contributors to minimise errors in this process.

Once the grains are labelled, surface meshes are generated using openVDB, a C++ library designed for efficient manipulation of sparse, time-varying volumetric data [7]. Meshes are created at varying densities to meet different computational needs. One mesh is generated directly from the original voxel-based 3D arrays, but this can be rather inefficient for numerical simulations. For this reason, the Sand Atlas provides lower-density meshes with 100, 30, 10, and 3 elements along the shortest axis of the grain. An example of these meshes for Hostun particle sand [8] is illustrated in Figure 1.

The obtained meshes are then used to measure the grain properties using scikit-image [5], SPAM [6], and SHAPE (SHape Analyser for Particle Engineering) [9], which include functions to extract and quantify shape descriptors from three-dimensional particles. The aim is to provide a detailed characterisation of the grains, including metrics that quantify their geometry and morphology.

All datasets are uploaded to the Sand Atlas server and made available for download on the website, contributing to a growing collection of sand samples from a wide range of environments. The collection features “traditional” samples from terrestrial sources such as Houston and Ottawa sands, as well as samples from undersea environments and extraterrestrial materials. It also includes unique and unconventional samples like the Caicos Ooids, and non-geological grains such as couscous and coffee beans. The downloadable data includes meshed grains in .STL format, level set files in .VDB format, the original labelled images, the raw data from which the images are derived, and a .CSV table with major descriptors.

Acquiring images requires significant resources, time, and expertise. The Sand Atlas aims to support researchers by providing readily accessible and open-access datasets and streamline the

integration of image-based data into numerical studies. Additionally, it could serve as a reference for imaging practices, offering standards that help ensure consistency.

Contributions to the Sand Atlas are welcomed. For more information, suggestions and to access the data, visit the Sand Atlas website (https://sand-atlas.scigem.com).

References

[1] Kawamoto, Reid, *et al*. "All you need is shape: Predicting shear banding in sand with LS- DEM." *Journal of the Mechanics and Physics of Solids* 111 (2018): 375-392.

[2] Villanova, J., *et al*. "Synchrotron X-Ray Nano-Analysis for Material Science: from 2D to 4D." *Microscopy and Microanalysis* 30.Supplement_1 (2024).

[3] Sansom, Travers M., *et al*. "Low radiodensity µCT scans to reveal detailed morphology of the termite leg and its subgenual organ." *Arthropod Structure & Development* 70 (2022): 101191.

[4] Van der Walt, Stefan, *et al*. "scikit-image: image processing in Python." *PeerJ* 2 (2014): e453.

[5] Berg, Stuart, *et al*. "Ilastik: interactive machine learning for (bio) image analysis." *Nature methods* 16.12 (2019): 1226-1232.

[6] Stamati, Olga, *et al*. "Spam: software for practical analysis of materials." *Journal of Open Source Software* 5.51 (2020): 2286.

[7] Museth, Ken, *et al*. "OpenVDB: an open-source data structure and toolkit for high-resolution volumes." *Acm siggraph 2013 courses*. 2013. 1-1.

[8] Wiebicke, Max, *et al*. "On the metrology of interparticle contacts in sand from x-ray tomography images." *Measurement Science and Technology* 28.12 (2017): 124007.

[9] Angelidakis, Vasileios, Sadegh Nadimi, and Stefano Utili. "SHape Analyser for Particle Engineering (SHAPE): Seamless characterisation and simplification of particle morphology from imaging data." *Computer Physics Communications* 265 (2021): 107983.

Figures

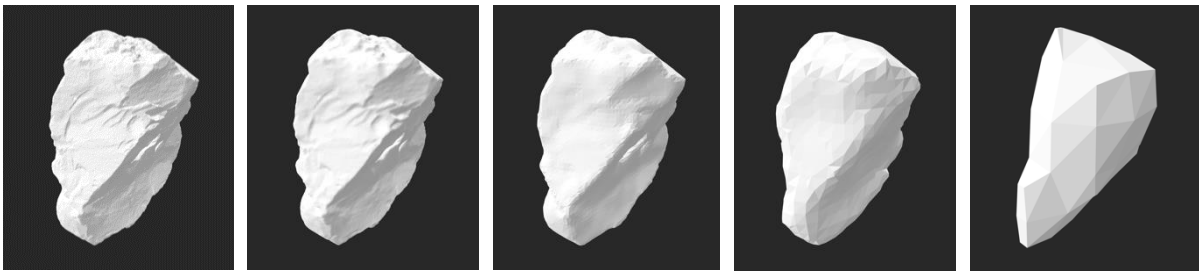

Figure 1: *Example of the meshing procedure for a Hostun particle sand grain [8]. The left image displays voxel-based meshing with a voxel size of 1 µm. The right images illustrate meshes with densities of 100, 30, 10, and 3 elements along the shortest axis.*

Altering the Macroscopic Behavior of Granular Materials by Adding Fines

Abhijit Hegde, Nadia Benahmed, Antoine Wautier, Pierre Philippe

INRAE, Aix Marseille Univ., RECOVER 3275 Route de Cézanne, CS 40061, 13182 Aix-en-Provence Cedex 5, France

abhijit.hegde@inrae.fr; nadia.benahmed@inrae.fr; antoine.wautier@inrae.fr; pierre.philipee@inrae.fr

Keywords: fines injection, suffusion permeameter, moist tamping, undrained triaxial tests

Abstract

It has been well established that the complex mechanical properties displayed by granular materials arise from the intricate interaction between the particles at the level of contacts. So, it follows that one should be able to make changes at the level of particle contacts and expect a change in the mechanical response at the ensemble level [1]. In our experimental work, this idea has been put to test by trying to alter the contact scale mechanics by making use of fines. Two sets of granular assemblies are prepared; in the first case, granular mixtures are prepared by injecting a granular column consisting of only coarse-grains with fines, and in the second set, the coarse samples are reconstituted at the same fines concentration using the moist tamping method. We choose Hostun 1 /2.5 sand (D_{50} ~ 1.71mm) for the coarse column and we have used sieved Fontainebleau sand falling in the size range 0.1-0.125mm for fines. Injection experiments are performed using a Suffusion Permeameter Device (Figure. 1) [2], and the final fines concentration in the injected sample is close to 4-5%. This is followed by subjecting the injected and reconstituted samples to triaxial tests under undrained conditions. The results of these experiments are presented in Figs. 2-3, and indicate a clear distinction in the mechanical behavior of the injected and reconstituted samples. The reconstituted samples are seen to partially liquefy before the commencement of the dilation phase whereas for the injected sample, the stresses are seen to monotonically increase without showing any tendency to liquefy. The stress paths in the p'-q space also tell a similar story with the reconstituted samples being more contractive than the injected samples. We hypothesize that this difference is a direct manifestation of the changes we have been able to affect at the microscopic level. In the reconstituted samples we expect the fines to occupy positions in between the coarse particles as shown in Figure 4, whereas for the injected samples, fines are only present at the pore throats, adjacent to the contact points. Therefore, the reconstituted samples are more contractive while the injected samples are stabilized by the additional constraint provided by the aspecting fines. Thus, indeed we can expect to engineer granular materials with desired properties by directly the influencing the mechanics at the level of particle contacts.

References

1. Antoine Wautier, Stéphane Bonelli, and François Nicot. (2019). Rattlers contribution to granular plasticity and mechanical stability. International Journal of Plasticity, 112:172–193.

2. Nguyen, C. D., Benahmed, N., Andò, E., Sibille, L., & Philippe, P. (2019). Experimental investigation of microstructural changes in soils eroded by suffusion using X-ray tomography. Acta Geotechnica, 14, 749-765NSSGA (2013).

Figures

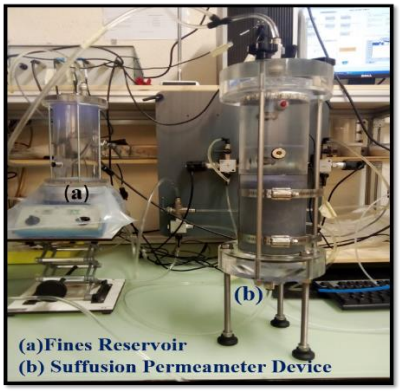

Figure 1: *Experimental Setup.*

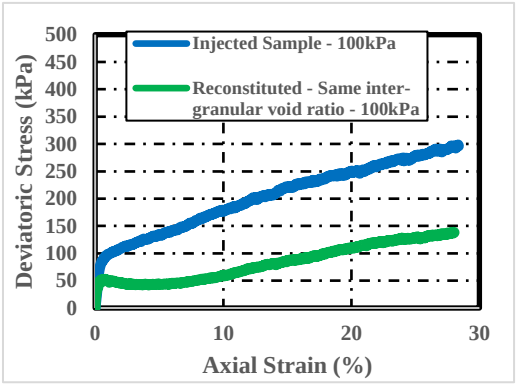

Figure 2: *Comparison of the undrained mechanical behavior between injected and reconstituted samples in the q-ϵ_a space.*

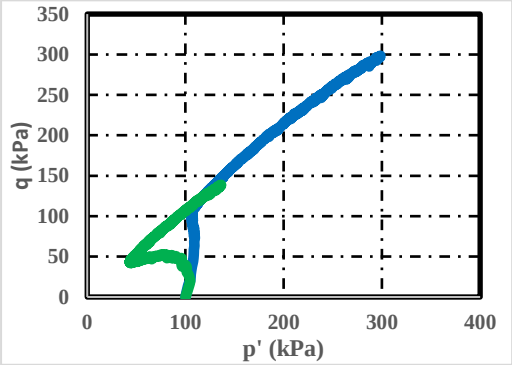

Figure 3: *Undrained stress path of injected and non-injected samples.*

Figure 4: *Proposed micromechanics behind the observed mechanical behavior.*

Advances in Earthquake Prevention: Controlling Slip-Rate in Seismic Faults and Seismicity Rate in Underground Reservoirs

Diego Gutiérrez-Oribio, Alexandros Stathas, Ioannis Stefanou

Nantes Universite, Ecole Centrale Nantes, CNRS, GeM, UMR 6183, F-44000, Nantes, France

diego.gutierrez-oribio@ec-nantes.fr, alexandros.stathas@ec-nantes.fr, ioannis.stefanou@ec-nantes.fr

Keywords: earthquake prevention, control theory, energy production, Artificial Intelligence

Abstract

Earthquakes pose significant risks, causing widespread damage and loss of life. This work presents two cutting-edge approaches that leverage control theory to mitigate seismic activity.

In the first one [1], we introduce a novel method to control the slip rate of a mature seismic fault using fluid injection as the control input. By managing the set-valued Coulomb coefficient, this approach aims to prevent earthquake-like behavior, offering a proactive measure to reduce seismic risks (see Fig 1).

In the second result [2], we focus on underground reservoirs where fluid injections, often used for clean energy production, can induce seismicity. Our control strategy minimizes the seismicity rate while ensuring continued energy production, effectively balancing safety and sustainability. Furthermore, a reinforcement learning approach [3] is also used for selecting the controller parameters in real-time to operate with minimal control power (see Fig. 2).

Both methods demonstrate how control theory provides a powerful framework for addressing complex geomechanical challenges, particularly in environments with inherent uncertainties and disturbances. These advances represent a significant step forward in the prevention and management of earthquake risks.

References

[1] D. Gutiérrez-Oribio, I. Stefanou, and F. Plestan, “Passivity-based control of underactuated mechanical systems with coulomb friction: Application to earthquake prevention”, Automatica, vol. 165, no. 111661, 2024. doi: 10.1016/j.automatica.2024.111661.

[2] D. Gutiérrez-Oribio and I. Stefanou, “Insights of using control theory for minimizing induced seismicity in underground reservoirs”, Geomechanics for Energy and the Environment, p. 100 570, 2024, doi: 10.1016/j.gete.2024.100570.

[3] D. Gutiérrez-Oribio, A. Stathas, and I. Stefanou, “AI-Driven approach for sustainable extraction of earth’s subsurface renewable energy while minimizing seismic activity”, 2024, doi: 10.48550/arXiv.2408.03664.

Figures

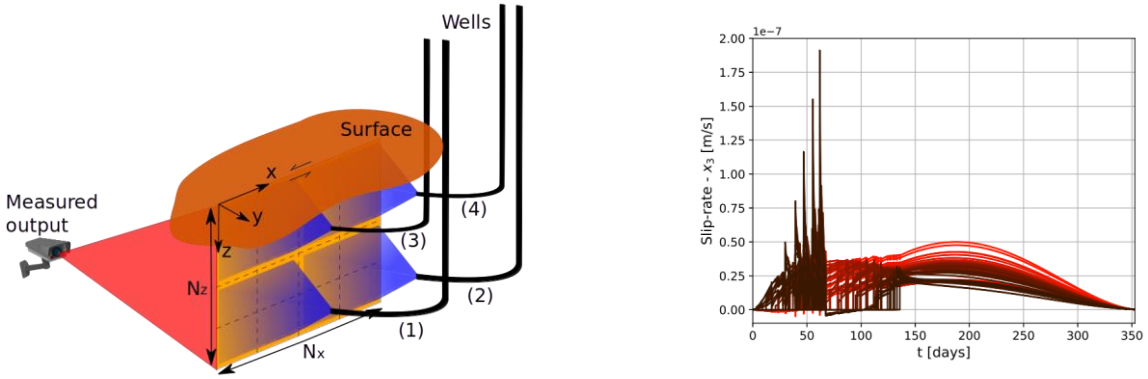

***Figure 1**: Earthquake prevention by controlling slip-rate of a fault by fluid injection.*

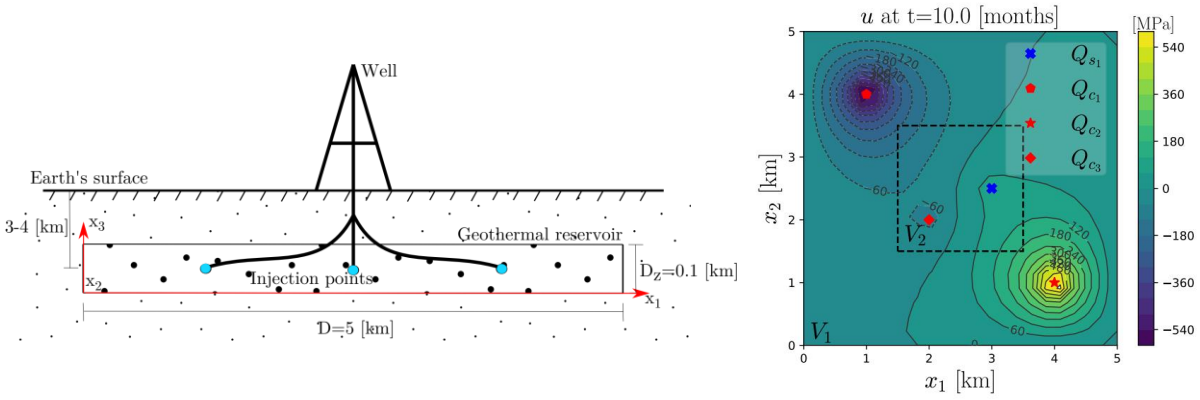

***Figure 2**: Induced seismicity minimization in an underground reservoir for energy production and storage.*

On the Emergence of Micromorphic Continua through the Upscaling of a Cauchy Medium

Alexandros Stathas, Ioannis Stefanou

Ecole Centrale de Nantes

alexandros.stathas@ec-nantes.fr

Keywords: micromorphic continua, asymptotic homogenization, upscaling, periodic unfolding

Abstract

Modern technological advances in material manufacturing have given rise to innovative composite geomaterials whose behavior is not completely understood in the framework of the classical theory of simple Cauchy continua (see [1]). Instead, these materials are often modelled through the use of higher order continuum theories such as second gradient theories (see [2]) or the theory of micromorphic continua (see [3]). However, while the emergence of higher gradient theories is understood in the framework of asymptotic homogenization this is not yet the case for micromorphic continua. In this work we present a method for the emergence of micromorphic continua from the classical Cauchy continuum using periodic unfolding (see [4]). We achieve this by searching the solution of the variational problem of classical elasticity in a richer functional space by expanding the test function space. This is done through the use of a suitable *lever* function (see also Figure 1), which allows for the emergence of the generalised stresses (e.g. moments) in the final two-scale variational problem and the suitable determination of consistent boundary conditions. Our approach allows -by means of numerical analyses- for the determination of the material properties of such micromorphic continua without further simplifying assumptions.

References

[1] Lee, W., Kang, D. Y., Song, J., Moon, J. H., & Kim, D. (2016). "Controlled unusual stiffness of mechanical metamaterials." *Scientific reports* 6.1 (2016): 20312.

[2] Mindlin, R. D. (1965). Second gradient of strain and surface-tension in linear elasticity. *International journal of solids and structures*, *1*(4), 417-438.

[3]Eringen, A. C. (1966). Linear theory of micropolar elasticity. *Journal of Mathematics and Mechanics*, 909-923.

[4]Cioranescu, D., Damlamian, A., & Griso, G. (2008). The periodic unfolding method in homogenization. *SIAM Journal on Mathematical Analysis*, *40*(4), 1585-1620.

Figures

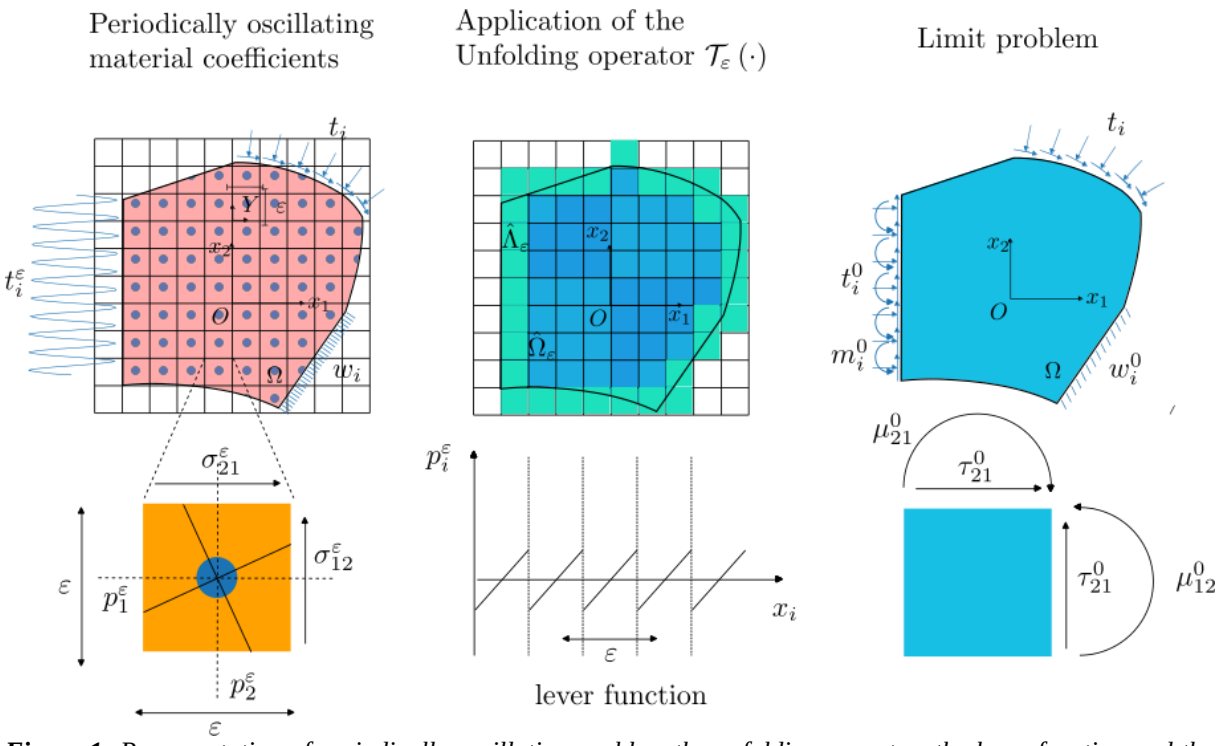

***Figure 1**: Representation of periodically oscillating problem the unfolding operator, the lever function and the limit problem.*

ALERT Geomaterials

The Alliance of Laboratories in Europe for Education, Research and Technology